

Naturally Sourced Epoxies for High-Performance Composite Applications

A feasibility study of renewable algae-derived epoxy resin system

Pranshul Gupta

Delft University of Technology



Naturally Sourced Epoxies for High-Performance Composite Applications

A feasibility study of renewable algae-derived
epoxy resin system

Thesis report

by

Pranshul Gupta

submitted in partial fulfillment of the degree of Master of Science
at the Delft University of Technology
to be defended publicly on May 17, 2024 at 13:00

Thesis committee

Supervisors: Dr. B. Kumru
Dr. Ing. S.G.P. Castro
Dr. Ir. R.C. Alderliesten
Daily Supervisor: William E. Dyer
Place: Faculty of Aerospace Engineering, Delft
Project Duration: September 2023 - May 2024
Student number: 5806054

An electronic version of this thesis is available at <http://repository.tudelft.nl/>.

“The greatest threat to our planet is the belief that someone else will save it.”

- Robert Swan

Preface

This research culminates from an idea and interest in developing bio-composites and contributing to sustainability goals. The successful culmination of this research is due in large part to the invaluable support of those around me. I want to express my deep appreciation for the love and support of my family, friends, supervisors, and the research group during this journey. Their constant encouragement, trust, patience, guidance, and unwavering presence have been a source of strength and motivation for me, especially during the highs and lows of this academic endeavor.

This thesis is divided into several sections. The first section lays the theoretical groundwork, followed by a detailed account of the experimental approach, findings, and their implications. The final sections discuss the broader context of the study and suggest directions for future research.

As I contemplate my future, this research has not only strengthened my dedication to sustainable engineering but has also sparked a desire to delve deeper into this field. My goal is to make a significant contribution to the advancement of eco-friendly materials and to motivate others to participate in this crucial endeavor.

*Pranshul Gupta
Delft, May 2024*

Naturally Sourced Epoxies for High-Performance Composite Applications

A feasibility study of renewable algae-derived epoxy resin system

Research Question: Can an epoxy resin system be prepared with PHTE that holds the potential to replace the current epoxies used for high-performance aerospace structural applications?

Composite materials have revolutionized the world as we know it, but along the way, we have transformed that world, which is changing and suffering from global warming. This thesis examines the possibility of using bio-based resins for high-performance composite applications. Specifically, it focuses on PHTE, a biobased epoxy made from brown algae. The research investigates the feasibility of PHTE to replace BADGE epoxy, a bisphenol-A-based toxic and synthetic fossil-fuel-derived epoxy that comprises a major portion of aerospace composites. To complement and maximize strength, an aromatic diamine DDS was selected as the curing agent, and the stoichiometric ratios were estimated for both systems by maximizing the glass transition temperature (T_g). The study involves comprehensive material analysis and testing, including an examination of thermal, physical, and mechanical performance and a comparison of both systems. The resin systems were also used to prepare a composite to develop and assess the feasibility of using traditional manufacturing techniques. PHTE had a T_g 34 °C higher with a lower activation energy as compared to BADGE. PHTE has a 23.8 % lower tensile strength but it has a 33.6 % higher Young's Modulus and a 39.6 % higher flexural modulus which is beneficial for composite applications. It also has a 15 % higher fracture toughness in a single-edge notched bend. The PHTE:DDS resin system yields a bio-based content of 64.31 %. In conclusion, PHTE demonstrated excellent mechanical and thermal properties with high bio-based content, although its high viscosity posed challenges for traditional manual manufacturing techniques, especially composite manufacturing. The promising properties motivate us to study and develop the recipe further for other high-performance applications as well apart from aerospace.

Key words : Bio-based resins, composite manufacturing, bio-based epoxy, phloroglucinol triglycidyl ether, sustainable materials, high-performance, mechanical properties, glass transition temperature, bio-based carbon, environmental sustainability.

Contents

Preface	iii
Abstract	v
List of Figures	xi
List of Tables	xiii
1 Introduction	1
2 Composites	3
2.1 Reinforcement	3
2.1.1 Bio-Composites	4
2.1.2 Natural Fibers	4
2.2 Matrix	4
2.2.1 Thermosets	5
2.2.2 Thermoplastics	5
2.2.3 Vitrimers	6
2.2.4 Thermosets or Thermoplastics?	6
2.3 Why focus on matrix than reinforcement?	7
3 Thermoset resins	9
3.1 Epoxy Resins	9
3.1.1 Advantages of Epoxies	10
3.1.2 Issues of Epoxy Resins	10
3.2 Bio-based epoxies	11
3.2.1 Available or existing Bio-based Monomers	12
3.2.2 Drawbacks of existing Bio-based epoxies	13
3.2.3 Why aromatic resins?	13
3.3 PHTE	13
3.3.1 Current applications of Phloroglucinol	14
3.3.2 Cost Reduction and effectiveness	14
4 Research question and methodology	15
5 Curing agent selection	17
5.1 Kofler bench testing	18
6 Stoichiometric ratio estimation	23
6.1 Theoretical stoichiometric ratios	23
6.2 Why is stoichiometric ratio estimation required?	23
6.3 Temperature dependency of polymers	23
6.4 Ratio estimation procedure	25
6.4.1 Thermo-gravimetric analysis (TGA)	25
6.4.2 Differential scanning calorimetry (DSC)	26
6.5 BADGE:DDS - Stoichiometric ratio estimation	30

6.6	Continued ratio estimation procedure.	31
6.6.1	Dynamic mechanical analysis (DMA)	31
6.7	PHTE:DDS stoichiometric ratio estimation	37
7	Resin characterization	43
7.1	Thermal analysis	43
7.1.1	Thermal behavior - Thermo-gravimetric analysis (TGA)	43
7.1.2	Activation energy - Differential scanning calorimetry (DSC).	45
7.1.3	Coefficient of thermal expansion (CTE) - Thermo-mechanical analysis (TMA)	47
7.1.4	Glass transition temperature (T_g) - Dynamic mechanical analysis (DMA)	48
7.1.5	Viscosity measurement - Dynamic Rheometry.	48
7.2	Physical Characterization.	49
7.2.1	Surface hydrophilicity - Water contact angle	50
7.2.2	Water absorption.	52
7.2.3	Gel content	52
7.2.4	Bio-based content	53
7.3	Mechanical testing	53
7.3.1	Density	53
7.3.2	Tensile strength and Young's modulus.	54
7.3.3	Flexural strength and modulus	57
7.3.4	Fracture toughness: Single edge notched bend	60
8	Composite trials	67
8.1	Test selection	67
8.2	Reinforcement selection	67
8.3	Composite manufacturing	67
8.3.1	Issues faced during composite manufacturing	69
8.4	Inter-laminar shear strength testing (ILSS).	69
8.4.1	Sample preparation.	69
8.4.2	Testing	70
8.4.3	Test Validity check.	71
8.4.4	Shear Strength Calculation	72
9	Conclusion	75
9.1	Curing agent selection	75
9.2	Stoichiometric ratio estimation	76
9.3	Resin characterization	76
9.4	Composite trials.	78
9.5	Conclusion and cost considerations	78
10	Recommendations and Future Work	79
	References	85
11	Woven fabric composite trials	87

Nomenclature

List of Abbreviations

ASTM	American society for testing and materials
BADGE	Bisphenol-A diglycidyl ether
BPA	Bisphenol-A
CD	Constant Deformation
CF	Carbon fiber
CR	Constant Rotation
DDE	4,4'-diaminodiphenyl ether
DDM	4,4'-diaminodiphenylmethane
DDS	4,4'-diaminodiphenylsulfone
DICY	Dicyandiamide
DMA	Dynamic Mechanical Analysis
DSC	Differential scanning calorimetry
FRP	Fiber reinforced plastic
GF	Glass fiber
HDPE	High-density Polyethylene
HMPA	Hexahydro- 4-methyl phthalic anhydride
ISO	International organization for standardization
MNA	Methyl nadic anhydride
PAEK	Polyaryletherketone
PAN	Polyacrylonitrile
PEEK	Polyether ether ketone
PHTE	Phloroglucinol triglycidyl ether
PMMA	Poly(methyl methacrylate)
PP	Polypropylene

PPS	Polyphenylene sulfide
RPM	Rotations per minute
TGA	Thermogravimetric analysis
TMA	Thermomechanical Analysis
UD	Unidirectional

List of Symbols

μm	micrometer
T_g	Glass Transition Temperature
T_m	Melting Temperature
atm	atmosphere
g	gram
GPa	Giga Pascal
Hz	Hertz
mg	milligram
ml	milliliter
mm	millimeter
MPa	Mega Pascal
N	Newton
$^{\circ}\text{C}$	Degree Celsius

List of Figures

1.1	Materials used for primary structures in Boeing 787 [2]	1
2.1	Composition of Composites [2]	3
2.2	Different Types of Reinforcement [2]	4
2.3	Types of Polymer Molecular Structure and their properties [9]	5
3.1	Chemical Structure of Epoxide [15]	9
3.2	Epoxy reaction with Amines and Anhydride [15]	9
3.3	Chemical Structure of B isphenol- A D iglycidyl E ther (BADGE) [15]	10
3.4	tris(4-hydroxyphenyl) methane triglycidyl ether (THPMTGE) or Tactix 742 [18]	11
3.5	Chemical Structure of Bisphenol-A (BPA) [15]	11
3.6	Chemical Structures of available Bio-based Resins	12
3.7	Chemical Structure of Phloroglucinol	14
3.8	Chemical Structure of Phloroglucinol triglycidyl ether (PHTE)	14
5.1	Chemical Structures of Anhydride Curing Agents	17
5.2	Chemical Structure of DDS	18
5.3	Chemical Structure of DDM	18
5.4	Chemical Structure of DDE	18
5.5	Chemical Structure of DICY	18
5.6	Kofler bench	19
5.7	Curing cycle DSC plot comparison for curing agents	21
6.1	Melting and softening behaviour of semicrystalline and amorphous materials [8]	24
6.2	Initial thermogravimetry of the resin systems	26
6.3	PHTE-DDS theoretical stoichiometric ratio DSC at varying heating rates	28
6.4	BADGE-DDS theoretical stoichiometric ratio DSC at varying heating rates	29
6.5	DSC plots for BADGE:DDS Stoichiometric Ratio Estimation	30
6.6	Mould design for DMA samples	33
6.7	Weighing Boats with PHTE-DDS molar ratios in degassing chamber	33
6.8	Initial molding trials for PHTE-DDS	34
6.9	Cured PHTE-DDS samples with bubbles	34
6.10	Resin preparation in Polypropylene Containers	35
6.11	Resin preparation in Polypropylene Containers	36
6.12	Final Cured PHTE-DDS samples	36
6.13	DMA PHTE-DDS Frequency Sweep	37
6.14	PHTE-DDS 1 st stoichiometric DMA data	37
6.15	PHTE-DDS Storage modulus data for molar ratios 1.4-1.8	38
6.16	DMA samples post-cured at multiple temperatures	39
6.17	Storage modulus data for post-cured PHTE samples	39
6.18	PHTE-DDS 2nd Stoichiometric with 210 °C post-curing	40
6.19	PHTE-DDS 2nd Stoichiometric with 220 °C post-curing	40
7.1	TGA PHTE-DDS with $T_{5\%}$ and $T_{50\%}$ marked	44

7.2	TGA BADGE-DDS with $T_{5\%}$ and $T_{50\%}$ marked	44
7.3	Difference in thermal behavior of both resin systems	45
7.4	DSC data at varying heating rates for both resin systems	46
7.5	Kissinger model fitting for both resins	47
7.6	Coefficient of thermal expansion evaluation of both resins	47
7.7	Visc-elastic behaviour of both resin systems	48
7.8	Viscosity variation with temperature for both resins	49
7.9	Calibration for Water Contact Angle	50
7.10	BADGE Water Contact Angle measurements	51
7.11	PHTE Water Contact Angle measurements	51
7.12	Tensile Specimens	55
7.13	Tensile Stress vs. Strain Curves	56
7.14	Flexural Stress vs. Strain Curves	59
7.15	SENB Samples - PHTE (Left) and BADGE (Right)	60
7.16	SENB Testing setup	62
7.17	SENB Force Vs Displacement Plot	62
7.18	Determination of C and P_Q	64
8.1	Hand Lay-up process for Composite manufacturing	68
8.2	Closed with hand laid composite layers before curing	68
8.3	Composite laminate of both resins	69
8.4	Short beam shear setup for ILSS (Inter-Laminar Shear Strength)	70
8.5	ILSS Force vs. Displacement testing data	71
8.6	Successful ILSS test with failure through a lamina	71
11.1	Composite laminate manufacturing trials with the resin systems	87

List of Tables

3.1	Comparison of mechanical properties of BADGE and PHTE with Anhydride curing agents [22] [32]	13
5.1	Kofler bench test timings - PHTE DDS	19
5.2	Kofler bench test timings - PHTE DICY	20
5.3	Kofler bench test timings - BADGE DDS	20
6.1	BADGE-DDS Inflection temperatures at different molar ratios	30
6.2	BADGE-DDS Inflection temperatures at different molar ratios	31
6.3	PHTE-DDS Inflection temperatures at different molar ratios	38
6.4	PHTE-DDS 2nd stoichiometric inflection temperatures	41
7.1	Final TGA Data	45
7.2	Peak temperatures for both resins at varying heating rates	46
7.3	Viscosity variation of resin systems with temperature	49
7.4	Contact Angles made by a water droplet on BADGE samples	51
7.5	Contact Angles made by a water droplet on PHTE samples	51
7.6	Water Absorption by BADGE-DDS for multiple durations	52
7.7	Water Absorption by PHTE-DDS for multiple durations	52
7.8	Gel Content of Post-cured and Non-Post cured samples of both resins	53
7.9	Density Measurement - BADGE:DDS	54
7.10	Density Measurement - PHTE:DDS	54
7.11	Tensile Specimen data - BADGE:DDS	55
7.12	Tensile Specimen Data - PHTE:DDS	56
7.13	Flexural Specimen Data - BADGE:DDS	57
7.14	Flexural Specimen Data - PHTE:DDS	57
7.15	BADGE Specimen Data	61
7.16	PHTE Specimen Data	61
7.17	Calculation of K_Q , the conditional K_{IC} value	65
7.18	Check for validity of tests	65
8.1	Sample Dimensions of Carbon composite with BADGE resin	70
8.2	Sample Dimensions of Carbon composite with PHTE resin	70
8.3	Inter-Laminar Shear strength calculation for Carbon composite with BADGE resin	72
8.4	Inter-Laminar Shear Strength Calculation for Carbon Composite with PHTE resin	72
9.1	Comparison table - PHTE and BADGE resin systems with DDS	77

1

Introduction

The aerospace industry is one of the most demanding and challenging, requiring the best of technology and equipment. Aerospace structures have been revolutionized with the advent of composites. [1] Composites have made aircraft possible as we know them today. The Airbus A380 was possible due to GLARE and fiberglass, whereas the latest Boeing 787 is possible due to carbon fiber composites.[2] Composite materials are widely used in the modern aircraft industry. They provide advantages such as lighter weight, greater stiffness, higher operating temperatures, higher reliability, and increased affordability. They allow for special needs such as good radio-frequency-compatible radomes made of fiberglass or quartz radomes or airframes for stealth aircraft. [1]

High-performance composites were developed because no single homogeneous structural material had all the desired properties. The constituent materials retain their identities in the composites and do not dissolve or otherwise merge completely into each other. Together, the materials create a *hybrid* material that has improved structural properties.

Figure 1.1 shows the range of materials used in the 787, as can be seen 50% of the materials are composites. Also, as mentioned, the 777 uses only 12% composites. This proves that the use of composites is also rising at a very high rate and thus it is important to tackle issues related to them. [2]

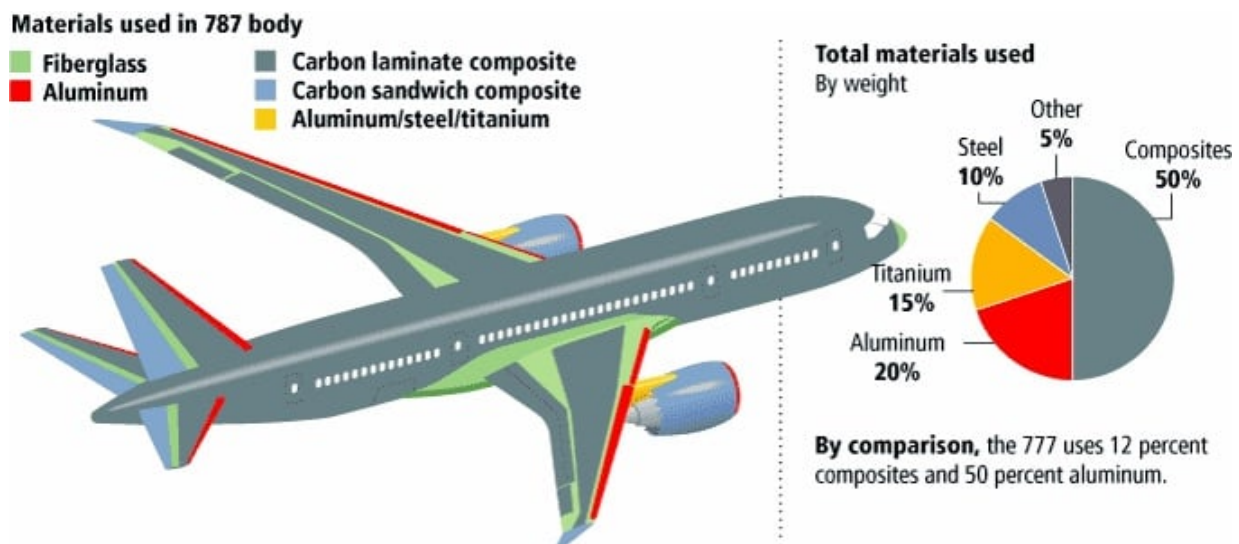


Figure 1.1: Materials used for primary structures in Boeing 787 [2]

High-performance applications employ what are called fiber-reinforced plastics. Wiliam et.al.

discuss at length the developments in the aerospace industry and materials. The ongoing global concern around global warming, fast-depleting fossil fuels, and toxic materials-related issues are driving a need to search for alternatives in all facets of the industry and the aerospace composites industry is not untouched by it. [3]

The current state of polymer composites employed in aerospace applications is far from being sustainable, both from a materials and manufacturing perspective. Resin recipes are composed of toxic and hazardous starting products obtained from petro refineries, the environmental footprint of CF production is immense, and composite manufacturing is associated with massive energy consumption. [3] There is a huge demand for new materials that can tackle these issues, and there is a great research focus on naturally sourced composite alternatives.

Chapter 2 introduces composite materials and the current research around bio-composites. It also discusses why is it essential to focus on resin rather than reinforcement. Chapter 3 discusses epoxy resin systems, their advantages and their issues, current developments around bio-epoxies, their advantages and drawbacks, and why PHTE holds potential as a good epoxy monomer for study along with the appropriate curing agent selection. Aerospace utilizes composites and due to the running environmental issues, it is high time a new resin system is formulated that is natural and non-toxic. Therefore, the main research objective of this thesis is:

Research Objective

To formulate an epoxy resin system from naturally sourced and non-toxic raw materials that can compete with and hold the potential to replace the current epoxies used for high-performance structural applications.

The specific research question is:

Research Question

Can an epoxy resin system be prepared with PHTE that holds the potential to replace the current epoxies used for high-performance structural applications?

This thesis aims to formulate an epoxy resin system using PHTE monomer to replace the BADGE resin system used in the aerospace industry.

Chapter 4 provides an insight into a stepwise list of objectives to achieve this aim. Chapter 5 focuses on the selection of an appropriate curing agent. Chapter 6 develops the stoichiometric ratio and the processing parameters of the resin systems. Chapter 7 explores and compares the resin systems utilizing various techniques and parameters. Chapter 8 checks the feasibility of manufacturing and comparison of composites manufactured from both resin systems. Chapter 9 concludes the study and current issues, and finally recommendations and future work are addressed in chapter 10.

2

Composites

Composites are a combination of 2 or more materials, split mainly into two categories: reinforcement and matrix. Composites combine the properties of the materials and provide a material whose properties can be tailored as per application, as shown in figure 2.1.

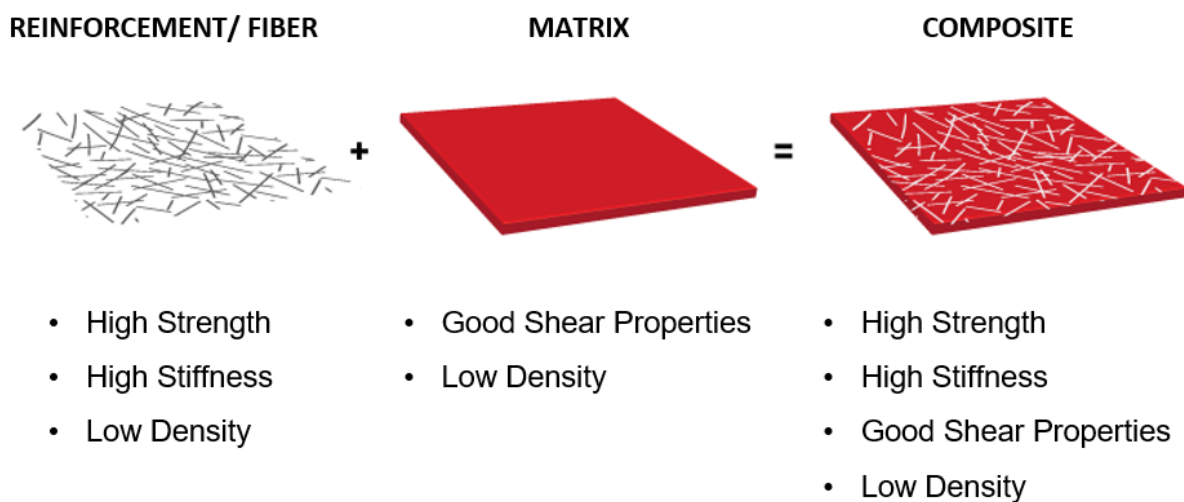


Figure 2.1: Composition of Composites [2]

2.1. Reinforcement

The main strengthening part of the composite is called a reinforcement. It can range from pebbles in concrete, to fibers used in bulletproof vests. Figure 2.2 shows types of reinforcement that can be used. The aerospace industry almost always uses fiber-reinforced composites. Fibers can be either continuous or discontinuous.

As fibers strengthen the composite along their length, it is important to utilize continuous fibers. Fibers are far stronger as compared to resin, especially longitudinally. Currently, fiberglass or carbon fiber is employed in high-performance applications such as aerospace, as shown in figure 1.1.

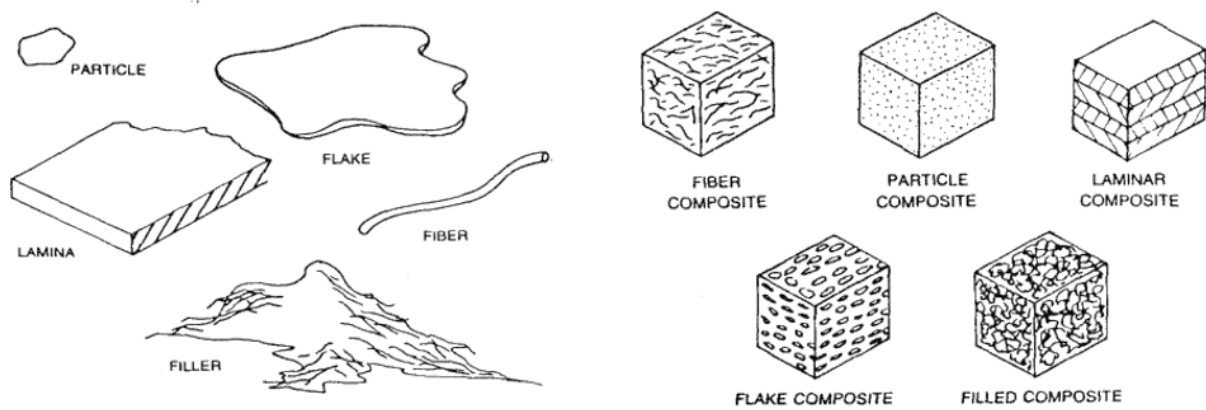


Figure 2.2: Different Types of Reinforcement [2]

Although these fibers have amazing properties, they have a number of drawbacks, such as high energy processing requirements (around 3000 °C for carbon fiber, 1400 °C for glass fiber), petroleum-derived products (precursor for carbon fiber, PAN (Polyacrylonitrile) is derived from crude oil processing), non-recyclable or decomposable, etc. [4] With the increasing concerns over global warming, depleting fossil fuels, ever-increasing waste production, and environmental concerns, it has become crucial to find alternate solutions to the existing solutions.

2.1.1. Bio-Composites

To tackle these issues, the need for bio-composites is at an all-time high. Bio-composites consist of using either natural fibers, resins, or both together and may serve as alternatives to petroleum-based, non-renewable plastics. Bio-composites are mostly non-toxic and hold the potential to lower the overall ecological footprint, making them safer for humans and avoiding the ill effects of synthetic materials on the environment. Moreover, some of the bio composite-based fibers and resins are recyclable and reusable.

2.1.2. Natural Fibers

A lot of studies are being conducted on natural fibers acting as a viable alternative to replacing the existing synthetic fibers. There is a vast range of natural fibers available that have been researched for composite use, such as jute [5], flax [6], hemp [6], sugarcane [7], bamboo [6], etc. They tackle almost every environmental concern mentioned but they have several drawbacks as far as aerospace is concerned.

They cannot be used for primary structures in aerospace due to their low strength, inconsistent properties, short fiber length, flammability and chemical degradation, water absorption, and low-temperature tolerance. They also pose issues related to deforestation and might even generate competition for food upon further industrialization.

Thus, due to their low mechanical properties, it is crucial to use either fiberglass or carbon fiber for aerospace composites and find other ways to tackle the issues at hand. [2]

2.2. Matrix

The reinforcement alone cannot form a structure and a matrix is required to hold it together. The matrix is the component of the composite that shapes the composite, holds everything together, and imparts rigidity to the structure. Matrix can also range from cement in concrete to resins in fiber-reinforced composites. As aerospace majorly employs fiber-reinforced composites that utilize resins, the discussion will only be focused on the resins. [2]

Majorly, resins can be of 2 types based on their internal structure: thermosets and thermoplastics. The structural characteristics that are most important in determining the properties of polymers are:

- The degree of rigidity of the polymer molecules,
- The electrostatic and van der Waals attractive forces between the chains,
- The degree to which the chains tend to form crystalline domains and
- The degree of cross-linking between the chains.

Both types of resins hold the potential to impart the required chemical and mechanical properties but behave differently under heat and pressure. Due to differences in their chemical structure, they have different properties and behaviors, as shown in figure 2.3. [8]

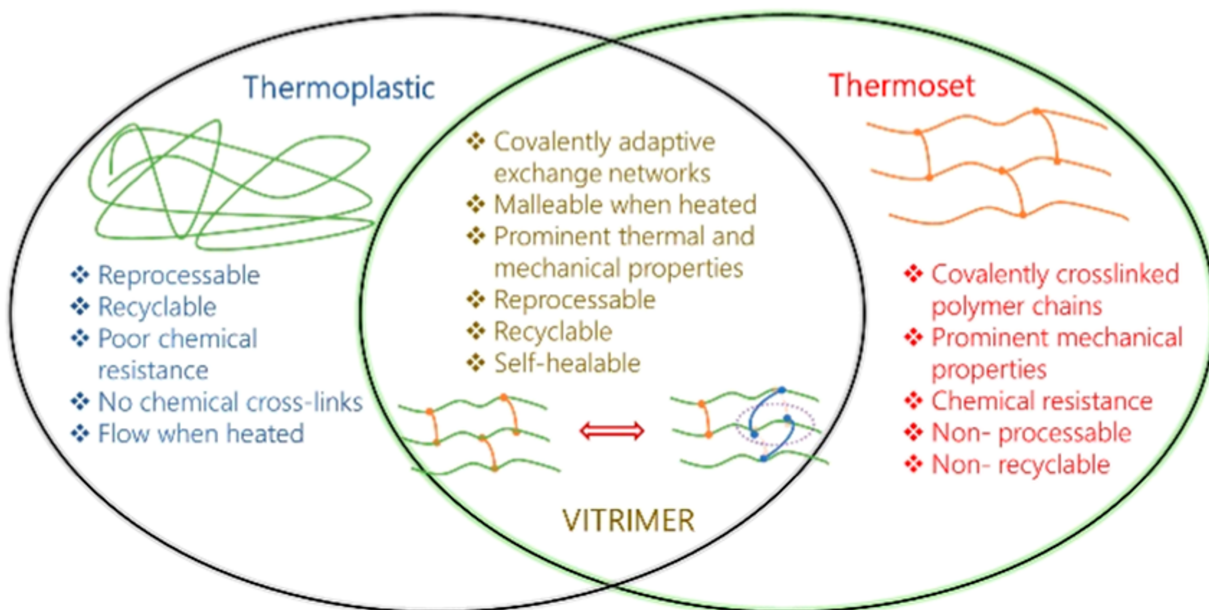


Figure 2.3: Types of Polymer Molecular Structure and their properties [9]

2.2.1. Thermosets

Thermoset polymers are one of the oldest known polymers and have been around and researched for decades. A lot of thermoset resin systems have been perfected over the years. Thermosets are usually monomeric or individual molecules that undergo a catalytic chemical reaction known as curing. During curing, these molecules form covalent bonds, which form a three-dimensional network with high-crosslinking densities of polymer chains that convert them into hard, brittle solids that, once formed, cannot be melted or reformed traditionally. Examples of thermosetting resins include epoxy resins, polyester resins, phenolic resins, etc. [2]

2.2.2. Thermoplastics

Alternatively, thermoplastics are linear or branched polymers that can be melted and reformed many times without chemical change. They are of high molecular weight whose strength and stiffness depend on the properties of the monomer units and their molecular weight. The breaking of intermolecular interactions in crystalline regions allows thermoplastics to flow and deform when heated. Examples of thermoplastic resins include polyethylene, polypropylene, and polycarbonate including the new ones with greater strength such as PEEK, PAEK, etc. [2]

Thermosets and thermoplastics are also processed differently. Thermosets are typically cured using heat, pressure, or a combination of both. This process can be done at room temperature or elevated temperature, depending on the specific resin and hardener used. Once cured, thermosets cannot be reshaped or melted without breaking the covalent bonds that hold the polymer chains together. Thermoplastics, in contrast, can be processed in a variety of ways, including injection molding, extrusion, blow molding, and thermo-forming. These processes heat the resin to its melting point and shape it into the desired shape using a mold or die. The resin is then allowed to cool and solidify, retaining its new shape. [8]

2.2.3. Vitrimers

A new unique field of polymer networks has emerged in recent times which combines the permanent structure of thermosets with the malleability and reprocessability of thermoplastics. These new polymer materials are called vitrimers and were introduced by Leibler and co-workers in 2011. Vitrimers are a new class of materials, which are fast emerging as thermosets with reprocessing capabilities. This is possible due to the presence of permanent networks of polymer chains connected via dynamic covalent bonds, which allow the network to change its topology while maintaining a constant number of chemical bonds at all temperatures. Due to this, vitrimers can achieve a compelling balance of robust mechanical properties and processability. Some examples include Diels-Adler adducts, PMMA/HDPE vitrimers, etc. [10] Due to the presence of dynamic covalent bonds, vitrimers exhibit lower strength and have greater creep resistance as compared to thermosets; thus, they cannot be used for high-performance applications.

2.2.4. Thermosets or Thermoplastics?

As per Airbus, the typical service life of a commercial aircraft is over 30 years. One characteristic that long-service components must have in addition to the necessary strength and functional qualities is creep resistance. Thermosets have a significant advantage over thermoplastics in terms of creep resistance. Creep is the deformation that occurs over time under a constant load, and the cross-linked molecular structure of thermosets provides them with better resistance to this phenomenon. During the manufacturing process, thermosets undergo curing and cross-linking, which chemically bond the polymer chains into a rigid structure. This restricts chain movement and reduces the material's tendency to deform under load. In contrast, thermoplastics have linear or branched structures that allow them to be melted and reformed multiple times but make them prone to creep. [2][8]

In addition to their superior creep resistance, thermosets offer other advantages. They can withstand high temperatures without melting or losing shape, making them suitable for high-temperature environments like aerospace applications. Thermosets are also resistant to various chemicals, acids, and bases, making them well-suited for use in harsh chemical environments. Once cured, traditional thermosets become hard and strong, exhibiting high mechanical properties, impact resistance, and abrasion resistance. Overall, the crosslinked structure of thermosets provides them with better dimensional stability and resistance to long-term deformation, making them advantageous for specific applications. [9] [11]

In addition, thermosets are often used in life-critical applications. Thermosets maintain their shape and size over a wide range of temperatures and humidity, making them ideal for use in applications where dimensional stability is critical, such as electronic components and structural composites. Along with this, many thermosets have excellent electrical insulating properties, making them useful in applications where electrical conductivity is undesirable or even dangerous.

With growing landfill concerns, thermoplastics are seen as a solution as they can be re-melted or reused. However, the recycling aspect of thermoplastics doesn't work for aerospace applications as

the melting temperature is very high and the product recovered from a thermoplastic composite is usually highly down-cycled. Also, the properties of thermoplastics degrade over time and it is impossible to re-use thermoplastics in aerospace. [12] Kumru et. al evaluate and insist on assessing the difference brought about by thermoplastics conducting life-cycle assessment studies before the implementation of thermoplastics for sustainability purposes.[13]

2.3. Why focus on matrix than reinforcement?

As mentioned before, amidst growing concerns about global warming, depleting fossil fuels, and toxic materials, the need to rethink and find alternate materials is at an all-time high. For the aerospace industry, as discussed, it is impossible to utilize natural fibers for primary structures due to their low mechanical properties and inconsistent properties. Thus, it is important to work on the matrix to make use of natural sources and shift the petroleum dependence and use of toxic materials. Thus, we will focus on thermoset resins and evaluate naturally derived materials.

3

Thermoset resins

Thermosets have been successfully employed in the aerospace industry for several decades now. The key role played in their success can be attributed to epoxy resins. Epoxy resins are the most widely used resins in the composite industry. [14]

3.1. Epoxy Resins

Epoxy resins were discovered by Prileschajew, who defined them as low molecular weight compounds with multiple epoxide groups as in figure 3.1 capable of polymerizing to form cross-linked polymers. [15]

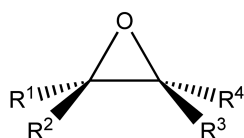


Figure 3.1: Chemical Structure of Epoxide [15]

Epoxy resins are versatile materials with a wide range of applications in coatings, adhesives, composites, and electrical insulation. Their properties can be varied as per requirements by using various monomers and curing agents or reinforcements. They are extensively used in the aerospace industry for weight reduction and efficiency improvement in aircraft structures. Epoxy coatings are done on concrete structures to prevent or protect from corrosion, epoxy adhesives are even used to adhere metals, plastics, and ceramics in industries as stringent as automotive, aerospace, or electronic applications. [15]

Epoxy resins are formed by the reaction of epoxy functional groups with curing agents such as amines and anhydrides as in figure 3.2.

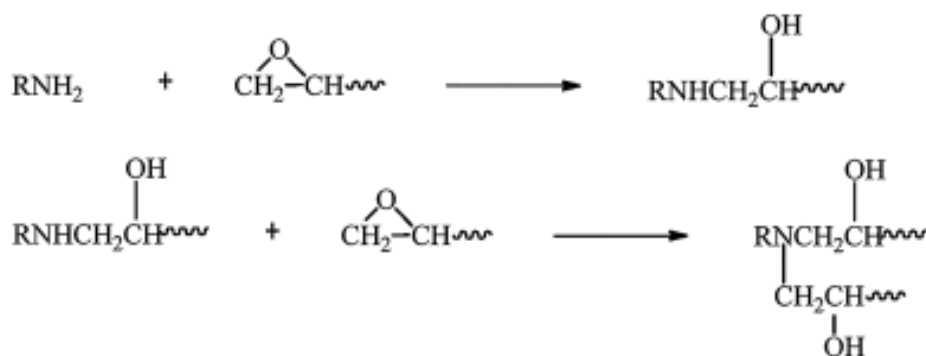


Figure 3.2: Epoxy reaction with Amines and Anhydride [15]

3.1.1. Advantages of Epoxies

Each amine reacts with two epoxies, which leads to a highly cross-linked network as in figure 3.2. The alcohol group formed upon epoxy ring opening polymerization also gives rise to strong inter-molecular interactions or hydrogen bonding which results in even greater molecular bonding. All of this leads to a material that has excellent mechanical, thermal, electrical, and adhesive properties along with good process-ability, dimensional stability, and compatibility with fillers or other polymers. [16] The mechanical properties of epoxy resin can be adjusted by adjusting curing conditions such as temperature and time or varying the epoxy monomers or curing agents, which affects the overall chemical structure.

In conclusion, they have excellent mechanical, thermal, electrical, and adhesive properties along with good process-ability, dimensional stability, and compatibility with fillers or other polymers. [16]

3.1.2. Issues of Epoxy Resins

Although these epoxy resins have excellent properties, these thermoset resins have important drawbacks that are necessary to be addressed, which are:

1. **Dependence on fossil fuels:** Most epoxy matrices are unsustainable, they are derived from fast-depleting non-renewable petroleum-based sources. **Bisphenol-A Diglycidyl Ether (BADGE)** as in Figure 3.3, which accounts for almost 90% of the resin systems, especially in high-performance or primary structural applications in Aerospace, is obtained by the reaction between Bisphenol-A (BPA) as shown in figure 3.5 and Epichlorohydrin. [14]

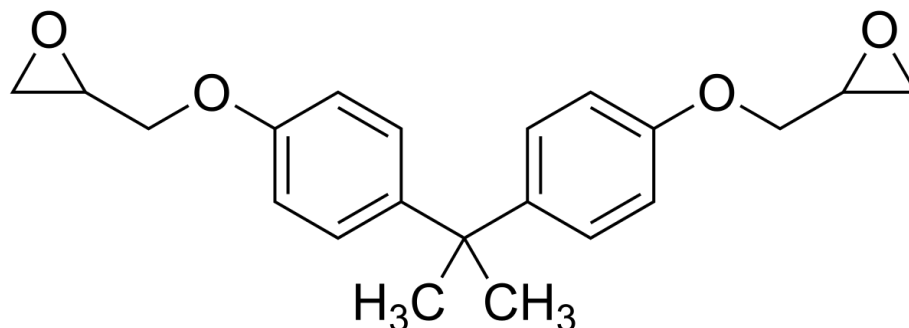


Figure 3.3: Chemical Structure of Bisphenol-A Diglycidyl Ether (BADGE) [15]

Similarly, tris(4-hydroxyphenyl) methane triglycidyl ether (THPMTGE) epoxy monomer (commercially available as Tactix 742 by Huntsman) is a trifunctional epoxy with a high aromatic ratio. [17] It has a high T_g due to which, it has high heat resistance even in high-strength applications. Thus, it is used mainly around turbines/hot areas of the aircraft, whereas BADGE is not used for such high-temperature applications. Tactix is formed by condensation of phenol with benzaldehyde followed by glycidylation. Phenol and benzaldehyde both are synthesized from benzene, which is obtained from petroleum-based sources.

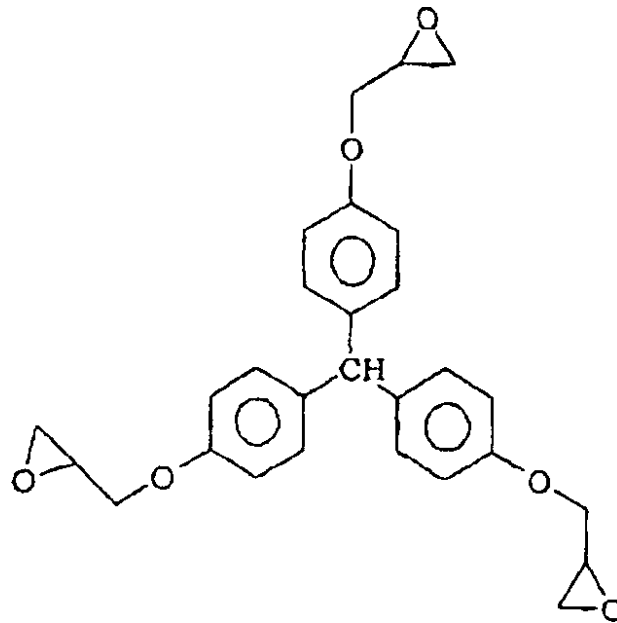


Figure 3.4: tris(4-hydroxyphenyl) methane triglycidyl ether (THPMTGE) or Tactix 742 [18]

2. **Toxic raw materials:** The raw materials involved in the synthesis of epoxy resins can be highly toxic. BPA has been found to have carcinogenic, mutagenic, and reprotoxic effects. [19] Awareness of BPA toxicity has led to the restriction of its use in numerous countries, thus generating an industrial crisis and an imminent need to find alternatives to epoxy resins that meet and provide characteristics like or even better than those generated by BADGE. [20]

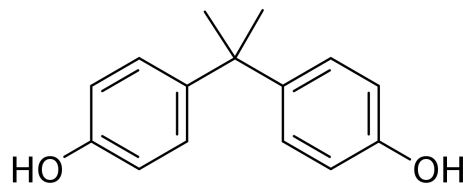


Figure 3.5: Chemical Structure of Bisphenol-A (BPA) [15]

Similarly, phenol and benzaldehyde are toxic materials that are used as raw materials for TACTIX synthesis.

3. **Issue of landfilling:** With the popularization of plastics, the issue of disposing of waste has become a daunting challenge. These resins have a highly cross-linked molecular architecture that hinders reprocessing, repairing, and recycling. [14] Yang et al. discuss the following recycling types for thermoset composites: [21]
 - Mechanical recycling: grinding or milling for reuse as fillers,
 - Thermal recycling: pyrolysis for fiber and matrix recovery, incineration, etc., and
 - Chemical recycling: Chemical dissolution of matrix, solvolysis, etc.

3.2. Bio-based epoxies

As the available solutions do not tackle the issues at hand, the development of thermosets from bio-based and environmentally friendly sources as alternatives to toxic and petroleum-based ones

is essential. It is an efficient way to mitigate environmental pollution, being in line with the sustainable development concept. [16] Some works even mention the recyclability or reprocessability of bio-based monomers, [22] [23] [19] but it is out of scope for this study and will not be discussed further.

3.2.1. Available or existing Bio-based Monomers

The research on bio-based monomers has been going on for quite some time now. A lot of work has been already done and there is a wide variety of bio-based monomers among them, itaconic acid [24], cardanol [5] [25], furan derivatives [26], sugars [27], or fatty acids [28] [29], linseed oil [30], soybean oil [31] are worth mentioning. These resins are derived from natural sources, are non-toxic, and often originate from the waste of other processes.

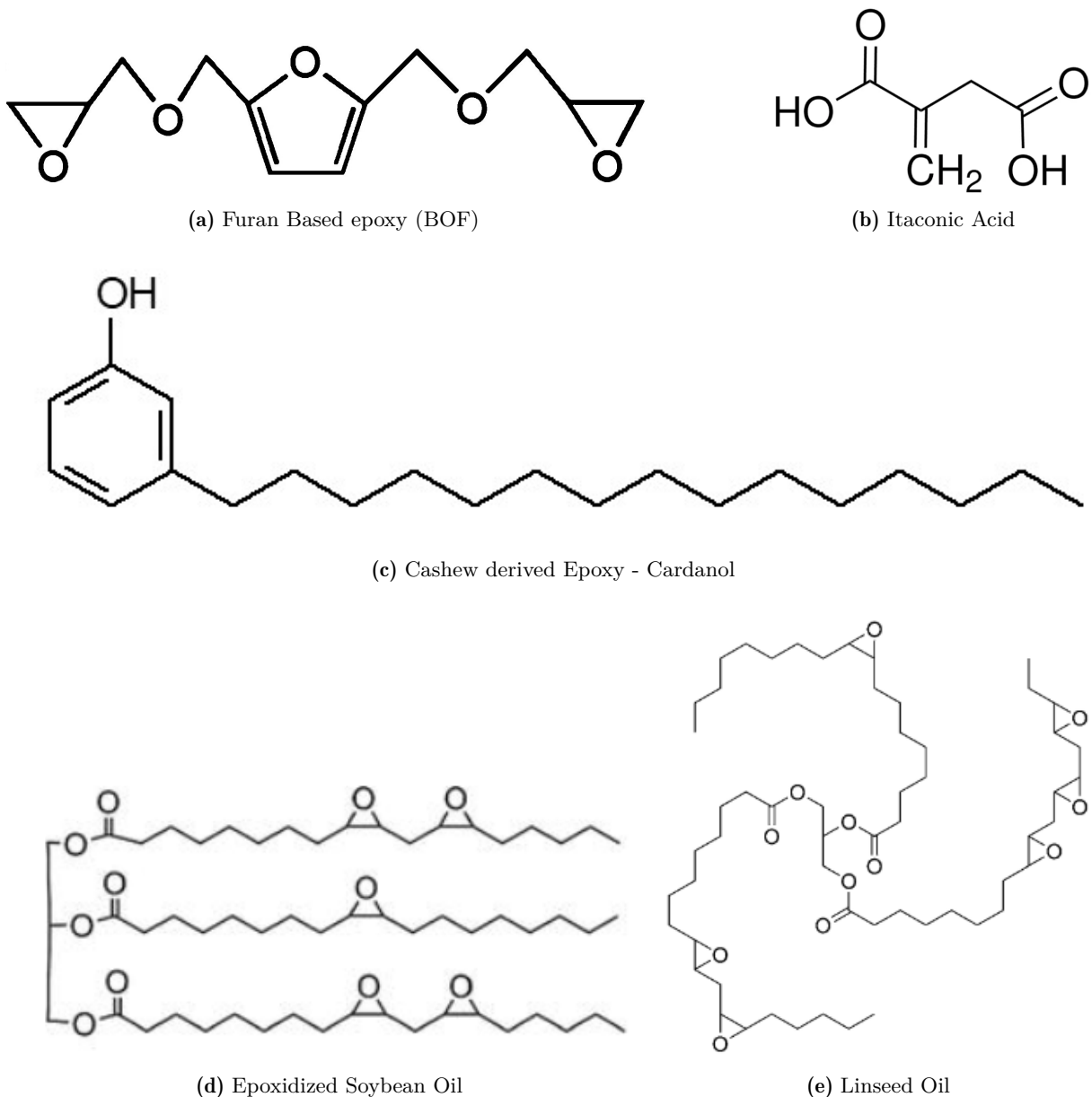


Figure 3.6: Chemical Structures of available Bio-based Resins

3.2.2. Drawbacks of existing Bio-based epoxies

Although the existing bio-based epoxies tackle the issues of epoxy resins as mentioned before, they have their drawbacks which limit their use, especially for high-performance or primary structural applications. The existing solutions:

- have low strength,
- emerge from wastes that highly depend on one source,
- are expensive,
- have high moisture uptake,
- compete with food, and
- have low interlaminar strength.

Keeping in line with the aim of this study, the best option in the preparation of high-performance thermosetting materials that can substitute BADGE thermosets is those having phenolic groups because the rigidity of the aromatic structure allows them to reach excellent thermal and mechanical performances. [18]

3.2.3. Why aromatic resins?

As can be inferred from the chemical structures in figures 3.3 and 3.4, the structures have aromatic components. Aromatic compounds confer more toughness, stiffness, and temperature stability to the final material thanks to the presence of $\pi - \pi$ stackings in the structure. [22]

Dinu et.al have wide expertise in the synthesis of epoxy monomers from natural resources. Their works with triglycidyl eugenol derivative, tetra glycidyl bis-eugenol derivative, and, more recently, with triglycidyl phloroglucinol, evidenced that these phenolic compounds are a great alternative. These works along with others confer a great deal of promise on phloroglucinol-derived resins in their performance as well as availability. [16] [18] [22] [23]

Sample	Tg-DSC [°C]	Young's modulus [GPa]	Tensile stress [MPa]
BADGE-HMPA	125	2.9	68
PHTE-HMPA	178	1.32 ± 0.15	55 ± 8.3
PHTE-MNA	184	1.20 ± 0.09	69 ± 10.2

Table 3.1: Comparison of mechanical properties of BADGE and PHTE with Anhydride curing agents [22] [32]

Table 3.1 shows the mechanical properties of the epoxy monomers cured with anhydride curing agent: methyl nadic anhydride (MNA) and hexahydro- 4-methyl phthalic anhydride (HMPA). As can be inferred from the table, PHTE holds the potential to achieve properties closer as compared to BADGE. Dimitrios et al. also have researched PHTE along with a commercial Bisphenol-A derived epoxy system, Epikote 04908 epoxy with the available commercial Epikure 04908 hardener. [33] These studies motivate the selection of PHTE as an epoxy monomer for research on high-performance matrix applications.

3.3. PHTE

Figure 3.8 shows the chemical structure of PHTE, or **Phloroglucinol Triglycidyl Ether**. It is obtained from the triglycidylation of phloroglucinol (1,3,5-trihydroxy benzene) as in figure 3.7, which is generally found in marine brown algae (*Ecklonia cava*) or the bark of fruit trees. It can also be obtained by synthetic route from benzene. [19]

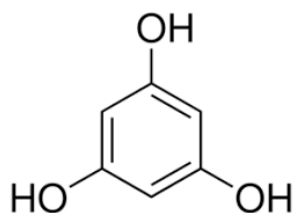


Figure 3.7: Chemical Structure of Phloroglucinol

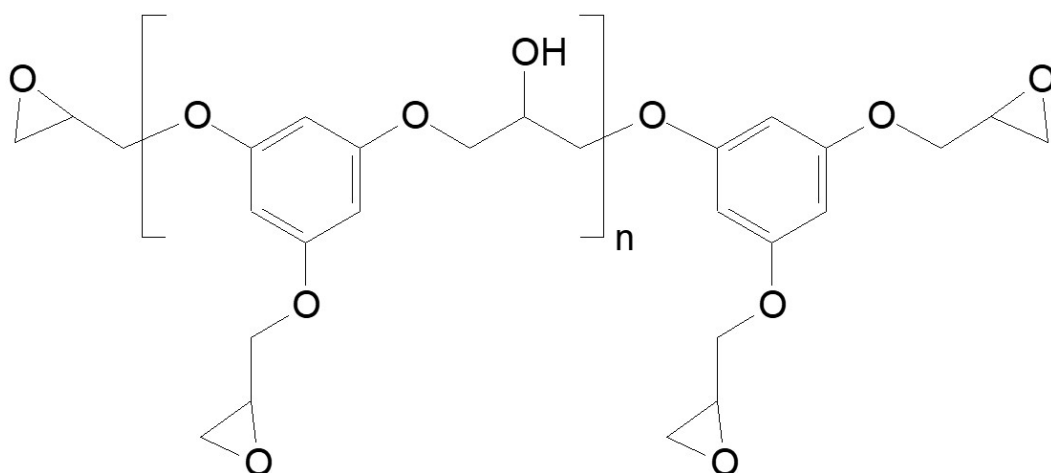


Figure 3.8: Chemical Structure of Phloroglucinol triglycidyl ether (PHTE)

3.3.1. Current applications of Phloroglucinol

One of the most important applications of phloroglucinol is in the medical field due to its beneficial effect on health such as anti-allergic, anti-inflammatory activity, antioxidant, or anti-carcinogenic. Currently, due to its good chemical characteristics, phloroglucinol has begun to be studied as a potential renewable resource for the development of various epoxy monomers or resins. [16] [19] [34] [33]

3.3.2. Cost Reduction and effectiveness

Phloroglucinol as of now is prepared mainly for medical or pharmaceutical use, due to which it is important to maintain a high level of purity and thus is expensive. It is already a multi-million dollar market and is expected to grow in the upcoming years. Upon exploration of PHTE for industrial use, it will lead to an increase in the production of phloroglucinol, which in turn might lead to a significant reduction in cost. To motivate this, the study explores the effectiveness of PHTE.

4

Research question and methodology

As discussed, PHTE holds the potential to be a contender for a sustainable matrix material for high-performance composites. To further investigate this, and specifically its applications in high-performance composites, an investigation using an aromatic curing agent is of interest. The central research question formed from the objective is:

Research Question

”Can an epoxy resin system be prepared with PHTE that holds the potential to replace the current epoxies used for high-performance structural applications?”

The objective is to formulate a resin system with PHTE epoxy monomer and study its characteristics and properties while comparing it with BADGE systems. To limit the scope of the study and for a fair comparison, it was decided to use a BADGE epoxy monomer, as commercial products tend to contain several additives. Also, it was decided to keep the curing agent constant for both monomers for a proper comparison.

Research Methodology

This study would provide insight into the natural alternate solutions to synthetic epoxies used for high-performance composite applications such as aerospace structures. To ensure a comprehensive and structured approach to the research, the following sub-objectives or tasks have been formulated:

1. **Curing agent selection:** Finalize a curing agent based on workability, availability, and properties.
2. **Stoichiometric ratio estimation:** Finalize an optimum mixing ratio for both the resin systems to maximize cross-linking and properties.
3. **Processing parameters:** Finalize a resin mixing procedure and decide on an appropriate curing cycle for proper cross-linking and maximum properties.
4. **Resin characterization:** Perform suitable characterization tests using ASTM/ISO standards to evaluate and compare the performance of the resin systems.
5. **Composite manufacturing trials:** Based on the results of the resin testing, progress to composite production and decide on an appropriate composite production technique.
6. **Composite testing:** Perform suitable mechanical tests using ASTM/ISO standards to investigate fiber-matrix interactions and composite performance of both resin systems.

Hypothesis Setting

Adhering to fundamental principles and key aspects of experimental research is crucial due to the experimental nature of the proposed study. This involves several crucial components, such

as creating and testing specific hypotheses, utilizing techniques for data collection and analysis, and conducting comparative studies to evaluate the potential of bio-based resins for composite manufacturing.

The primary hypotheses, which will serve as the cornerstones of the research, can be summarized as follows:

- **Hypothesis 1:** It is possible to prepare a resin system from PHTE and a suitable curing agent with easier processing.
- **Hypothesis 2:** The PHTE resin system holds the potential to compete with the synthetic BPA-based resin system.
- **Hypothesis 3:** Traditional composite manufacturing techniques can be adapted and effectively applied to composites with a bio-based matrix.

Throughout the research process, these hypotheses will guide the experiments, data collection, and analysis, helping to draw meaningful conclusions and insights regarding the viability of bio-based resins for composite manufacturing. The subsequent chapters of this study provide an in-depth exploration of the methodology, experimental procedures, results, and discussion in the pursuit of answering the research questions and testing the hypotheses.

5

Curing agent selection

As thermoset resin systems are 2 component systems, it is important to select the curing agent (also called B-Part or hardener) properly as it also plays a major role in the properties of the system.

As discussed in chapter 3, aromatic structures confer more strength and stiffness to material due to the presence of $\pi - \pi$ stacking in the structure. Dinu et. al. have researched PHTE majorly with anhydrides such as methyl nadic anhydride (MNA) and hexahydro-4-methyl phthalic anhydride (HMPA) having chemical structures as shown in figure 5.1. [22][16] As is evident from the chemical structures, aromatic structures are not present in these curing agents.

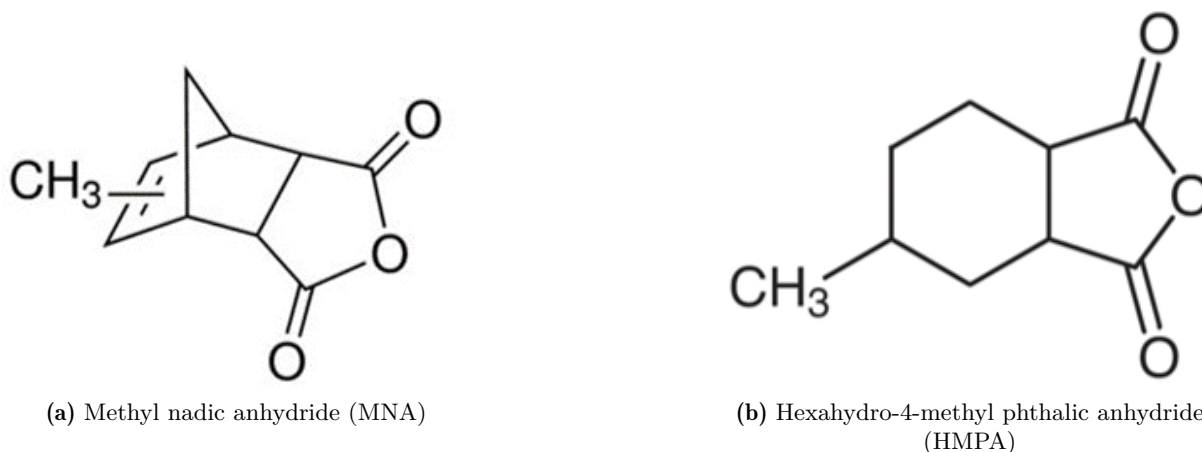


Figure 5.1: Chemical Structures of Anhydride Curing Agents

Table 3.1 motivates to search for different curing agents to be able to replace BADGE resin systems for aerospace applications. The anhydride curing agents produce resins with lower aromatic ratios, leading to lower mechanical properties as compared to other curing agents.

Sukanto et. al discusses epoxies and the use of amine and anhydride curing agents for composite matrix applications. Aromatic diamine curing agents regularly used in aerospace are DDS, DDM, and DDE as shown in figures 5.2, 5.3 and 5.4. Another curing agent regularly used in aerospace is DICY as in figure 5.5 due to its small structure as compared to other curing agents, which can be utilized to increase the aromaticity. [35][36][37]

Finally, the following 4 curing agents were worked upon:

- 4,4'-diaminodiphenylsulfone (DDS) sold commercially by Huntsman as Aradur 976.

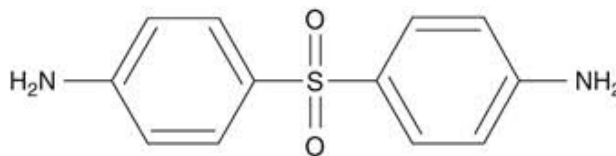


Figure 5.2: Chemical Structure of DDS

- 4,4'-diaminodiphenylmethane (DDM)

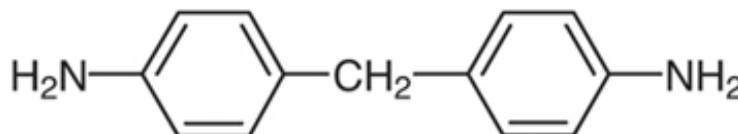


Figure 5.3: Chemical Structure of DDM

- 4,4'-diaminodiphenyl ether (DDE)

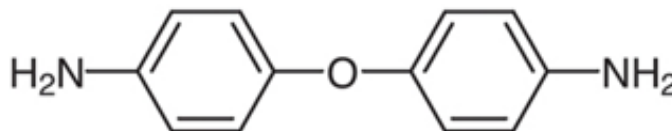


Figure 5.4: Chemical Structure of DDE

- Dicyandiamide (DICY)

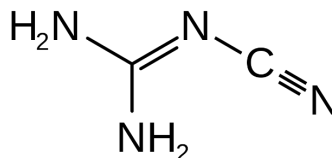


Figure 5.5: Chemical Structure of DICY

A resin dispersion was prepared of PHTE with the four curing agents. As all these curing agents are solid, it is essential to disperse them and prepare a colloiddally stable dispersion to avoid uncured areas in the matrix. As DDS is a commercially available product, it is available in a micronized powder that disperses well and gives a homogenous mixture. DDM and DDE are available as small crystals. They were ground into a fine powder, but still getting them to the fineness of DDS was not possible locally. Also, DDM and DDE are toxic, and converting them into fine powder for use in the lab would have been hazardous. Thus, it was decided to eliminate DDM and DDE.

5.1. Kofler bench testing

Moving forward with DDS and DICY, a testing methodology was essential to finalize the curing agent. The reactivity of a resin system is an important parameter, as it defines the processing time

available for a resin system. DDS has a low reactivity and is useful in creating large components. [35]

An initial testing method to test the reactivity and finalize a curing agent is a *kofler bench test*. It is used in the industry often due to its simplicity and effectiveness. It is a metallic heating plate setup with constantly varying temperatures from 50 °C to 300 °C as shown in the figure 5.6. It was used to study the behavior of the resins at different temperatures as a function of time.

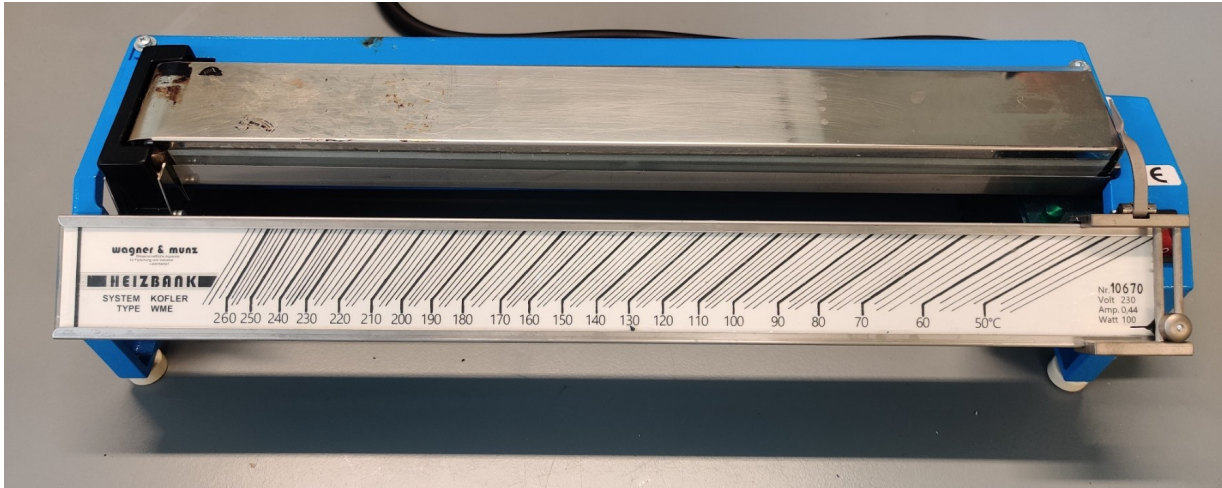


Figure 5.6: Kofler bench

The Kofler bench is thoroughly cleaned with acetone, and 3–4 layers of a chemical release agent (Marbocote 227) are applied at intervals of 5 minutes to allow proper drying. After this, it is plugged in and turned on. The Kofler bench takes around 10 minutes to heat up, after which the prepared resin sample is placed at the desired temperature. A PHTe stoichiometric mix was prepared with both DDS and DICY and placed at intervals of 20°C from 70°C to 210°C. The melting temperature of DDS is $\simeq 170^\circ\text{C}$ and that of DICY is $\simeq 205^\circ\text{C}$, which were kept in consideration for temperature range selection.

Tables 5.1 and 5.2 give the results from the Kofler bench test. The timing was noted at three points:

- Dissolution time - The cloudy mix of the resin becomes transparent with a runny consistency.
- Gelation time - The resin begins to thicken and starts to stick to the spatula.
- Curing time - The resin becomes solid and doesn't stick to the spatula.

Temperature (°C)	Dissolution time (min.)	Gelation (min.)	Curing (min.)
70, 90, 110	No progression till 60 minutes		
130	35	No gelation	No curing
150	7	45	57
170	5	22	28
190	3	10	14
210	1	5	9
250	2 minutes (burnt and gas formation)		

Table 5.1: Kofler bench test timings - PHTe DDS

From table 5.1, it can be inferred that no progression or change was seen below 130°C until 60 minutes for PHTE:DDS. The resin started dissolving at 130 °C and cured above it. At 250°C, the resin mix burned with a cloud of smoke. As expected, temperatures higher than the melting point of DDS give comparatively shorter times for use. A good processing temperature window was found to be between 70 and 110 °C, due to no progression or change meanwhile the viscosity becomes low, which will help in the handling of the resin.

Temperature (°C)	Dissolution time (min.)	Gelation (min.)	Curing (min.)
70, 90, 110, 130	No progression till 60 minutes		
150		20	30
170	7	8	12
190	30 seconds		1
210	15 seconds burn		
230	5 seconds burn		

Table 5.2: Kofler bench test timings - PHTE DICY

Similarly, from table 5.2 it can be inferred that no progression was seen below 150°C until 60 minutes for PHTE:DICY. The majority of the time spent here is in dissolution at lower temperatures as compared to the melting point of DICY. The dissolution and gelation occur simultaneously here, giving no processing window.

Although Kofler bench testing is a qualitative kind of test, the difference in the behavior of the curing agents along with PHTE is sufficient to motivate DDS as the curing agent of choice. Thus, DDS was finalized as the curing agent for this study.

Keeping with the aim of the study of comparing PHTE with BADGE, it is essential to keep all the parameters or components the same for a fair comparison starting from the curing agent. Table 5.3 shows the behavior of BADGE with DDS on the kofler bench. It can be inferred that no progression was seen below 150°C until 60 minutes. DDS dissolves instantly above 150°C, with a good processing window.

Temperature (°C)	Dissolution time (min.)	Gelation (min.)	Curing (min.)
70, 90, 110, 130	No progression till 60 minutes		
150	10		
170	30 seconds		
190	30 seconds	32	50
210	30 seconds	19	27
250	Instant	2	5

Table 5.3: Kofler bench test timings - BADGE DDS

To quantify the curing behavior of the curing agents, DSCs were run for theoretical stoichiometric ratios for the curing agents. A plot of 'Heat flow vs temperature' was created as shown in figure 5.7. The rise in heat flow means the absorption of heat or energy by the resin system which leads to dissolution of the curing agent and ring-opening polymerization, which leads to cross-linking and curing. As curing is an exothermic reaction, it leads to a release of energy, and the heat absorbed from the system drops.

The width of the peak defines the kinetics of the reaction and the processing window. The plot for DICY has a sharp peak indicating a fast curing and a short processing window, whereas DDS has a wide peak indicating a slow cure as seen during kofler testing.

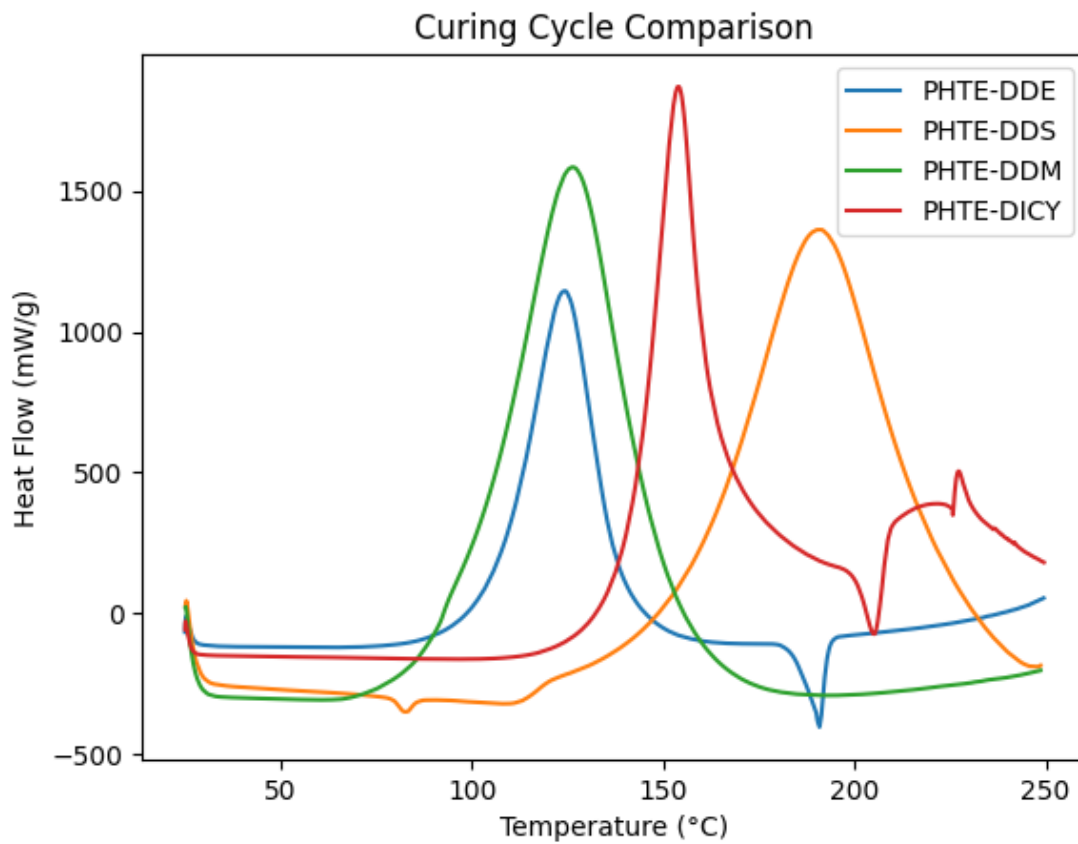


Figure 5.7: Curing cycle DSC plot comparison for curing agents

6

Stoichiometric ratio estimation

Upon finalizing the materials, it is important to study the properties of the resin system as they depend on the epoxy and the curing agent, their nature and functionality, and the extent of their cross-linking. Thus, it is important to study both the epoxy monomers, curing agent, and mix to optimize the ratio to generate fully cross-linked networks and optimize the curing procedure. [30]

The stoichiometric ratio between epoxy resin and curing agents significantly influences its physical and mechanical properties. Theoretically, a crosslinked thermoset polymer structure is obtained when equimolar quantities of resin and hardener are combined. However, in practical applications, epoxy formulations are optimized for performance rather than equimolar quantities which are discussed further. [30]

6.1. Theoretical stoichiometric ratios

As discussed, to generate fully cross-linked networks it is essential to mix the epoxy and the curing agent in the correct or optimum proportion. Each epoxy unit reacts with one terminal hydrogen of the amine. This is defined as the functionality of the monomers.

As PHTE has 3 epoxy groups in its chemical structure, it is a tri-functional monomer whereas BADGE has 2 epoxy groups, thus it is a bi-functional monomer. On the other hand, the curing agent is a diamine and each amine consists of 2 reactive terminal hydrogen units. Thus, it has a functionality of 4.

From this, the theoretical stoichiometric ratios are calculated to be 1.33 for PHTE:DDS and 2:1 for BADGE:DDS. (NOTE - These are molar ratios and need to be converted to mass ratios during mixing.)

6.2. Why is stoichiometric ratio estimation required?

Although the stoichiometric ratios have been calculated as per monomeric structures of the components, it is essential to calculate the actual stoichiometric ratio. This is because during the synthesis of epoxy monomers, the reaction or the product is not purely monomeric and some internal cross-linking is present which leads to what is known as oligomericity or oligomeric products. This drives the overall functionality of the monomer down and thus it is important to estimate the mixing ratio for proper cross-linking, also known as stoichiometric ratio. This reduces the extent of cross-linking and subsequently the properties. Thus, it is essential to optimize the mixing ratio to obtain the highest properties. [38]

6.3. Temperature dependency of polymers

Almost all polymers at room temperature are usually in a solid state. The molecular chains have less energy to travel when they are solid. The polymer starts to expand when heat is applied

because the molecular chains gather energy and can move farther than before. Eventually, when the long structural chains absorb more energy, they have enough energy to flow freely as a viscous fluid, commonly referred to as a melt. The materials harden to maintain their shape as they cool and the energy between the chains contracts because of the chains losing energy. [8]

Almost all materials or polymers undergo a series of thermal events with varying temperatures as shown in figure 6.1. The major two transition temperatures are:

- **Glass transition temperature (T_g)**- The amorphous areas undergo a transition from a stiff to a more flexible state at the glass transition temperature, which causes the temperature to change from a solid to a rubbery state. Glass transition temperature is a property of amorphous materials or the amorphous portion of semi-crystalline materials. The molecular chains of amorphous materials get locked in place and act like solid glass when the surrounding temperature is below T_g . T_g is lower for plastic materials with flexible backbones and higher for plastic materials with stiff, hard, and inflexible molecules. [8]
- **Melting temperature (T_m)**- The melting point is the critical temperature above which the crystalline regions in semi-crystalline plastics can flow. Semi-crystalline polymers begin to soften above T_g , however, they do not demonstrate fluid behavior until the T_m range is achieved. In general, the T_m of a semi-crystalline polymer is higher than its T_g . At temperatures above T_g but below T_m , there is a “rubbery region,” where the material can exhibit large elongations under low loads as shown in figure 6.1. [39]

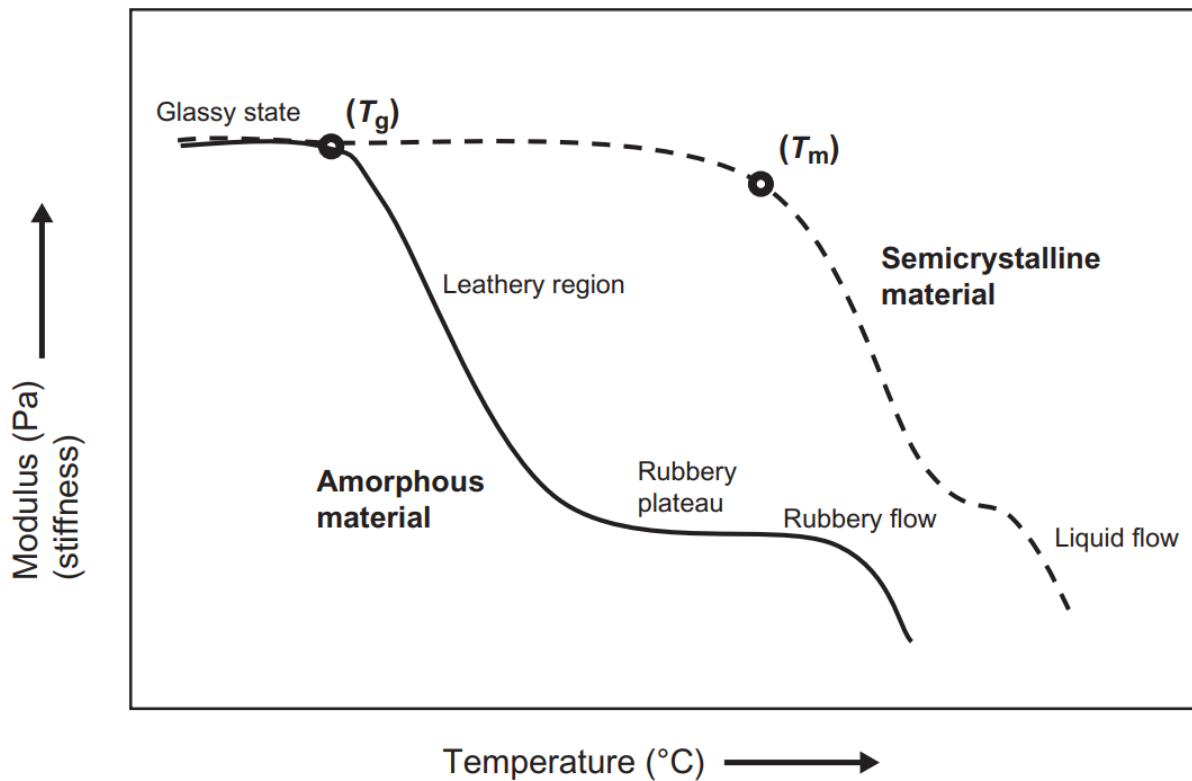


Figure 6.1: Melting and softening behaviour of semicrystalline and amorphous materials [8]

Plastic materials are made up of uneven chain lengths and require different amounts of energy to move, which means that T_g or T_m for amorphous and semi-crystalline polymers is not one definite temperature but a range of temperatures during which all the chains start to move and experience complete flow.

We can see from the figure 6.1 that the usable region for any application is T_g , as the properties plummet immediately after the T_g . The T_g aids in identifying a material's potential flexible and stiff applications. Thus, it is essential to figure out the T_g for our polymers and the stoichiometric ratio by getting the highest T_g while also looking at the behavior of the material with temperature.

6.4. Ratio estimation procedure

As mentioned, to estimate the stoichiometric ratios, T_g optimization was done here. To figure out the T_g of the resin mix, thermal analysis techniques are utilized. Thermal analysis is a set of techniques used to monitor a sample's property over time or temperature while programming the temperature of the sample in a specific atmosphere. They are also used for calculating several other parameters which are discussed later.

There are several thermal analysis techniques which can be used, namely:

- Thermo-gravimetric analysis (TGA)
- Differential scanning calorimetry (DSC)
- Thermo-mechanical analysis (TMA)
- Dynamic mechanical analysis (DMA)

These techniques are discussed along with the experiment results.

6.4.1. Thermo-gravimetric analysis (TGA)

Thermo-gravimetric analysis (TGA) is a method to analyze a material's thermal stability and the amount of volatile components present by monitoring the weight change of a sample as it is heated. The measurement is usually carried out in air, helium, argon, or nitrogen, and the weight is recorded as the temperature increases. The thermo-gravimetric analysis method involves heating a sample in an inert or oxidizing atmosphere while measuring its weight. The weight changes during specific temperature ranges, providing indications of the sample's thermal stability and composition. [40]

TGA is usually the first test while developing a new material, especially polymers. Thermo-gravimetric data is critical to setting proper temperature limits for the development of differential scanning calorimetry testing methods. Other common usages include thermal and oxidative stability of materials, moisture and volatile contents, composition of multi-component materials, decomposition kinetics and estimated lifetime of a product, and effects of reactive or corrosive atmospheres. [41]

Sample testing

From the literature review, a preliminary testing method was prepared. [22][42] This includes taking samples weighing around 10 mg and testing them till 800 °C at a heating rate of 10 °C/min under an airflow of around 20 ml/min.

Figure 6.2 shows the weight change % variation of both the resins with temperature. The PHTE:DDS sample was prepared with the theoretical stoichiometric ratio of 1.33:1 weighing 9.58 mg, and the BADGE:DDS sample with a ratio of 2:1 weighing 9.65 mg.

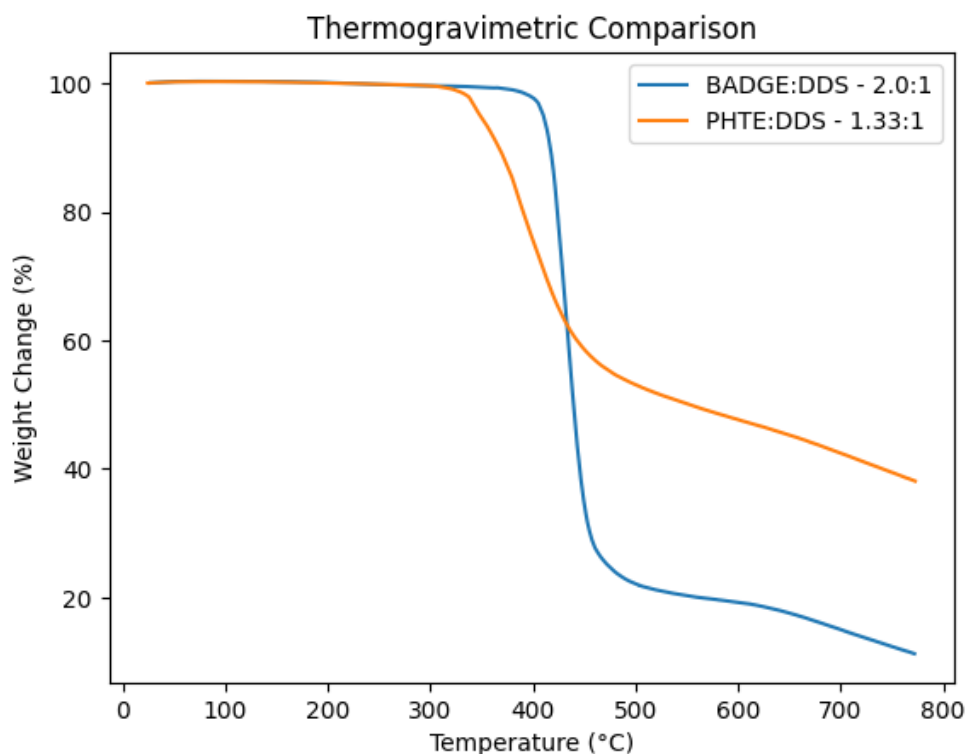


Figure 6.2: Initial thermogravimetry of the resin systems

TGA can be used for a lot of parameters, but the primary aim here was to set an upper limit of temperature for other testing techniques to avoid ruining the equipment. This temperature is taken as the point where the onset of degradation or reduction in weight % initiates, also called the onset temperature. The onset temperature was observed to be 310 °C for PHTE-DDS and 375 °C for BADGE-DDS. To keep a safe window of working temperature for both the resin systems, an upper limit range of 300 °C was taken for all kinds of thermal analysis. This helps to conduct the testing safely and avoid ruining the equipment.

6.4.2. Differential scanning calorimetry (DSC)

DSC is a kind of quantitative differential thermal analysis that consists of a sample and reference whose temperatures are increased, and the difference in the amount of heat required is measured as a function of temperature or time. As these reactions require energy, usually in the form of heat, it is assumed that the degree of cure of the resin can be related to the heat of the reaction. [43]

DSC is an essential characterization technique that enables the measurements of the temperature behavior of the resin and obtains transition points such as the glass transition, melting point, and crystallization. As discussed, the T_g optimization is the initial method used for stoichiometric ratio estimation, which is also commonly used in the industry. [19] The aim is to retrieve these points along with the whole curing to decide on an appropriate curing cycle and times such as pot life, gel time, etc.

Principle

As discussed, when a sample undergoes a physical transformation, such as a phase transition, more or less heat will need to flow to it rather than to the reference (typically an empty sample pan) to maintain the same temperature for both. The amount of heat that must flow to the

sample depends on whether the process is exothermic or endothermic. Usually, it is expected to see major heat exchange occurring at transition points, from which we can estimate the T_g .

Mechanism types

Differential Scanning Calorimetry can be classified into two types, based on the mechanism of operation: [44]

- **Heat flux DSC:** A heat flux DSC consists of a thermoelectric disk placed in a furnace. Two pans are placed on this disk: an empty reference pan and another one consisting of the sample material enclosed in the same material pan. The furnace is heated at a specified heating rate, and the heat is absorbed by both the pans through the thermoelectric disk. The sample pan, consisting of the sample, takes up more heat than the reference pan, due to which there is a temperature difference between both pans, which is measured by the area thermocouples, and the required heat flow to maintain the same temperature is determined by the thermal equivalent of Ohm's law. [45] [44]
- **Power compensated DSC:** A power-compensated DSC consists of separate furnaces with separate heaters. The sample material is enclosed in a pan; it is placed along with the reference pans in separate furnaces, and the same temperature is maintained for both. The sample pan requires greater thermal power for the same temperature, and this thermal power difference is measured and plotted as a function of temperature or time. [45] [44]

Sample preparation

To obtain good data from DSC, proper sample preparation is of critical importance. Sample preparation starts with selecting the correct kind of pans, which are guided by the requirements and type of sample. There are majorly four types of pans available commonly, apart from special-purpose pans:

- Aluminium - Flat aluminium pans
- Aluminium hermetic - Flat aluminium hermetic pans up to 3 atm.
- Tzero aluminium - High-performance flat aluminium pans.
- Tzero hermetic aluminium - High-performance flat aluminium hermetic pans up to 3 atm.

Each sample pan has a set of fixtures for sample preparation. It is important to prepare samples properly and maintain the flat surface of the pans as they might give varying results otherwise. Also, the pans should be handled carefully and not contaminated by touch, as it can alter the test data.

Literature review

A literature review was done to understand the equipment and the parameter requirements for our application. Dinu et. al use a DSC 3 Mettler Toledo apparatus. They ran a mix of uncured formulations in dynamic conditions, from 25 °C to 250 °C at 10 °C/min. They ran two heating and cooling cycles to determine the T_g between 0 and 280 °C at a rate of 10°C/min. The T_g values were reported as the inflection point of the second heating scan of the DSC curves. [22] [18] David et. al used a Mettler DSC3+ 700/970 calorimeter and studied the curing process at 10°C/min from 20 °C to 275 °C. They determined the T_g of these cured samples in dynamic scans at 20 °C/min, from 50 °C to 150 °C. [17]

Testing trial and expected results

As DSC is quite a complex testing technique with a number of parameters to choose from, it is essential to work on these parameters to get the correct data. The first is the mechanism selection; the heat flux DSC was used as that is the equipment available; both methodologies are suitable

for use here. The next selection is the sample pan selection. The aluminum hermetic pans were used to avoid any gas dissipation and keep the samples sealed. After equipment selection, the next step is the cycle parameters.

As mentioned, DSC is being used here for stoichiometric ratio estimation using T_g optimization, so to check DSC data, it was decided to run the T_g cycles for both PHTE and BADGE with DDS at the theoretical stoichiometric ratio. As mentioned before, an upper-temperature limit of 300 °C was obtained from TGA. Thus, it was decided to run the T_g estimation cycle from 25°C to 300°C. A trial was conducted with theoretical stoichiometric ratios of PHTE:DDS at varying heating rates. From the literature review, ASTM Standard D3418 [46] and the equipment Guide specifies a heating rate of 10-20 °C/min and a sample weight of 10-20 mg for T_g estimation.

To decide the heating rate for testing, a T_g estimation cycle with varying heating rates was run to compare the data received. A sample weighing around 10 mg was prepared and run at varying heating rates from 25°C to 300°C. Multiple trials were done for PHTE:DDS as shown in figure 6.3 but no drops were seen to estimate T_g . As discussed in section 6.3, a drop in the graph is expected to estimate T_g . Also, the increase in heat flow seen in the plots after 250-260 °C, indicates a ring-opening polymerization of the phenolic groups. It should be avoided from happening as it would lead to a reduction in strength. As discussed, the aim was to maximize the aromaticity of the structure. Thus, it was decided to keep the processing temperatures below 250 °C to avoid this.

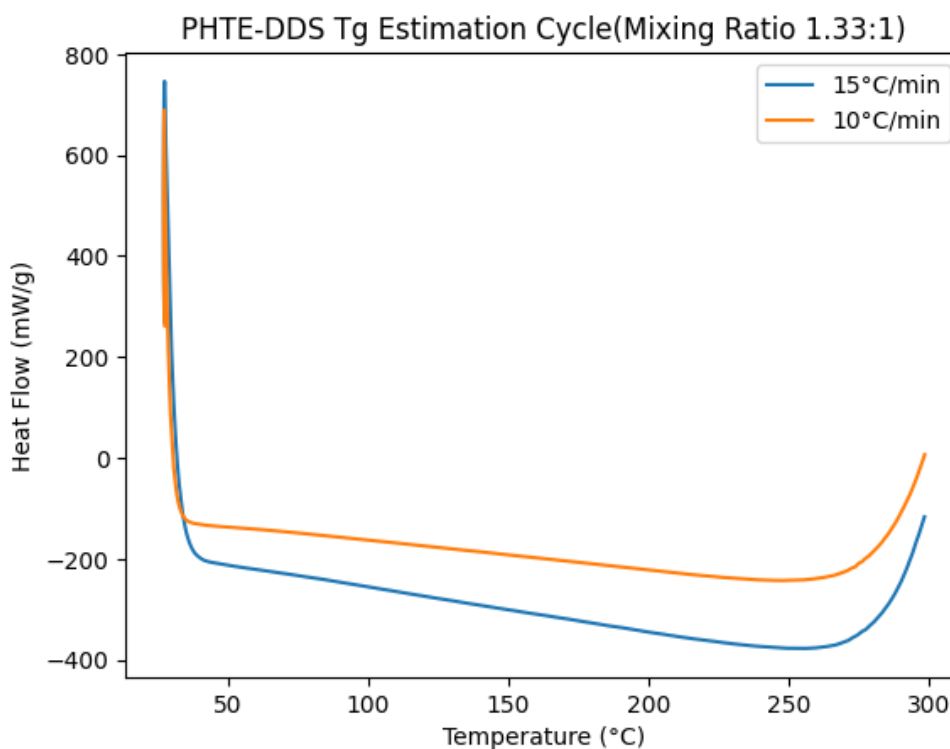


Figure 6.3: PHTE-DDS theoretical stoichiometric ratio DSC at varying heating rates

From the literature, the expected T_g values for BADGE-DDS were to be around 200°C. Thus, it was decided to run a similar cycle as above for the BADGE-DDS sample at heating rates of 10, 15, and 20 °C/min from 25°C to 250°C, avoiding ring-opening polymerization of phenolics as discussed. The results are as shown in figure 6.4.

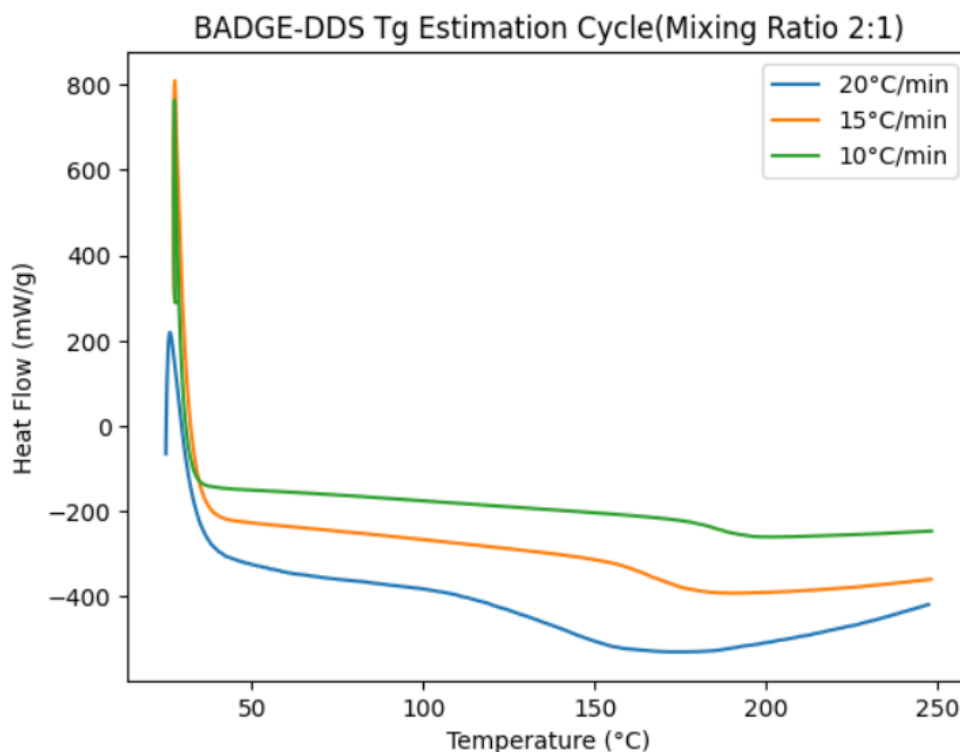


Figure 6.4: BADGE-DDS theoretical stoichiometric ratio DSC at varying heating rates

As can be inferred from the DSC data of PHTE-DDS in figure 6.3 no drops were received, and it was not possible to estimate T_g from the DSC for PHTE whereas BADGE-DDS graphs in figure 6.4 gave good drops for T_g estimation. As in the PHTE-DDS sample, the monomers are bulky, a more sensitive technique would be required for T_g estimation. Out of the available thermal analytical techniques, DSC, TMA, and DMA can be used for T_g estimation. DSC is the primary choice, but TMA is more sensitive, and DMA is the most sensitive technique available.

Thus, DSC was eliminated as the method to be used for stoichiometric ratio estimation of PHTE:DDS. So, BADGE:DDS stoichiometric ratio will be estimated using DSC as discussed here and other techniques will be attempted for PHTE:DDS further on.

Testing methodology

To finalize the testing methodology, it is essential to finalize the heating rate to be used. To interpret the data from the graphs properly, an understanding of the glass transition temperature is important. A T_g , while being a specific temperature, is not a definite temperature for a material, and it varies greatly with the chemical structure of the material as well as its thermal history. There are a lot of different points on the drop of the graph that can be considered as T_g such as the inflection point, midpoint, etc. A general practice in the industry is to take the inflection point as the T_g .

After developing an understanding of the expected results and T_g point, the BADGE-DDS DSC data in figure 6.4 is analyzed. To get an accurate T_g , a curve that has a sharp drop in a short temperature range is preferable; thus, a heating rate of 10°C/min was finalized. An appropriate heating rate selection is essential, as a low heating rate would not give a sharp drop in the graph as the bonds would have greater time for relaxation or movement, whereas a higher heating rate would miss the drop altogether.

6.5. BADGE:DDS - Stoichiometric ratio estimation

After finalizing all the parameters of DSC, the stoichiometric ratio estimation of BADGE-DDS was attempted. As mentioned before, the theoretical ratio should be 2:1. As BADGE is a fairly commercial monomer, a molecular weight of 340.41 g/mol was given by the supplier. From a theoretical molecular weight of 348 g/mol, a stoichiometric ratio of 2.06 was calculated for BADGE:DDS.

Although ratios can be calculated from the molecular weight, still it was decided to run DSCs for BADGE:DDS to check this. As the epoxy is the part of the mix that will show oligomericity, a slightly higher quantity of the epoxy will be required, which is BADGE in this case as also seen from the previous calculation. As it is difficult to assess the oligomericity, it was decided to split this study into 2 steps. It was decided to study the molar ratios with a difference of 0.1 first, and then study the five ratios around the optimum ratio from this study with a difference of 0.2 in the second study.

Thus, for the first stoichiometric study, it was decided to assess five ratios of BADGE-DDS, which consist of the theoretical ratio 2:1, one ratio on the lower side just for the whole spectrum, thus 1.9:1, and the remaining three above the stoichiometric ratio, thus 2.1, 2.2, and 2.3. Figure 6.5a shows the plots for the 5 molar ratios run at a 10 °C/min heating rate from 25°C to 250°C. Table 6.1 shows the inflection or onset point temperatures for all 5 molar ratios in figure 6.5a. As can be inferred, the highest T_g was received for 2.1.

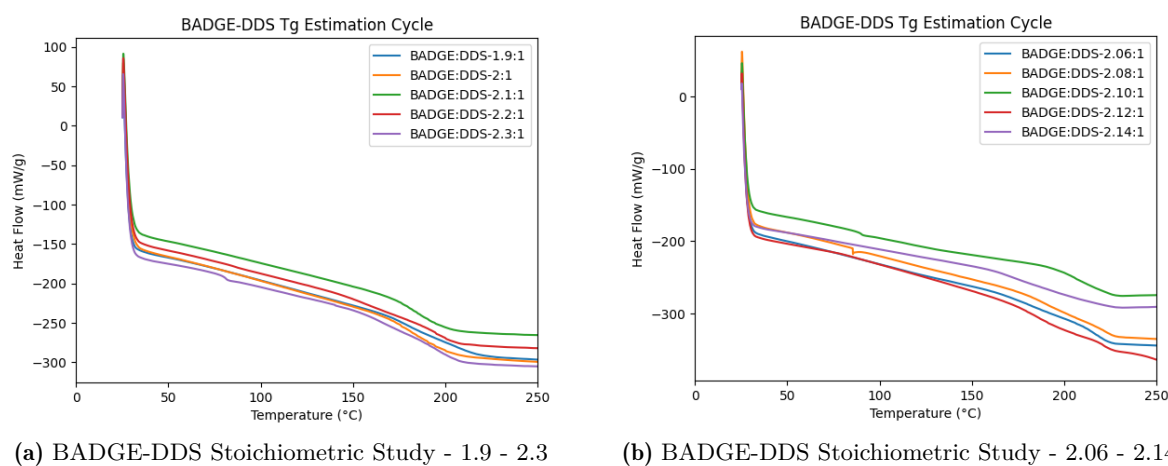


Figure 6.5: DSC plots for BADGE:DDS Stoichiometric Ratio Estimation

Molar Ratio	1.9	2	2.1	2.2	2.3
Onset Temperature (°C)	166.67	166.83	169.79	167.41	162.65

Table 6.1: BADGE-DDS Inflection temperatures at different molar ratios

To finalize the second digit of the stoichiometric ratio, five ratios with 2.1 as the mid-point were prepared. Thus, a second DSC study with ratios of 2.06, 2.08, 2.10, 2.12, and 2.14 was run similarly at a 10 °C/min heating rate from 25°C to 300°C, and the figure 6.5b shows the DSC graphs for these ratios.

Molar Ratio	2.06	2.08	2.10	2.12	2.14
Onset Temperature (°C)	191	191.41	194.1	171.14	161.97

Table 6.2: BADGE-DDS Inflection temperatures at different molar ratios

Table 6.2 shows the inflection or onset point temperatures for all 5 molar ratios in figure 6.5b. This study yielded inconsistent data, which could be attributed to a solid curing agent being dispersed inconsistently in the sample pan or variation in curing agent due to small quantities. This variation would in turn lead to a variation, especially with ratios as close. Thus, it was decided to move with the ratio calculated from the data provided by the supplier. Thus, 2.06:1 is the mixing ratio that will be used for BADGE:DDS in the study.

6.6. Continued ratio estimation procedure

The main task here was to estimate the stoichiometric ratio of PHTE:DDS. No data was received for PHTE from the supplier. Multiple trials had to be done which have been discussed in this section. As discussed earlier, DSC gave no results for PHTE and the next more sensitive technique that can be used is TMA (Thermo-mechanical analysis) which was tried for PHTE but no suitable results were seen as well. Thus it was decided to move on to DMA for PHTE:DDS ratios.

6.6.1. Dynamic mechanical analysis (DMA)

DMA is a visco-elasticity measurement technique that analyzes a sample's elastic and viscous response by measuring stress or strain under the application of a constant oscillating load and monitored against temperature, time, or frequency. [47]

Principle

As mentioned in DSC, materials undergo phase transitions with temperature. All materials undergo transitions as shown in figure 6.1, including elastic behavior or a glassy state at low temperatures and viscous behavior or a rubbery flow at higher temperatures. As this behavior can be better studied due to its mechanical phenomenon, DMA is more sensitive and can be used for T_g estimation for this case. DMA measures the changes in these molecular motions and the transitions in molecular structures, such as relaxation, crystallization, and curing reactions. [48]

DMA measures three visco-elastic properties, namely:

- **Storage modulus:** E' , G' (purely elastic component)
- **Loss modulus:** E'' , G'' (purely viscous component)
- **Loss tangent:** $\tan\delta$ ($= E''/E'$),

Testing modes

As DMA consists of studying the behavior of a sample against temperature, time, or frequency, the testing modes can be classified primarily into two modes:

- **Temperature sweep:** In a temperature sweep DMA, a sample is analyzed for a range of constantly varying temperatures at a constant frequency. This gives an operating temperature limit or operating range of temperature.
- **Frequency sweep:** In a frequency sweep DMA, a sample is analyzed for a range of frequencies at a constant temperature for a specified time. This gives a resonant frequency for the material or the operating range of frequency.

Types of fixtures

As DMA is a thermo-mechanical testing technique, the type of fixture is essential before finalizing the sample geometry. Various kinds of fixtures can be used to run DMA, namely:

- Tension/compression
- Simple shear
- Single cantilever bending
- Dual cantilever bending
- 3-point Bending

Literature review

As there are a lot of parameters to select from, a literature review was conducted. Dinu et al. carried out DMA with a Mettler Toledo DMA 1 using a three-point bending fixture. They ran a temperature sweep from -70 to 400 °C at a heating rate of 3 °C/min with a constant oscillation frequency of 1.0 Hz and a 20 μ m amplitude. [18] [23] Genua et al. investigated the thermo-mechanical behavior of the samples using a Mettler Toledo DMA 1 apparatus using a three-point bending clamp. They ran a temperature sweep from -50 °C to 280 °C at a heating rate of 3 °C/min with a constant 1.0 Hz oscillating stress and 20 μ m amplitude. [19]

Specimen geometry

From the literature review and ASTM standard D5023, a three-point bending fixture was finalized for analyzing the samples. Before other parameters of the test can be finalized, it was important to finalize the specimen geometry and manufacturing methods to prepare specimens for testing. The ASTM standard recommends a minimum L/t (length to thickness or depth) ratio of 16 along with 10% or a minimum 6.4mm overhang on each side. [49] The first restricting dimension is length, as the heater on the equipment could accommodate a sample of a maximum of 55 mm. Thus, a maximum of 2.6 mm-thick sample could be used keeping the L/t ratio to be 16. To keep the samples a bit shorter, a thickness of 2 mm was selected. This gave a required length of 32 mm. Adding an overhang of 6.4 mm on each side, a sample length of 45 mm was received. With the available mold design to accommodate 5 samples, a width of 9 mm could be achieved. As the width is accounted for by the software it can be any value below the width of the supports, which is 15 mm. Thus, the final sample size was 45 x 9 x 2 mm. Furthermore, the available supports were of a span of 10, 25, and 40 mm. As the usable length is 32 mm, the 25 mm span support was selected.

Mould design and sample preparation

After finalizing the specimen geometry, a good mold design is essential to preparing good-quality samples with a good surface finish to achieve consistent results. Multiple concepts were worked on, and a sandwich mold was finalized to allow a good surface finish while keeping the design relatively simple. This was also done keeping in mind the high viscosity of the resin, high-temperature curing, eliminating leaks, and having good and straight samples. To achieve a good surface, a vertical mold was designed to minimize uneven top surfaces.

As can be seen from the figure 6.6, the mold consists of two outer blocks made out of aluminum with bolt holes at constant distances and a funnel-shaped top for easy pouring. The center plate was machined out of steel, as the coefficient of thermal expansion is half that of aluminum and the hardness is way higher. This ensures consistent sample dimensions and negligible or lower mold damage with each use. This modular mold concept also gives you the freedom to change the center plate for multiple sample sizes. As mentioned before, the center plate can manufacture five different samples. The length was kept such that two samples of each type could be manufactured at a time to allow for proper testing.

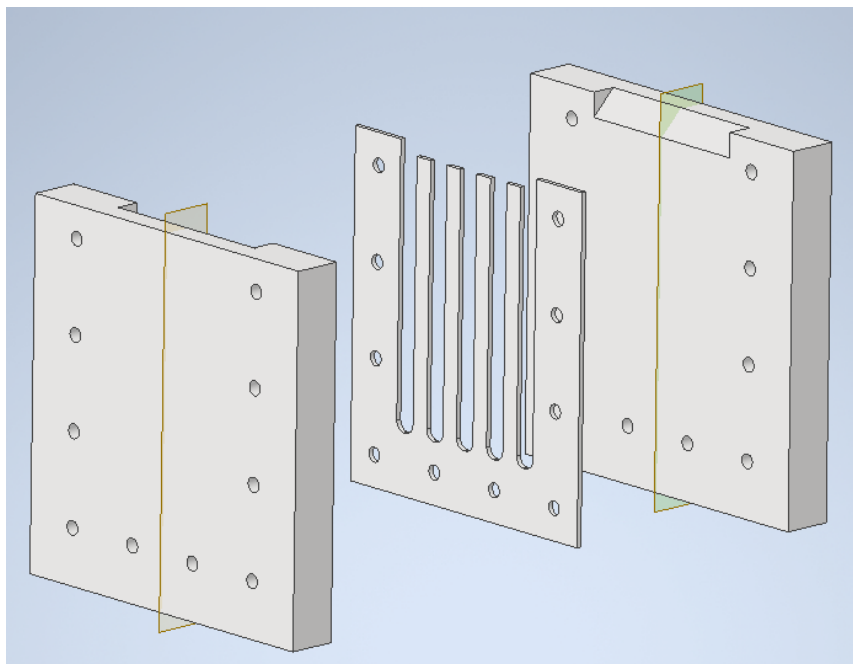


Figure 6.6: Mould design for DMA samples

Initial mould trials

After finalizing and getting the mold machined, samples were prepared. The theoretical stoichiometric ratio for PHTE:DDS is 1.33:1. As discussed for BADGE, PHTE is also oligomeric, and molar ratios 1.4, 1.5 to 1.8 were considered for the study. These molar ratios were prepared in weighing boats and placed in the degassing chamber for 30 minutes as shown in figure 6.7

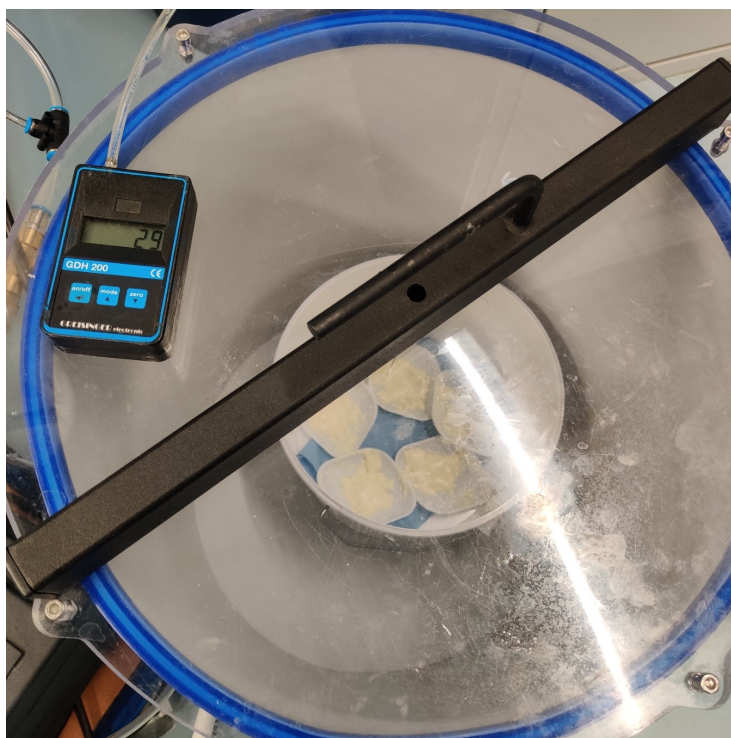
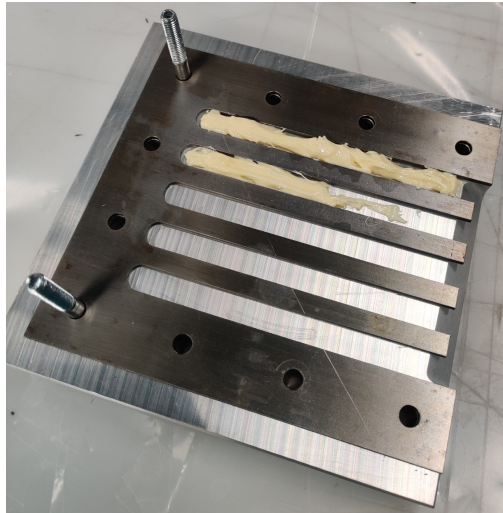
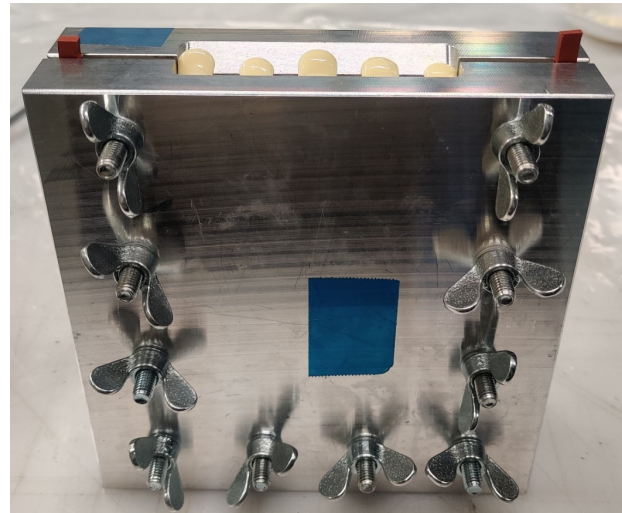


Figure 6.7: Weighing Boats with PHTE-DDS molar ratios in degassing chamber

After degassing, the resin needs to be applied to the mold as the resin is too viscous. The mold was prepared beforehand with a release agent, Marbocote 227. 4 layers were applied liberally on all internal surfaces with a 5-minute gap between each application to allow the release agent to dry and form a layer. Figure 6.8a shows the resin being applied to the mold and figure 6.8b shows the closed mold after resin application with excess resin oozing out of all the partitions.



(a) Resin being applied to the mould



(b) Closed mould with excess resin coming out

Figure 6.8: Initial molding trials for PHTE-DDS

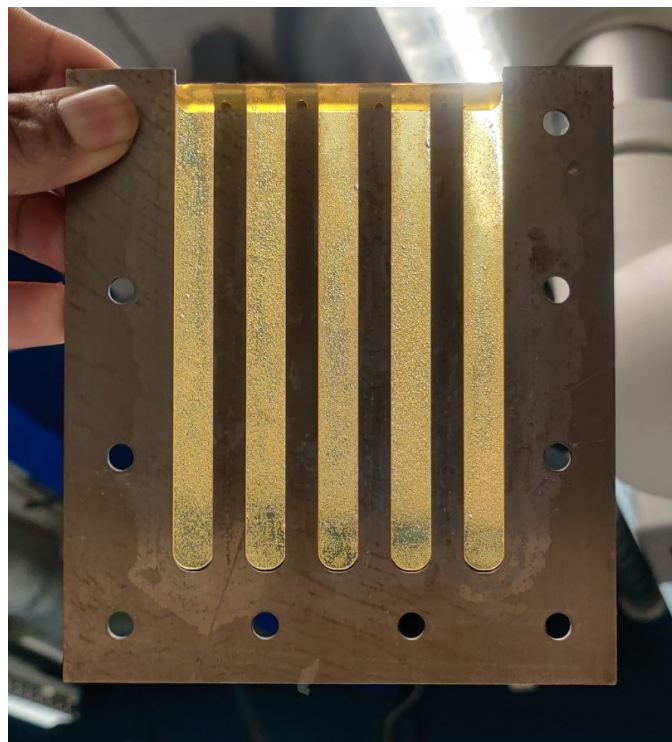


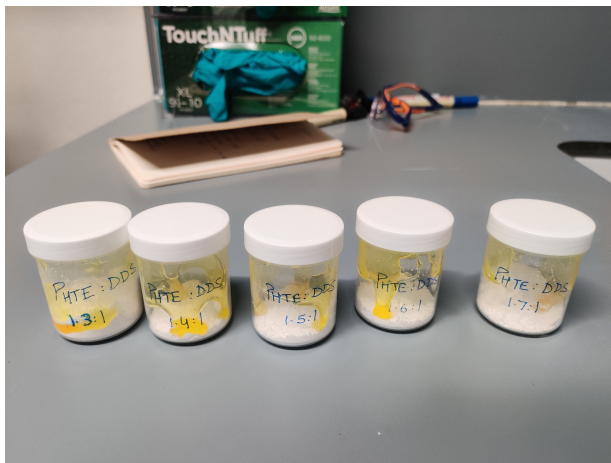
Figure 6.9: Cured PHTE-DDS samples with bubbles

After the preparation of the mold with the resin, it was essential to finalize an appropriate

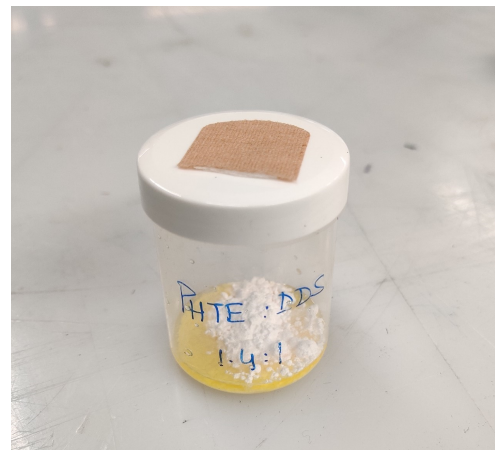
curing cycle. From the kofler bench results and initial DSCs of PHTE-DDS, a curing cycle was finalized. The temperature was raised to 100 °C at a rate of 5 °C/min and maintained at 100 °C for 30 minutes to allow the mold to gain temperature, the resin lowered in viscosity, and filled the gaps in the mold. The temperature was then raised to 180 °C at a rate of 5 °C/min and then maintained at 180 °C for 2 hours. Then it was cooled down to 25 °C at a rate of 5 °C/min. The samples are taken out of the mold and figure 6.9 shows the cured samples. The samples were full of air bubbles, and a need to improve this process was identified.

Process improvement

As PHTE has a high viscosity and DDS is a fine powder-like solid, it was difficult to mix them properly and homogeneously. It is difficult to handle PHTE as it is sticky and it takes 15-20 minutes to mix and prepare a resin sample. Thus, a better workflow was essential to handle PHTE. From the Kofler bench results, it can be inferred that PHTE lowers in viscosity near 50–60 °C, enabling better working. After multiple trials, a mixing method was generated. PHTE and DDS were put in a polypropylene container as in figure 6.10a and placed in an oven at 60 °C for 10–15 minutes. This temperature also cannot be exceeded, as the PP containers can handle a temperature of around 70 °C. Once the containers are heated, all the resin on the sidewalls, if any, drops to the bottom as in figure 6.10b. A hole is made in the cap of the container and a bandage is applied to allow air to pass through during degassing.



(a) PHTE-DDS resin mix in PP containers

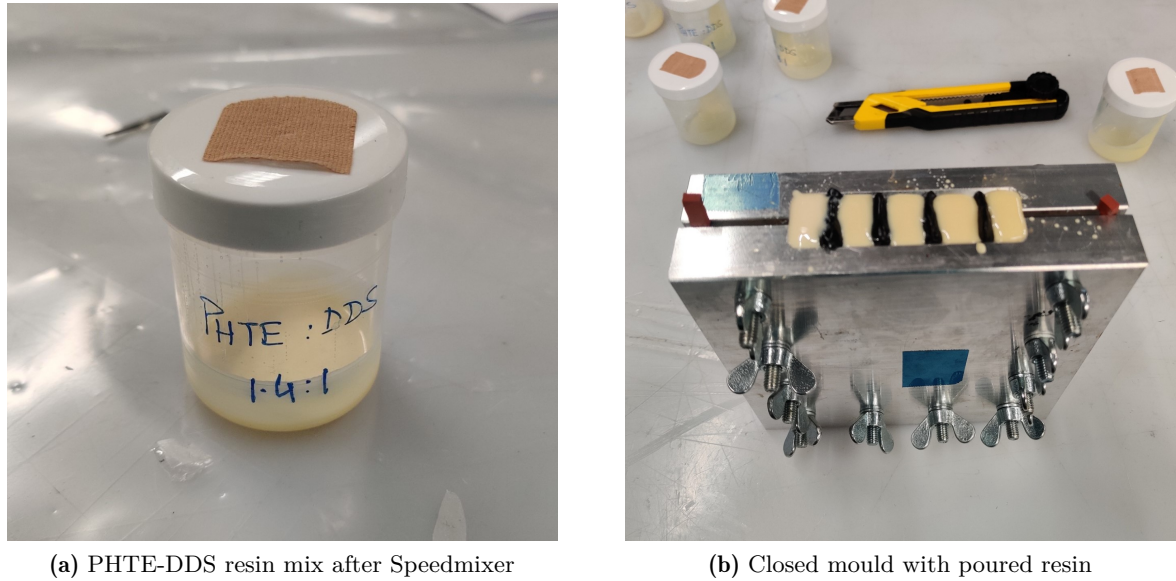


(b) PP container before Speedmixer

Figure 6.10: Resin preparation in Polypropylene Containers

The heated containers are put in a speed mixer and run at 2300 RPM for 5 minutes under a vacuum of 40 mBar pressure. This leads to a homogenous, degassed PHTE-DDS mix as in figure 6.11a.

After the mixing, the containers are again placed in the oven at 60 °C for 10–15 minutes. The resin lowers in viscosity making it easier to handle. Now, the resin can be poured into the mold for curing. To facilitate the pouring of multiple resin mixes simultaneously, the sample slots are separated by placing a kind of putty or sealant tape in between. As the viscosity is still high, the resin does not go inside the mold and fills the top as in figure 6.11b. The mold is placed in an oven at 100 °C for 30 minutes; this allows the resin to drop into the mold, and this process can be repeated until the resin fills the internal slots.



(a) PHTE-DDS resin mix after Speedmixer

(b) Closed mould with poured resin

Figure 6.11: Resin preparation in Polypropylene Containers

After the mold was prepared, the same curing cycle mentioned before was run. The samples are taken out of the mold, and figure 6.12 shows the cured samples. As can be seen, the samples were free of any bubbles, and the surface finish was also good.

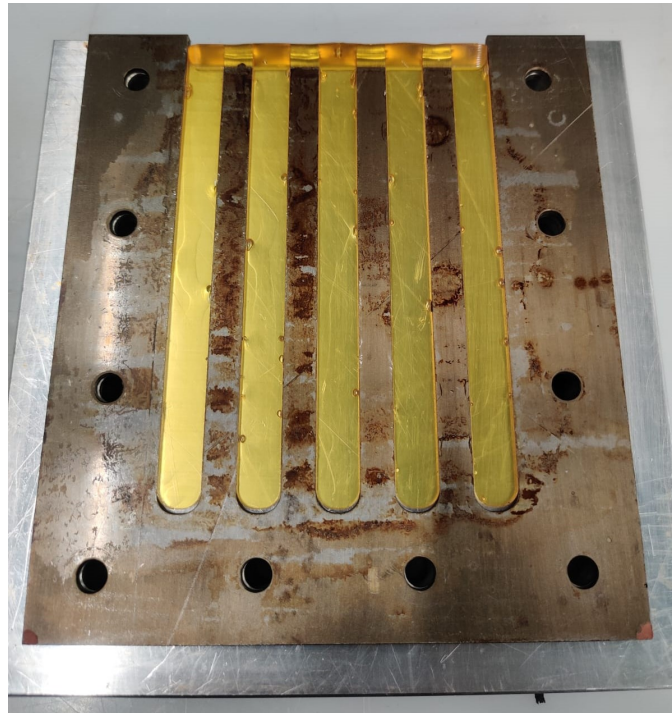


Figure 6.12: Final Cured PHTE-DDS samples

These samples were then cut using a rotary cutting machine and the ends are sanded for a smooth finish to a size of 45 x 9 x 2 mm.

Initial DMA trials and testing methodology

After preparing the samples, it was essential to finalize the testing parameters for DMA. A frequency sweep from 0.01 Hz to 100 Hz was run on a sample to understand the behavior of the samples with frequency and to figure out a frequency for the temperature sweep as shown in figure 6.13. It is important to test at a frequency where the sample has flat or consistent results. The data showed a flat graph from 0.1 Hz to 10 Hz as in the figure. From the literature review and frequency sweep, 1.0 Hz oscillating stress and 20 μm amplitude were selected.

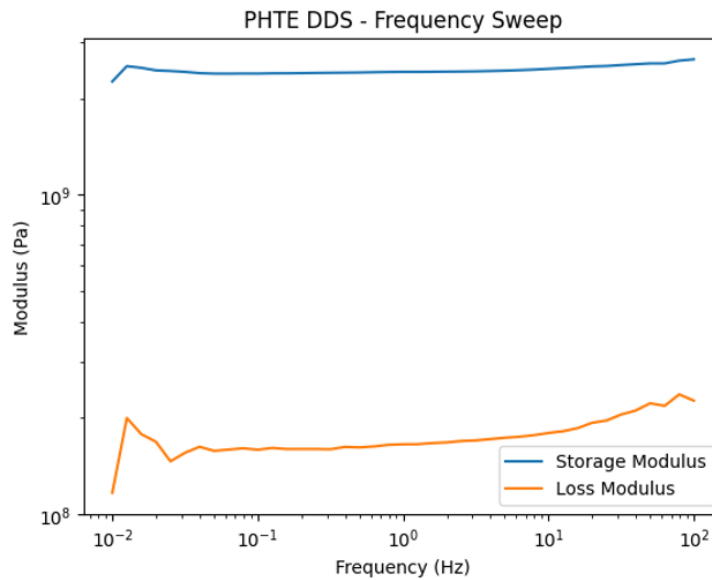


Figure 6.13: DMA PHTE-DDS Frequency Sweep

6.7. PHTE:DDS stoichiometric ratio estimation

After preparing defect-free samples and finalizing all the parameters for DMA, the samples were then tested with the parameters selected. Figure 6.14a shows the storage modulus (marked by S) and loss modulus (marked by L) data for the stoichiometric ratios 1.4 to 1.8. Similarly, figure 6.14b shows the $\tan\delta$ data for the stoichiometric ratios 1.4 to 1.8.

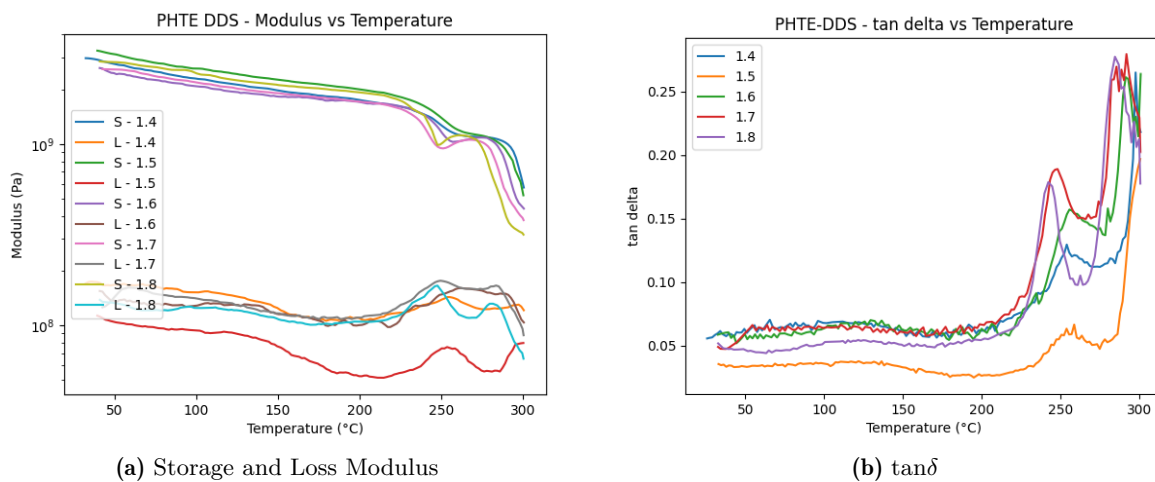


Figure 6.14: PHTE-DDS 1st stoichiometric DMA data

Multiple points can be regarded as the T_g in DMA but the onset inflection point of the storage modulus plots was taken as the T_g here which is also commonly used in the industry. Storage modulus represents the elastic solid behavior of a material and as discussed before, the material transitions from a glassy state to a rubbery state with temperature. Thus, taking the inflection point of the storage modulus is done as this maximizes the temperature at which the material can sustain its properties reliably. Figure 6.15 shows the storage modulus data for the stoichiometric mixes.

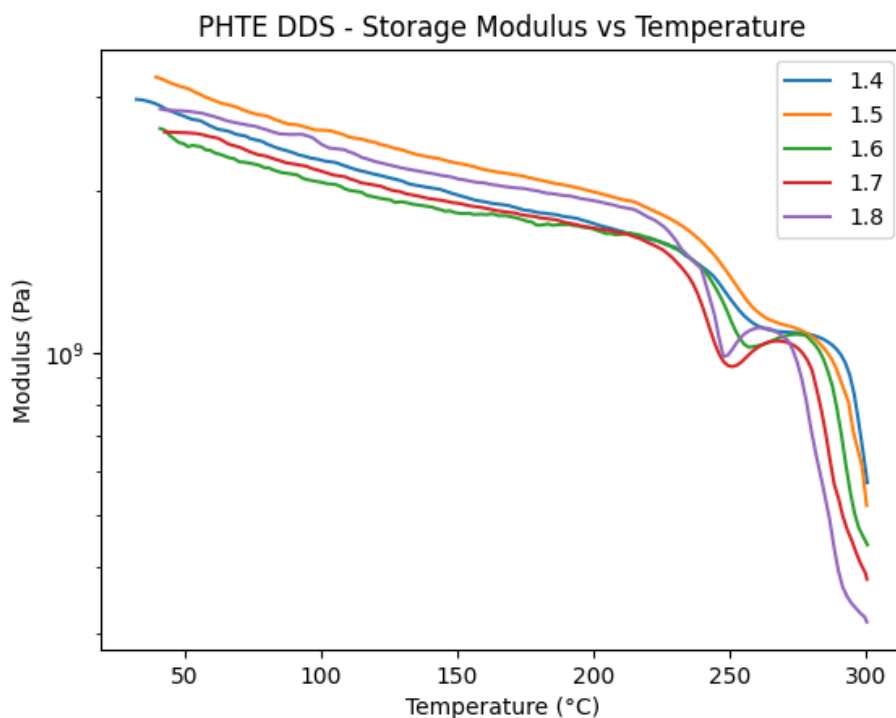


Figure 6.15: PHTE-DDS Storage modulus data for molar ratios 1.4-1.8

Table 6.3 shows the onset inflection point temperatures for the five stoichiometric molar ratios. As can be inferred, the highest T_g was received for the molar ratio of 1.5. The highest modulus was also seen for 1.5, which indicates the maximum cross-linking out of all resin mixes as the appropriate ratio will lead to the most cross-linking and highest properties.

Molar Ratio	1.4	1.5	1.6	1.7	1.8
Onset Temperature (°C)	232	235	234	231	230

Table 6.3: PHTE-DDS Inflection temperatures at different molar ratios

Post curing

The multiple drops in the DMA data indicate that the curing is not complete for the samples and post-curing might be required. To assess the post-curing temperature, five samples with a 1.5 molar ratio were prepared using the same curing cycle and then put for post-curing at varying temperatures from 200 °C to 240 °C for 30 minutes each and tested using DMA. Figure 6.16 shows the samples after post-curing, as can be seen the sample post-cured at 240 °C changed color to a dark black, which was considered to be degradation as seen in all the samples after DMA.

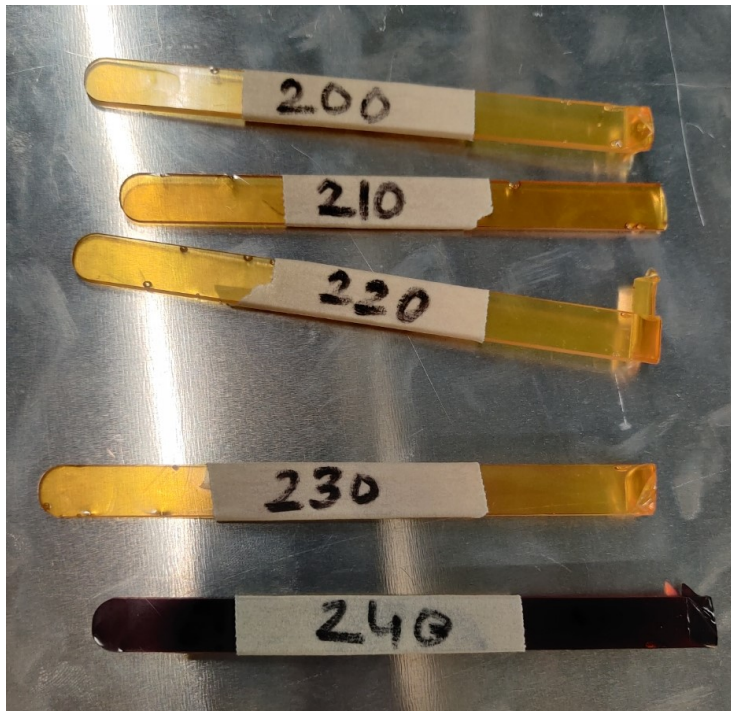


Figure 6.16: DMA samples post-cured at multiple temperatures

Figure 6.17 shows the DMA data for the post-cured samples. As can be inferred, all samples removed the double peak behavior. To ensure proper curing, a 210 °C post-curing was introduced in the curing cycle. Also, the 240 °C sample gave similar results as compared to the other samples, indicating that color changing to a darker shade here does not mean degradation, as opposed to what was thought initially.

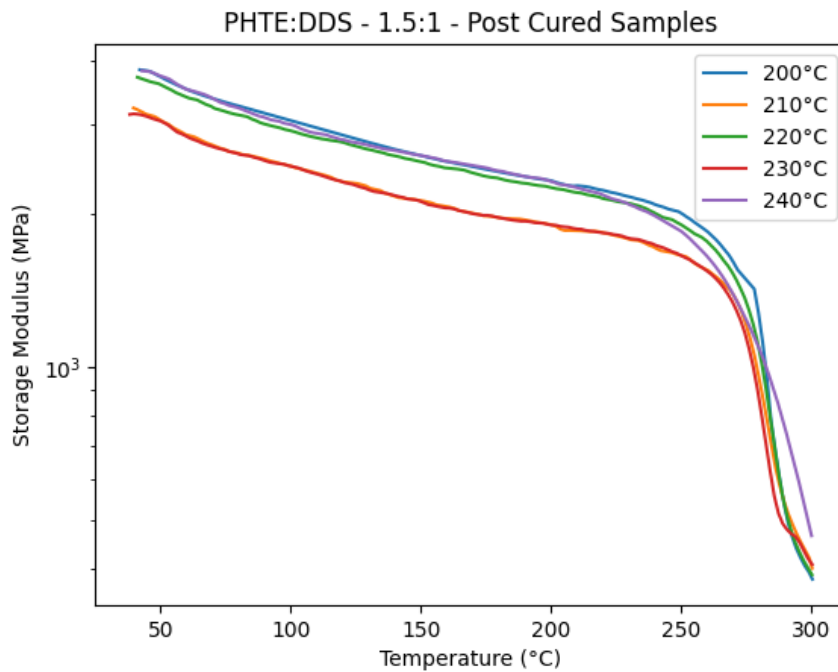


Figure 6.17: Storage modulus data for post-cured PHTE samples

Final stoichiometric ratio estimation

After finalizing the first stoichiometric ratio at 1.5 and introducing post-curing at 210 °C in the curing cycle, the estimation of the second decimal of the stoichiometric ratio was conducted. Five samples were prepared with molar ratios 1.46, 1.48 to 1.54 using the finalized technique. Figure 6.18 shows the DMA data for these five samples.

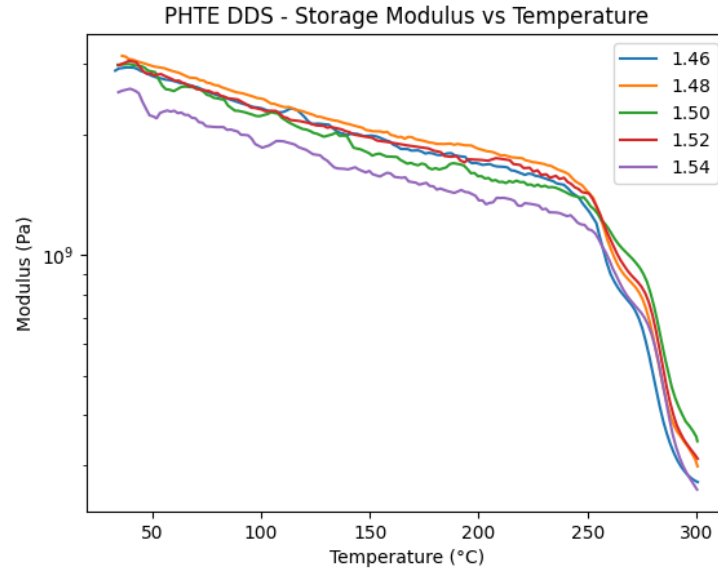


Figure 6.18: PHTE-DDS 2nd Stoichiometric with 210 °C post-curing

As can be seen from the figure, these samples still show double drop behavior as in the first study. Thus, it was decided to prepare a second set of samples with a 220 °C post-cure. As can be seen from figure 6.19, this post-cure temperature works and receives a final stoichiometric ratio of 1.52.

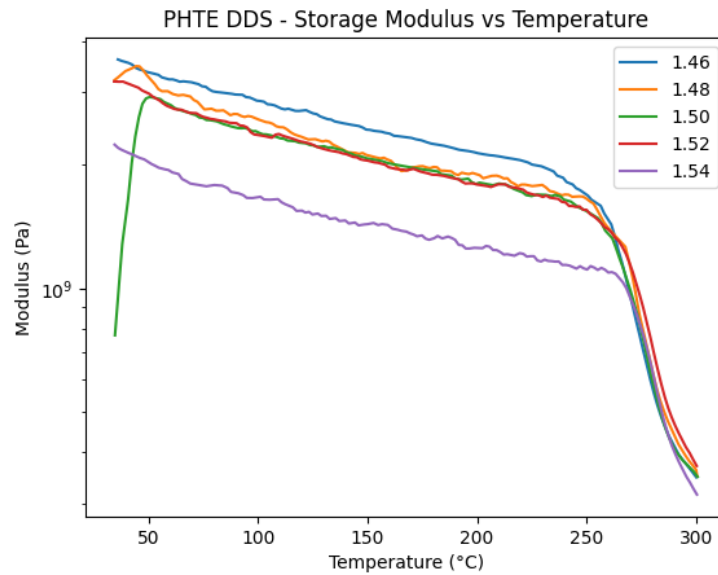


Figure 6.19: PHTE-DDS 2nd Stoichiometric with 220 °C post-curing

Molar Ratio	Onset Temperature (°C)	
	210 °C	220 °C
1.46	259.5	255
1.48	262.7	258.5
1.50	268.5	260.5
1.52	269.0	267.2
1.54	264	264

Table 6.4: PHTE-DDS 2nd stoichiometric inflection temperatures

Table 6.4 shows the onset inflection temperatures for the 2nd stoichiometric ratios at two different post-cure temperatures, 210 °C and 220 °C. It can be seen that the highest T_g was received for 1.52. Thus, 1.52 was finalized as the stoichiometric ratio for PHTE-DDS and will be used further in the study.

7

Resin characterization

After determining the stoichiometric ratios of both PHTE and BADGE with DDS, it is essential to study the resin and characterize it. The following methods can study the physicochemical and thermo-mechanical properties of the developed thermosets [19]:

- **Thermal analysis**
 1. Thermo-gravimetric analysis (TGA)
 2. Differential scanning calorimetry (DSC)
 3. Thermo-mechanical analysis (TMA)
 4. Dynamic mechanical analysis (DMA)
 5. Dynamic rheometry
- **Physical characterization**
 1. Water contact angle
 2. Water absorption test
 3. Gel content
 4. Bio-based content (BCC)
- **Mechanical analysis**
 1. Density
 2. Tensile test
 3. Flexural test
 4. Fracture toughness: Single edge notched bend

7.1. Thermal analysis

The first kind of comparison was done using thermal analysis. All polymers change behavior with temperature and to ensure optimum performance for the whole temperature range, these techniques are essential.

7.1.1. Thermal behavior - Thermo-gravimetric analysis (TGA)

In the context of thermal analysis, it is essential to study the thermal behavior of both resin systems, which was done here using TGA. Although TGA has already been discussed and run for both epoxy monomers, it is essential to run TGA for the actual stoichiometric mixes to get the correct operating temperature range and thermal stability of the epoxies.

The same procedure as before was followed. Samples weighing around 10 mg and tested until 900 °C at a heating rate of 10 °C/min under a constant airflow of around 20 ml/min. The $T_{5\%}$ and $T_{50\%}$ were calculated and marked on the data received. Figure 7.1 shows the behavior of the PHTE-DDS sample, and Figure 7.2 shows the behavior of the BADGE-DDS sample upon heating.

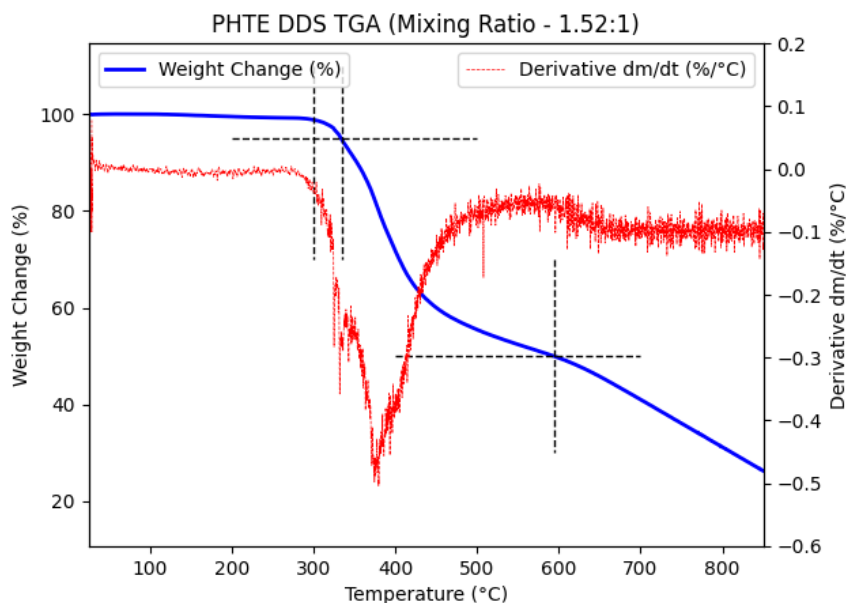


Figure 7.1: TGA PHTE-DDS with $T_{5\%}$ and $T_{50\%}$ marked

Figure 7.1 shows the TGA for a PHTE-DDS sample mixed in a stoichiometric ratio of 1.52:1. The sample weighed 12.95 mg. The blue curve shows the weight change percentage of the sample with temperature, and the red dashed line shows the derivative of the weight change or variation of weight for every temperature change. The dashed black lines mark the relevant transition temperatures, as mentioned in table 7.1.

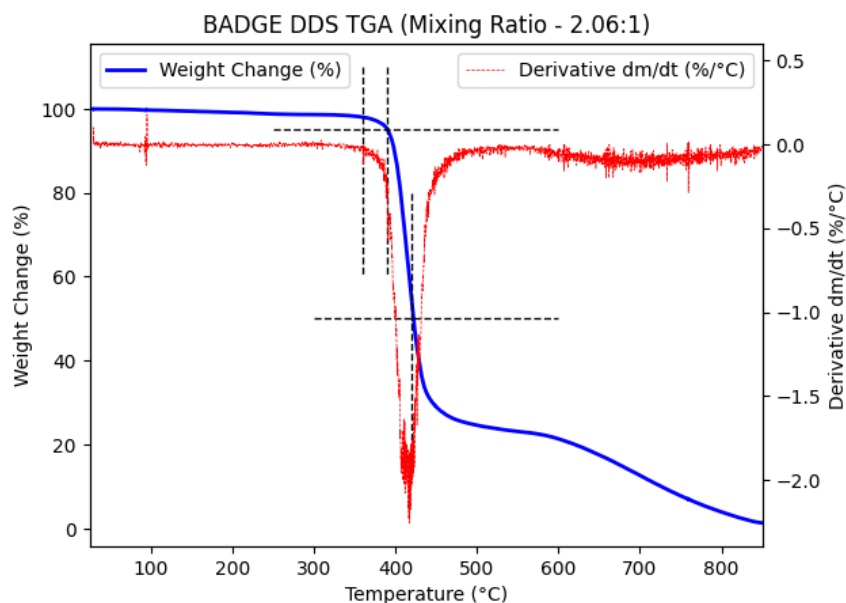


Figure 7.2: TGA BADGE-DDS with $T_{5\%}$ and $T_{50\%}$ marked

Similarly, Figure 7.2 shows the TGA for a BADGE-DDS sample mixed in the actual stoichiometric ratio of 2.06:1. The sample weighed 9.35 mg.

Resin Mix	T_{Onset} (°C)	$T_{5\%}$ (°C)	$T_{50\%}$ (°C)	Max dm/dt (°C)	Residual Mass (at 850 °C)
PHTE-DDS (1.52:1)	310	348	551	390	26.22%
BADGE-DDS (2.06:1)	360	390	420	417	1.30%

Table 7.1: Final TGA Data

As can be inferred from table 7.1, BADGE:DDS has greater thermal stability as compared to PHTE:DDS, but BADGE degrades rapidly once it surpasses $T_{5\%}$ as can be seen in figure 7.3. Also, the residual mass or char yield is higher in PHTE as compared to BADGE which is preferable as we do not want our resin to just disappear or act as more fuel, thus leading to a bigger fire in case of an incident.

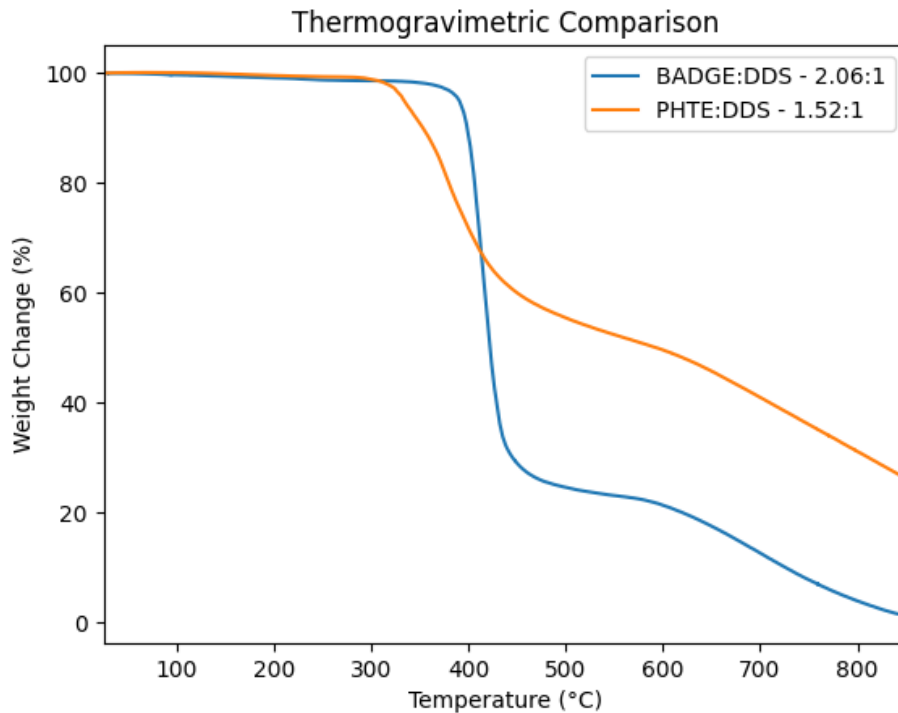


Figure 7.3: Difference in thermal behavior of both resin systems

7.1.2. Activation energy - Differential scanning calorimetry (DSC)

After understanding the thermal stability of both resins, understanding the activation energies required for the reaction of both resins is important. The minimum amount of energy required for the activation of atoms or molecules for them to undergo chemical transformation or physical transport is called activation energy. From the point of view of global warming, this parameter is essential, as a minor change in this value will affect energy usage, especially for large parts.

Kissinger model

The Kissinger model is a commonly used model that was employed to calculate the activation energy of the curing reaction here, which is:

$$E = -R \frac{dl \frac{\beta}{T_p^2}}{dT_p^{-1}}$$

Where:

- R: gas constant is taken as $8.3145 \text{ Jmol}^{-1}\text{K}^{-1}$
- β : heating rate
- T_p : the temperature corresponding to the position of the rate peak maximum

Parameters from DSC

As can be seen from the model, it required the peak temperatures at varying heating rates. Thus, DSC tests were carried out at varying heating rates ranging from 2.5 to 10 °C/min for both the resins over a temperature range from 25°C to 300°C, utilizing various heating rates ranging from 2.5 to 10 °C/min.

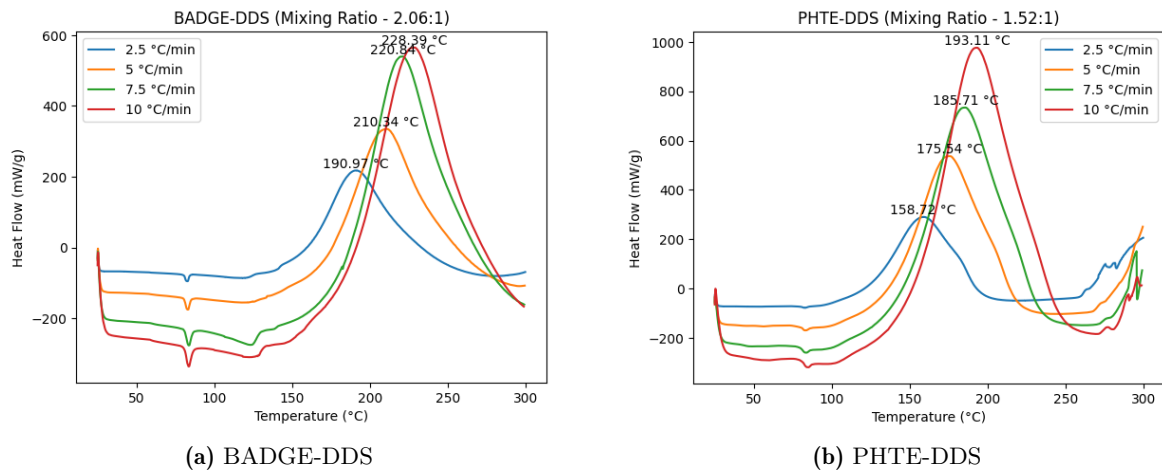


Figure 7.4: DSC data at varying heating rates for both resin systems

Figure 7.4 shows the DSC data for multiple heating rates for both resin systems. The peak temperatures are listed in table 7.2, which were used later for activation energy estimation.

(Heating Rate)	Peak Temperature (T_p)	Peak Temperature (T_p)
(°C/min)	BADGE-DDS (°C)	PHTE-DDS (°C)
2.5	190.97	158.72
5	210.34	175.54
7.5	220.84	185.71
10	228.39	193.11

Table 7.2: Peak temperatures for both resins at varying heating rates

Model fitting

Once the parameters have been estimated, model fitting is done for both resin systems as in figures 7.5a and 7.5b.

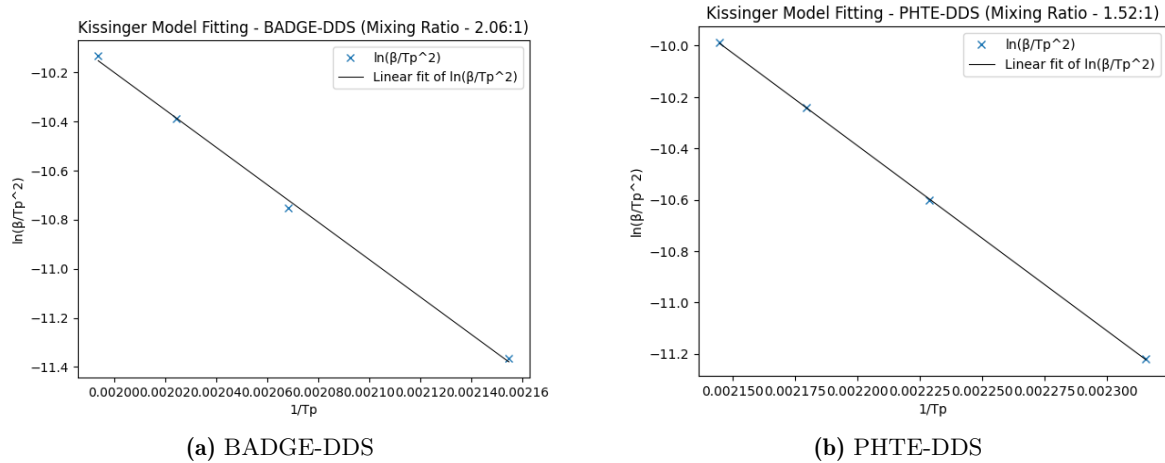


Figure 7.5: Kissinger model fitting for both resins

The slope of these plots is the derivative which is then plugged into the Kissinger model equation. The activation energies were calculated for both resins. 59.974 kJ/mol for PHTE and 63.417 kJ/mol for BADGE. PHTE has a 5.4 % lower activation energy, which is preferable as comparatively lower heating is required to fully cure the resin, keeping in mind global warming issues.

7.1.3. Coefficient of thermal expansion (CTE) - Thermo-mechanical analysis (TMA)

As discussed, all materials behave differently at different temperatures. This behavior also translates to dimensional changes which affect the usability of materials, especially in high-performance applications with a large variation in temperatures as seen in aerospace. TMA, or thermo-mechanical analysis, is a thermal technique that is used to study the change in dimensions of a sample as a function of temperature. A Perkin Elmer TMA4000 was used to evaluate the dimensional changes of both resins. Runs from 25 °C to 300 °C at a heating rate of 10 °C/min were done for both PHTE and BADGE.

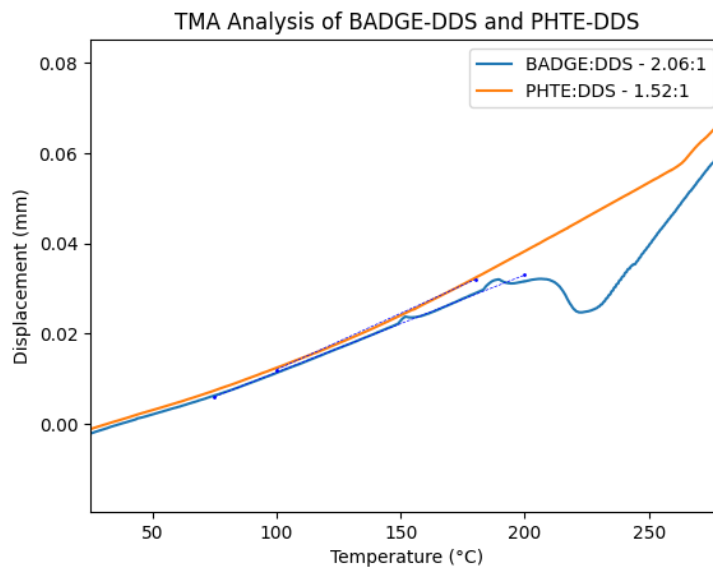


Figure 7.6: Coefficient of thermal expansion evaluation of both resins

A displacement vs. temperature plot is received. The slope of the plots gives the coefficient of thermal expansion. The CTE's received for the resin systems are as below:

- BADGE:DDS = $84.45 \times 10^{-6}/\text{K}$
- PHTE:DDS = $97.75 \times 10^{-6}/\text{K}$

These CTEs can be utilized to calculate the change in dimensions of a structure, which dictates the usable temperature range of a structure in a certain application.

7.1.4. Glass transition temperature (T_g) - Dynamic mechanical analysis (DMA)

As discussed extensively, T_g is an important parameter of a material as it dictates the usable temperature limit of a material. As seen from chapter 6, DMA is the most sensitive technique that could be used for T_g estimation. Thus, DMA was run for both resins. We can see in figure 7.7 that the T_g for PHTE is 260 °C as seen before, whereas for BADGE it is 226 °C as compared to 190 °C as seen before. This can be attributed to the difference in the measurement technique and the parameter being evaluated. Thus, using a common technique with the same parameters is essential to comparing both resins.

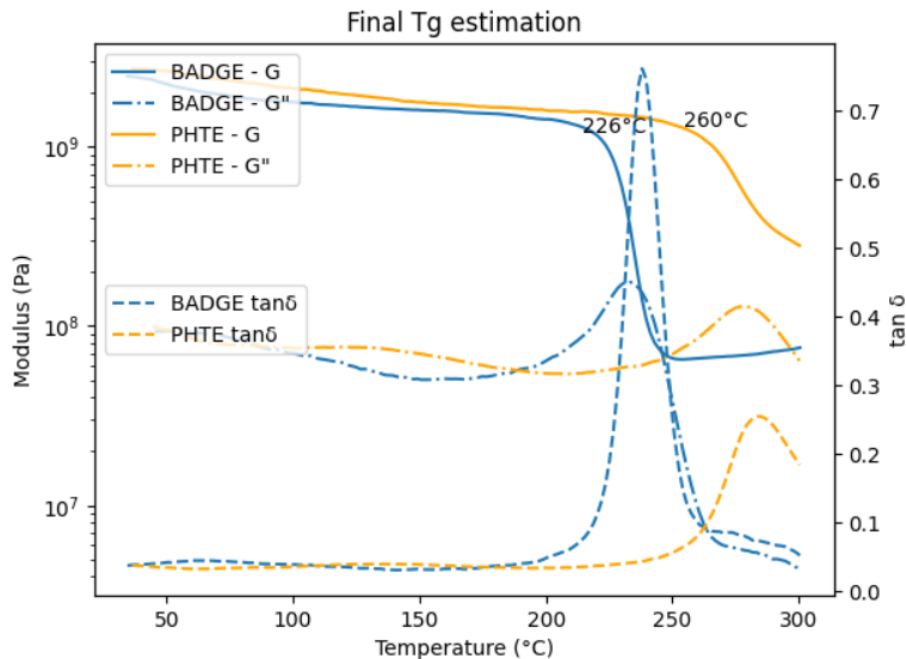


Figure 7.7: Visc-elastic behaviour of both resin systems

Also, as we see from figure 7.7, there is a sudden drop in the modulus for BADGE, which is not preferable as a resin of choice and places a hard temperature limit on its use.

7.1.5. Viscosity measurement - Dynamic Rheometry

Dynamic rheometry or rheology is a scientific study that deals with the flow and deformation of materials. In this field, deformation and flow are referred to as strain or strain rate, respectively. These terms indicate the distance that a body moves under the influence of an external force, or stress. By assessing these parameters, an understanding of the material is attained in terms of its viscosity varying over temperature or time.

Rheology is also concerned with the stress-strain relationships in materials. Viscosity measurement of the resins, especially with temperature, is essential for composite manufacturing to get an

understanding of the behavior of the resin and the kinds of pressures required during the process.

Rheological tests were conducted using a HAAKE MARS III rheometer. As the viscosity of the resins is high at room temperature, an understanding of the viscosity behavior with temperature is required to define a processing procedure.

To study the viscosity behavior with temperature, samples with flat pp20 (20 mm diameter) disposable aluminum circular plates were prepared and fixed to the rheometer. This experiment was carried out in Constant Rotation (CR) rotational mode with a rotational frequency of 10 Hz from room temperature to 100 °C at 10 °C/min. It focused on examining how the viscosity of the resin systems varied over a range of temperatures.

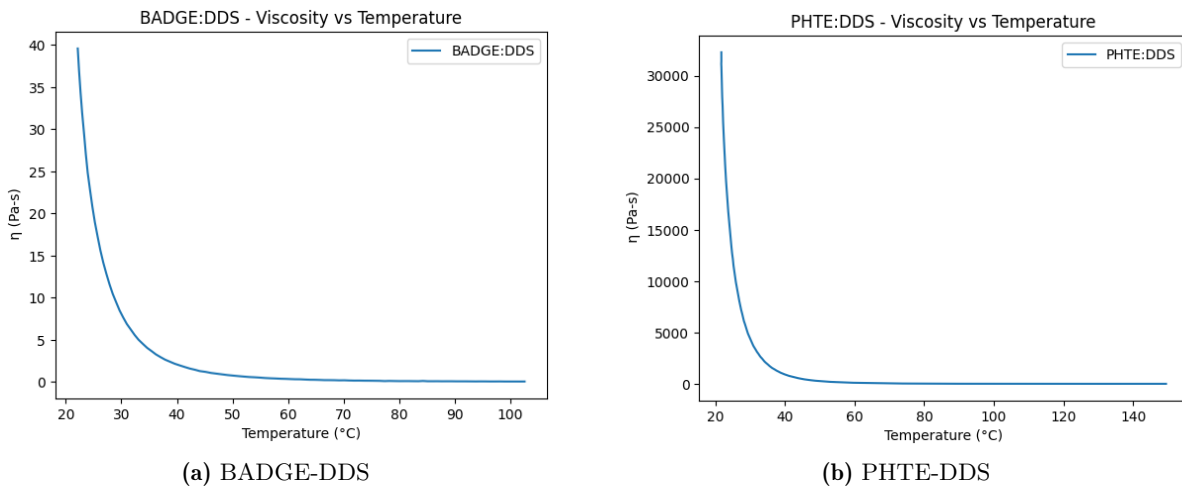


Figure 7.8: Viscosity variation with temperature for both resins

Figures 7.8a and 7.8b show the change in viscosity with temperature of BADGE:DDS and PHTE:DDS respectively. As can be seen, the viscosity is initially high, especially for PHTE but rapidly drops until 50 °C which is per the procedure of heating the resin to 60 °C for processing. The table 7.3 gives the development of viscosity with temperature for both resin systems.

Temperature	PHTE:DDS	BADGE:DDS
	Pa-s	Pa-s
25 °C	12300	19.3
40 °C	910	2.1
60 °C	101	0.5
100 °C	6.6	0.15

Table 7.3: Viscosity variation of resin systems with temperature

The main aim of these tests was to obtain valuable insights into the material properties and behavior of the resin systems under various thermal conditions and settings which will also aid in the processing, especially for composite manufacturing.

7.2. Physical Characterization

The physical characterization comprises parameters that can be used to understand the behavior of the resin systems with moisture and their surface characteristics.

7.2.1. Surface hydrophilicity - Water contact angle

Surface hydrophilicity or wettability is an essential parameter that needs to be assessed for a material as a hydrophilic surface would attract more water which is then absorbed by the material or might turn into ice and affect the performance of the part. Although, to tackle this coatings are used, but this parameter indicates the level of preventive measures to be taken to avoid water. Water contact angle measurement is the most common method used to quantify the wettability of a solid surface by a liquid.

For water contact angle measurements, an Attension Theta Optical Tensiometer by KSV Instruments was used. Five samples of both resins with flat surfaces were prepared, properly cleaned with acetone, and dried. The sample base was leveled using a spirit level and calibration was done using a 4mm diameter metal ball as shown in figure 7.9.

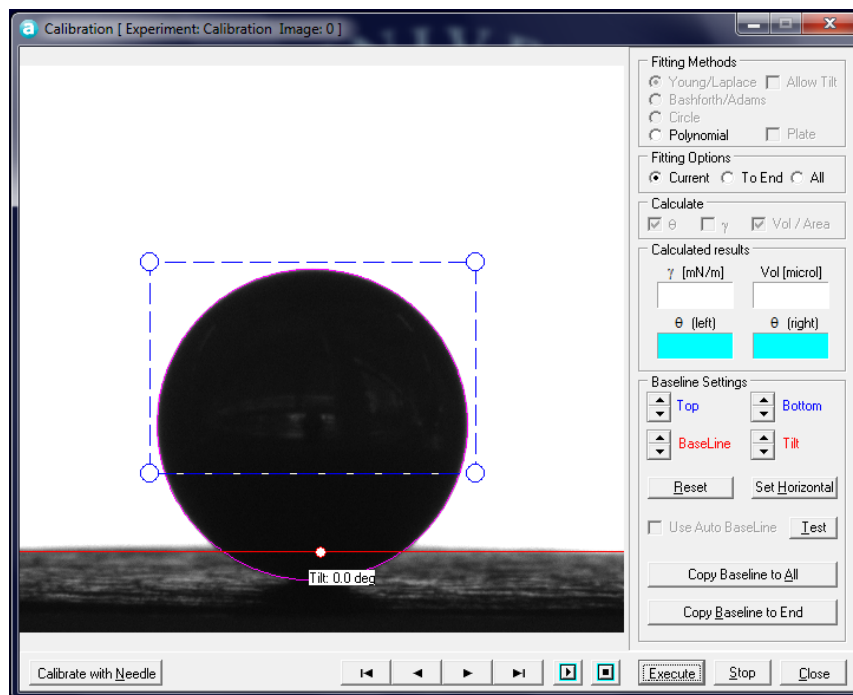


Figure 7.9: Calibration for Water Contact Angle

After calibration, the sample was placed on the base and a water droplet of 5 ml was carefully placed on each surface using a fin pipette, and a digital image was captured. The captured image was analyzed with Attension Theta software, and the droplet's left and right contact angles with the structure was measured as in table 7.4 and 7.5. Out of them, the average was taken for each sample.

Figure 7.11 shows the water contact angle analysis for PHTE whereas figure 7.10 shows the analysis for BADGE.

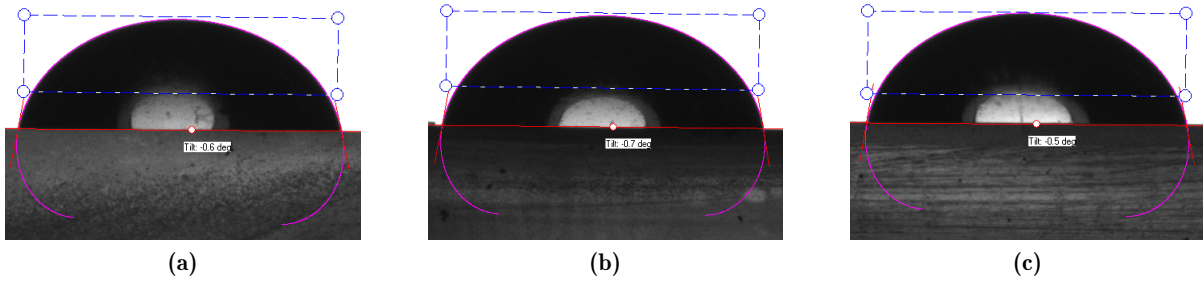


Figure 7.10: BADGE Water Contact Angle measurements

Sample	$\theta(\text{Left})$	$\theta(\text{Right})$	$\theta(\text{Average})$
1	79.95°	79.26°	79.61°
2	78.47°	82.38°	80.43°
3	79.68°	77.97°	78.83°
4	79.83°	80.23°	80.03°
5	80.74°	78.73°	79.74°

Table 7.4: Contact Angles made by a water droplet on BADGE samples

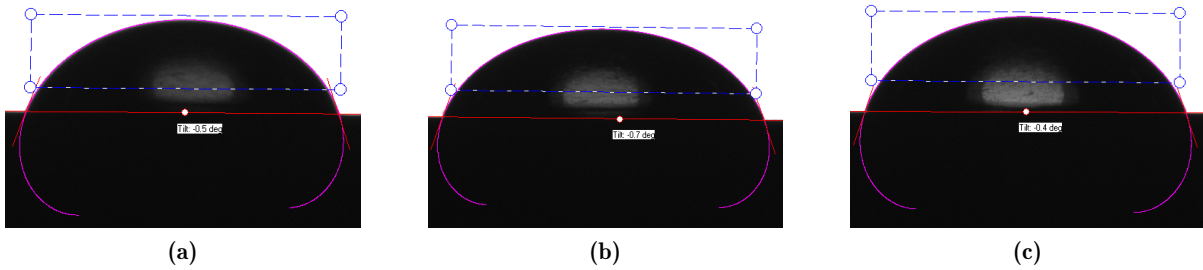


Figure 7.11: PHTE Water Contact Angle measurements

Sample	$\theta(\text{Left})$	$\theta(\text{Right})$	$\theta(\text{Average})$
1	67.88°	66.35°	67.12°
2	68.88°	71.96°	70.42°
3	70.12°	70.11°	70.12°
4	67.58°	67.20°	67.39°
5	71.33°	70.62°	70.98°

Table 7.5: Contact Angles made by a water droplet on PHTE samples

It can be inferred that the angle made by the water droplet on PHTE samples in table 7.5 is smaller than on BADGE in table 7.4. An angle equal to or greater than 90° means hydrophobic and less than means hydrophilic. PHTE making a smaller angle means it is more hydrophilic as compared to BADGE, which in turn means greater measures would be required to avoid water for PHTE-based components.

7.2.2. Water absorption

To properly check the water affinity of the resins, samples are immersed in water to get a proper understanding of the development in water absorption by the material. These tests were conducted as per the ASTM standard D570 ‘Standard test method for water absorption of plastics’. [50] Both resin and composite samples of varying mass from 0.3 to 0.4 g (W_0) were immersed in vials of distilled water and left for 24 h, 48 h, 7 days (168 h) and 14 days (336 h) respectively. After that, the samples were removed from the water, wiped with filter paper, dried with compressed air, and weighed (W_D). Water absorption was calculated using:

$$WA\% = \frac{W_D - W_0}{W_0} * 100$$

Where:

- W_D = Weight after submerging in distilled water
- W_0 = Initial weight of the sample

Sample	Duration	Initial Weight (mg)	Final Weight (mg)	Weight Change (mg)	Water Absorption (%)
BADGE:DDS	24 Hours	405.2	406.5	1.3	0.32
	48 Hours	396.0	397.8	1.8	0.45
	7 Days	521.2	525.2	4	0.76
	14 Days	787.7	795.3	7.6	0.96

Table 7.6: Water Absorption by BADGE-DDS for multiple durations

Sample	Duration	Initial Weight (mg)	Final Weight (mg)	Weight Change (mg)	Water Absorption (%)
PHTE:DDS	24 Hours	508.2	509.9	1.7	0.33
	48 Hours	462.0	464.1	2.1	0.45
	7 Days	543.1	547.6	4.5	0.82
	14 Days	666.6	675.3	8.7	1.30

Table 7.7: Water Absorption by PHTE-DDS for multiple durations

It can be inferred from table 7.7 that the water absorption % for PHTE is slightly higher as compared to BADGE in table 7.6, which as discussed in the previous section means greater measures would be required to avoid water absorption for PHTE-based components.

7.2.3. Gel content

A parameter indicative of cross-linking of the chemical structure is gel content. This testing consists of the immersion of samples in toluene, which leads to the separation of any unreacted or uncross-linked monomers or small molecular chains from the structure. ASTM D2765 ‘Standard test methods for determination of gel content and swell ratio of cross-linked ethylene plastics’ was used for the determination of the gel content of the PHTE resin and composite. [51] Samples of resin and composite were submerged in toluene for 72 hours, after which they were removed, dried using filter paper-compressed air, and weighed. The gel content was calculated using the following equation:

$$GC\% = \frac{W_f}{W_0} \times 100$$

Where:

- W_f = Mass of dried samples after toluene immersion
- W_0 = Initial mass of the sample before immersion

Sample		Initial Weight	Final Weight	Weight Change	Gel Content
		(mg)	(mg)	(mg)	(%)
PHTE:DDS	Post-Cured	445.4	445.2	0.2	99.95
PHTE:DDS	Non Post-Cured	442.7	442.3	0.4	99.91
BADGE:DDS	Post-Cured	369.8	369.8	0	100
BADGE:DDS	Non Post-Cured	419.9	419.3	0.6	99.85

Table 7.8: Gel Content of Post-cured and Non-Post cured samples of both resins

Table 7.8 shows the weight change and gel content of the post-cured and non-post-cured samples of both resins. Although there is slight variation in the Post-cured and Non-Post-cured samples, the gel content is almost 100 %, which states that the inter-linking percentage of the monomers is quite high. However, it is to be noted that even though the inter-linking percentage is high, it does not convert to complete cross-linking of the monomers.

7.2.4. Bio-based content

The main task of this study was to eliminate the use of toxic materials and reduce the use of synthetic materials. Thus, it was important to assess the bio-based content and maximize it as much as possible. This was done here by calculating the bio-based carbon content in the resin system.

As discussed in chapter 3, PHTE is achieved from two components, phloroglucinol and epichlorohydrin. Both of these components are completely bio-based materials, thus the bio-content of PHTE is taken as 100 %. As DDS is synthetic, it is essential to calculate the bio-based content of the resin system. The molecular weight of PHTE is 294 g/mol and that of DDS is 248 g/mol. The mixing ratio for PHTE:DDS is 1.52:1. We get a bio-based content of 64.31 % by weight.

7.3. Mechanical testing

Mechanical properties are often the most important properties related to technology. This is because mechanical loading is experienced to some degree in virtually all applications. Also, because these resins are being studied for high-performance applications, they are important.

7.3.1. Density

Material Density is an important parameter, especially for aerospace applications. The density of rectangular samples can be analyzed by calculating the ratio of mass to volume. To avoid potential errors, an average of five samples should be considered as the final value for each system. [16] [19]

Identical samples with visibly no defects were prepared using a Proth cutting machine equipped with a diamond-edge blade. Once the samples were prepared and optically tested, multiple measurements were done using a digital vernier caliper, and average sample dimensions and their weight were measured using a digital scientific scale and recorded as in table 7.9 and 7.10.

	Sample Dimensions				
Sample	Length	Width	Thickness	Weight	Density
	(mm)	(mm)	(mm)	(g)	(kg/m^3)
1	74.29	10.07	3.89	3.5545	1221.03
2	74.3	10.05	3.9	3.5582	1221.43
3	74.26	10.13	3.92	3.5876	1216.62
4	74.38	10.11	3.9	3.5691	1216.99
5	74.52	10.05	3.92	3.5371	1205.22
6	74.45	10.01	3.9	3.5488	1221.41

Table 7.9: Density Measurement - BADGE:DDS

	Sample Dimensions				
Sample	Length	Width	Thickness	Weight	Density
	(mm)	(mm)	(mm)	(g)	(kg/m^3)
1	73.85	10.09	3.92	3.9323	1345.78
2	73.91	10.14	3.92	3.9456	1343.03
3	74.07	10.04	3.92	3.9031	1339.34
4	74.18	10.13	3.94	3.9743	1342.36
5	73.95	10.14	3.94	3.9496	1336.40
6	73.92	10.13	3.94	3.821	1294.69

Table 7.10: Density Measurement - PHTE:DDS

Density was calculated for all the specimens. An average density of 1217 kg/m^3 for BADGE and 1333 kg/m^3 for PHTE was evaluated, which is 10.1 % higher as compared to BADGE. A higher density is not preferable and further mechanical testing is essential to assess if this can be offset by higher mechanical properties.

7.3.2. Tensile strength and Young's modulus

To assess the strength of a material or a sample, the first test that comes to mind is a tensile test. The samples are tested in tension, and a stress vs. strain curve is plotted as shown in figure 7.13. The testing was performed as per ASTM D638 "Standard test method for tensile properties of plastics.". A Type 5 specimen was selected, which is a smaller specimen size to keep the cost of this research lower. This selection does not affect the results.

Each tensile sample mold yields 4 samples, but due to the fragile and brittle nature of the samples, it was impossible to extract all 4 samples intact. Thus, 2 sets of samples were prepared, and the samples were numbered and marked to identify the batch they were taken from in case of variation in data. Tables 7.11 and 7.12 give the specimen details of both resins shown in figures 7.12.



Figure 7.12: Tensile Specimens

Sample	Length	Width	Section Width	Thickness	Weight	Remarks
	(mm)	(mm)	(mm)	(mm)	(g)	
1.1	89.63	9.41	3.3	3.9	3.3693	Good Sample with slight contractions on support, no mark on the middle portion, broke properly in the middle
1.2	90.36	9.48	3.28	3.91	3.3943	Good Sample with slight contractions and bubbles on support, no mark on the middle portion, broke properly in the middle
2.1	90.65	9.48	3.35	3.89	3.4618	Slight contractions and bubbles on sample, slight bubble in the middle portion, weird breaking from the tip
2.2	91.41	9.55	3.35	3.89	3.46	Slight contractions and bubbles on the sample, a minute bubble in the middle and a bubble at the curve of the middle portion, and some bubbles on support, broke slightly off center
2.3	87.52	9.51	3.22	3.91	3.1582	Lots of bubbles in the specimen, Specimen width not correct in data, broke from the middle near a bubble
2.4	87.39	9.5	3.25	3.89	3.2948	Slight contractions on support, multiple bubbles in the middle support and curve end, broke slightly off center, good data

Table 7.11: Tensile Specimen data - BADGE:DDS

Sample	Length	Width	Section Width	Thickness	Weight	Remarks
	(mm)	(mm)	(mm)	(mm)	(g)	
1.1	89.12	9.43	3.3	3.89	3.636	Slight Contractions, almost perfect sample, broke slightly off center
1.2	89.74	9.45	3.35	3.9	3.7051	Slight Contractions, slight bubbles on one side root, broke at the support tip
1.3	89.35	9.39	3.31	3.88	3.6545	Slight Contractions, slight bubbles in the middle, broke quite off center
2.1	90.15	9.45	3.35	3.88	3.7408	Slight contractions, no bubbles, broke at the support tip
2.2	89.54	9.41	3.26	3.91	3.6689	Slight contractions, a significant bubble in the middle, multiple bubbles on curve and supports, 0.5 mm/min test, broke slightly off center at the significant bubble
2.3	89.56	9.33	3.28	3.89	3.673	No contractions, slight bubbles on a curve on one side, broke at end of the curve at a bubble
2.4	90.92	9.38	3.32	3.92	3.7501	Slight contraction on one support, almost perfect sample, no bubbles, broke at the start of the curve

Table 7.12: Tensile Specimen Data - PHTE:DDS

The samples were fixed in the grips and tested in tension at 1 mm/min crosshead rate and a Force vs. Displacement data was received. This data was converted to a Stress vs. Strain curve as in figure 7.13

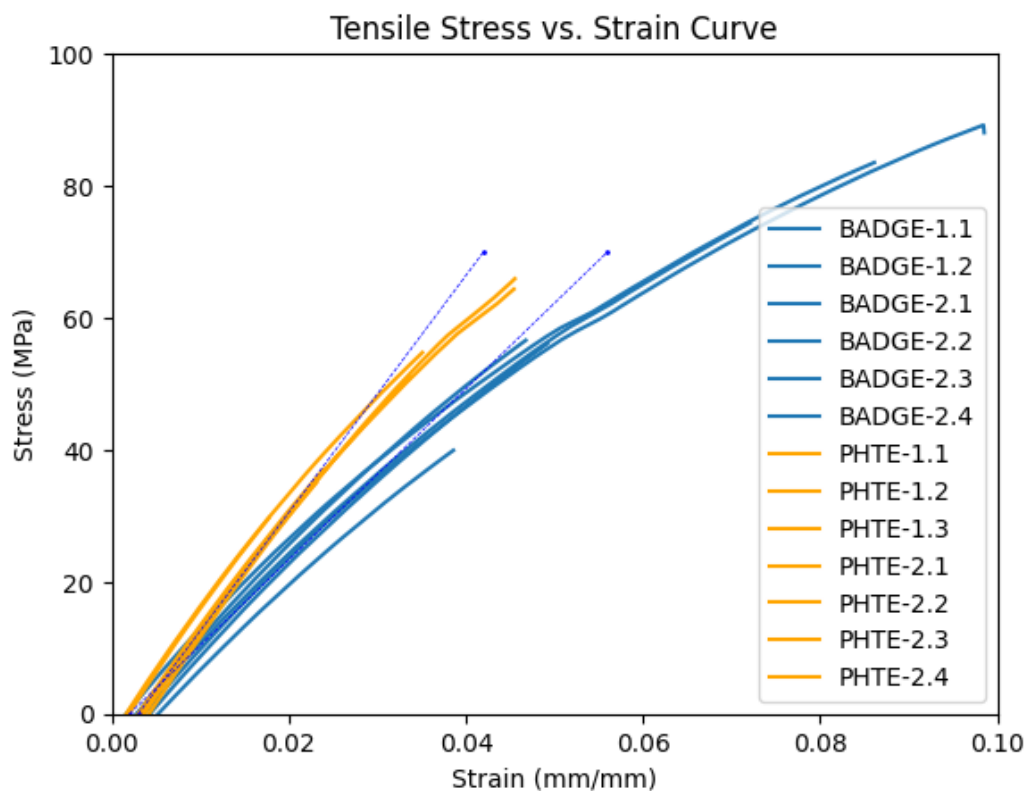


Figure 7.13: Tensile Stress vs. Strain Curves

The samples have a slight variation in their strength but are consistent in their behavior. Figure 7.13 shows the Stress vs. Strain curve for all the samples of both resins tested in tension. The ultimate tensile strength of PHTE is 67 MPa which is 23.8 % lower as compared to 83 MPa for BADGE. However, Young's Modulus for PHTE is 1.794 GPa which is 33.6 % higher as compared to 1.296 GPa for BADGE.

Now, to understand which resin system is better here, it is essential to understand its behavior with fiber in composites which is complex. In composites, the strength-imparting component is the fiber, and the function of the matrix is to impart the fiber structure and transfer load from one fiber to another. Also, fibers are comparatively stiffer and stronger as compared to matrix materials. Thus, for a matrix material, the most important parameter is stiffness as compared to strength, as once the matrix undergoes loading and starts extending, the next fiber takes up the loading and the matrix does not undergo great extension. As can be inferred from figure 7.13, BADGE has a higher strength but it comes at a high strain which often will be unusable. Thus, from a high-performance composite application point-of-view PHTE can be deemed to be a better matrix material as compared to BADGE.

7.3.3. Flexural strength and modulus

Another common mechanical properties evaluation is through flexural testing. The sample preparation and testing were performed as per ASTM D790 "Standard test methods for flexural Properties of unreinforced and reinforced plastics and electrical insulating materials". [52]

Resin plates were prepared of thickness 4 mm and cut to dimensions using a Proth cutting machine equipped with a diamond-edge blade. Tables 7.13 and 7.14 give the specimen details of both resins measured accurately using a digital vernier caliper.

Sample	Length (mm)	Width (mm)	Thickness (mm)	Remarks
1	74.29	10.07	3.89	No contractions, no bubbles
2	74.3	10.05	3.9	No contractions, no bubbles
3	74.26	10.13	3.92	No contractions, no bubbles
4	74.38	10.11	3.9	Slight contractions on top surface
5	74.52	10.05	3.92	Slight contractions on top surface
6	74.45	10.01	3.9	No contractions, no bubbles

Table 7.13: Flexural Specimen Data - BADGE:DDS

Sample	Length (mm)	Width (mm)	Thickness (mm)	Remarks
1	73.85	10.09	3.92	No contractions, no bubbles
2	73.91	10.14	3.92	No contractions, no bubbles
3	74.07	10.04	3.92	No contractions, no bubbles
4	74.18	10.13	3.94	No contractions, no bubbles
5	73.95	10.14	3.94	No contractions, no bubbles
6	73.92	10.13	3.94	Big bubble at the end, do not consider density

Table 7.14: Flexural Specimen Data - PHTE:DDS

The samples were tested in a 3-point bending setup. The standard mentions a support span-to-depth ratio of 16:1, which gives a span of 64 mm for a 4 mm thick sample which was used here. A Force vs. Displacement curve was obtained.

The flexural stress is calculated using the following equation as mentioned in the standard:

$$\sigma_f = \frac{3PL}{2bd^2}$$

where,

- σ_f = stress in the outer fibers at midpoint, MPa,
- P = load at a given point on the load-deflection curve, N,
- L = support span, mm,
- b = width of beam tested, mm, and
- d = depth of beam tested, mm.

The flexural strain is calculated using the following equation as mentioned in the standard:

$$\epsilon_f = \frac{6Dd}{L^2}$$

where,

- ϵ_f = strain in the outer surface, mm/mm,
- D = maximum deflection of the center of the beam, mm,
- L = support span, mm, and
- d = depth, mm.

The Flexural stress vs. strain curves were obtained as shown in figure [7.14](#).

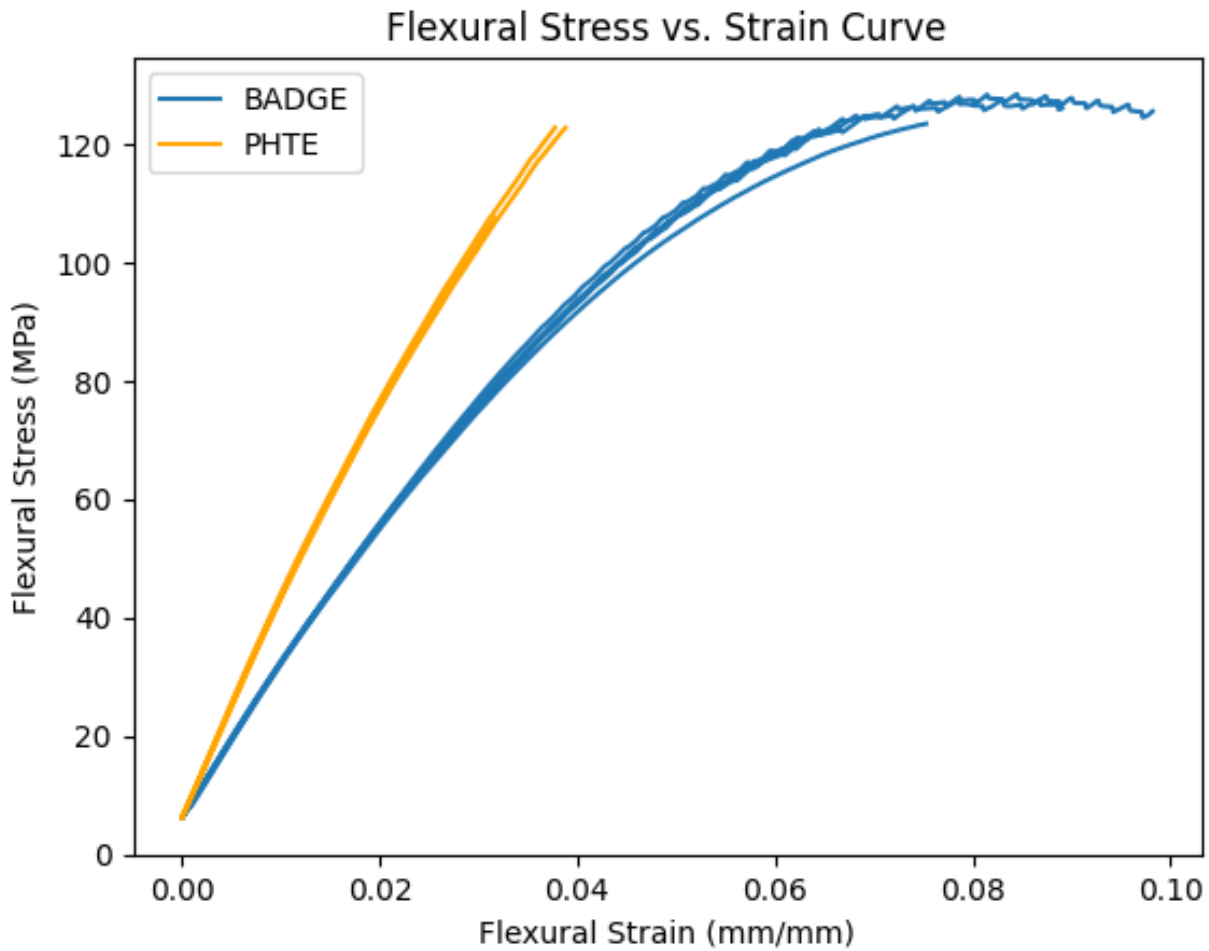


Figure 7.14: Flexural Stress vs. Strain Curves

Figure 7.14 shows the Stress vs. Strain curve for all the samples of both resins tested in flexure. As can be inferred from figure 7.14, the samples are quite consistent in their strength and behavior and the flexural strength is almost similar for both resin systems. The modulus of elasticity in bending is calculated using the following equation:

$$E_B = \frac{L^3 m}{4bd^3}$$

where:

- E_B = modulus of elasticity in bending, MPa,
- L = support span, mm,
- b = width of beam tested, mm,
- d = depth of beam tested, mm, and
- m = slope of the tangent to the initial straight-line portion of the load-deflection curve, N/mm of deflection.

The modulus of elasticity in bending or flexural modulus is calculated as 3.77 GPa for PHTE which is 42.3 % higher as compared to 2.6 GPa for BADGE. The higher flexural modulus might be beneficial in some cases where it can resist buckling more in a composite structure.

7.3.4. Fracture toughness: Single edge notched bend

Apart from the regular tensile and flexural tests, an important testing parameter is fracture toughness, especially for a matrix material. Fracture toughness is an estimate of the amount of stress required to propagate a pre-existing crack or defect. It is a very important material property, as defects are impossible to avoid in the processing, fabrication, or service of a material/component. Cracks, voids, metallurgical inclusions, weld faults, discontinuities in the design, or any combination of these may be signs of a defect. Since it cannot be certainly said that a material is defect-free, the component is assumed to consist of a fault of a certain magnitude, and a linear elastic fracture mechanics (LEFM) approach is taken to design important components.

The sample preparation and testing were conducted as per ASTM D5045 "Standard test methods for plane-strain fracture toughness and strain energy release rate of plastic materials". [53]

Sample preparation

- **Sample cutting:** It was decided to use the same 4 mm thick resin plate used for flexural testing for SENB samples. Thus, the thickness (B) was 4mm. As per standard, the width (W) should be twice the thickness, and the length should be 4.4 times the width. That gave a sample size of 35.2 X 8 X 4 mm. Similar to samples for flexural testing, the samples were cut from a 4mm thick resin plate using the Proth cutting machine with a diamond-edge blade.
- **Notch preparation:** The total crack length (A) consists of the notch length (a) and the pre-crack length (δa). The standard specifies the total crack length (A) to be nominally equal to the thickness (B) and between 0.45 to 0.55 times the width (W). This gives an A of 4 mm to 4.4 mm. Also, the pre-crack length δa should be at least twice the notch width (w).

To create the notch, a saw of the lowest available thickness of 0.4 mm was taken. This gives a minimum required pre-crack length of 0.8 mm. First, a notch with a length of 2.5 to 3 mm was created at the center of all samples. A diamond paste of 1 μm was used as a lubricant while processing to avoid excess stress on the samples.

- **Pre-crack initiation:** After creating the notches and measuring them under the microscope, creating a pre-crack was tried. As mentioned in the standard, a fresh razor blade was taken and lightly tapped on all sample notches to create the pre-crack. This process splits or breaks a lot of samples. With a lot of trials, 4 samples of both resins were created, as shown in figure 7.15.

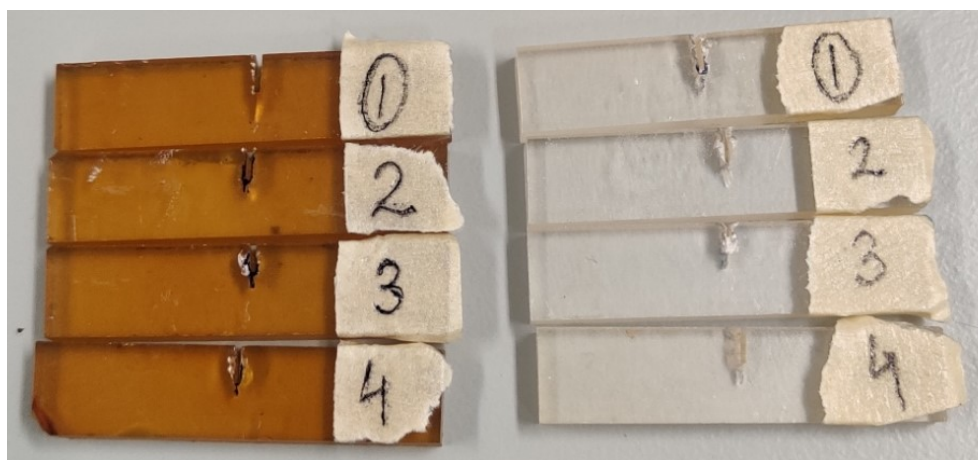


Figure 7.15: SENB Samples - PHTE (Left) and BADGE (Right)

- **Crack measurement:** The samples were put under a microscope to measure the required crack dimensions accurately. Along with the measurement of the notch, the standard mentions taking three measurements of thickness and width to ensure accuracy, as in table 7.15 and 7.16.

Sample	Thickness	Width	Length	Notch Specifications			
				B	W	L	A
1	3.94	8.2	34.57	5.0648	0.4906	3.4215	1.6433
2	3.92	8.18	35.45	4.8801	0.5353	3.218	1.6621
3	3.92	8.17	35.35	3.7079	0.5543	2.37	1.3379
4	3.93	8.18	35.44	4.39	0.5612	3.0529	1.3371

Table 7.15: BADGE Specimen Data

Sample	Thickness	Width	Length	Notch Specifications			
				B	W	L	A
1	3.94	8.19	35.39	5.2115	0.5033	3.4976	1.7139
2	3.92	8.18	35.42	4.1735	0.5161	2.8796	1.2939
3	3.91	8.18	35.44	3.9948	0.5543	2.4595	1.5353
4	3.92	8.21	35.42	4.3266	0.5033	3.1855	1.1411

Table 7.16: PHTE Specimen Data

From tables 7.15 and 7.16, we can infer that samples 1 and 2 of BADGE and sample 1 of PHTE are not up to standard. The standard mentions three replicate tests for a valid test, which is still possible here. To analyze this property further, more samples can be created and tested to get the fracture toughness.

Testing setup and conditions

Since this testing is for plastics which are visco-elastic materials, the standard mentions testing under the same temperature, which was 21.1 °C here and a crosshead rate of 10 mm/min. The testing was done in a short period to avoid the change in behavior due to temperature change.

The setup is a 3-point bending test with the span taken as four times the width, which is 32.2 mm here. The standard mentions the support and indenter diameter to be between $W/2$ and W , thus a setup of 6 mm diameter was taken here. Figure 7.17 shows the testing setup for BADGE and PHTE as per standard specifications. A loading cell of 100 N was used to get accurate data as the expected loads were 10 - 20 N, from an understanding of the materials from the previous mechanical testing (Flexural).

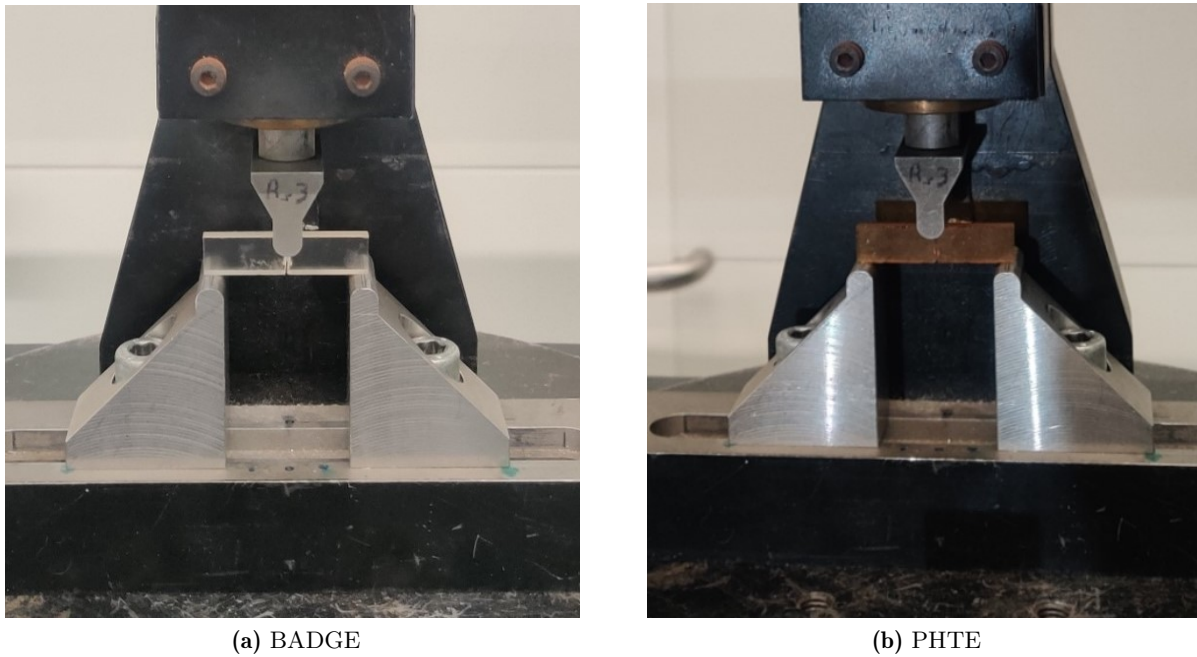


Figure 7.16: SENB Testing setup

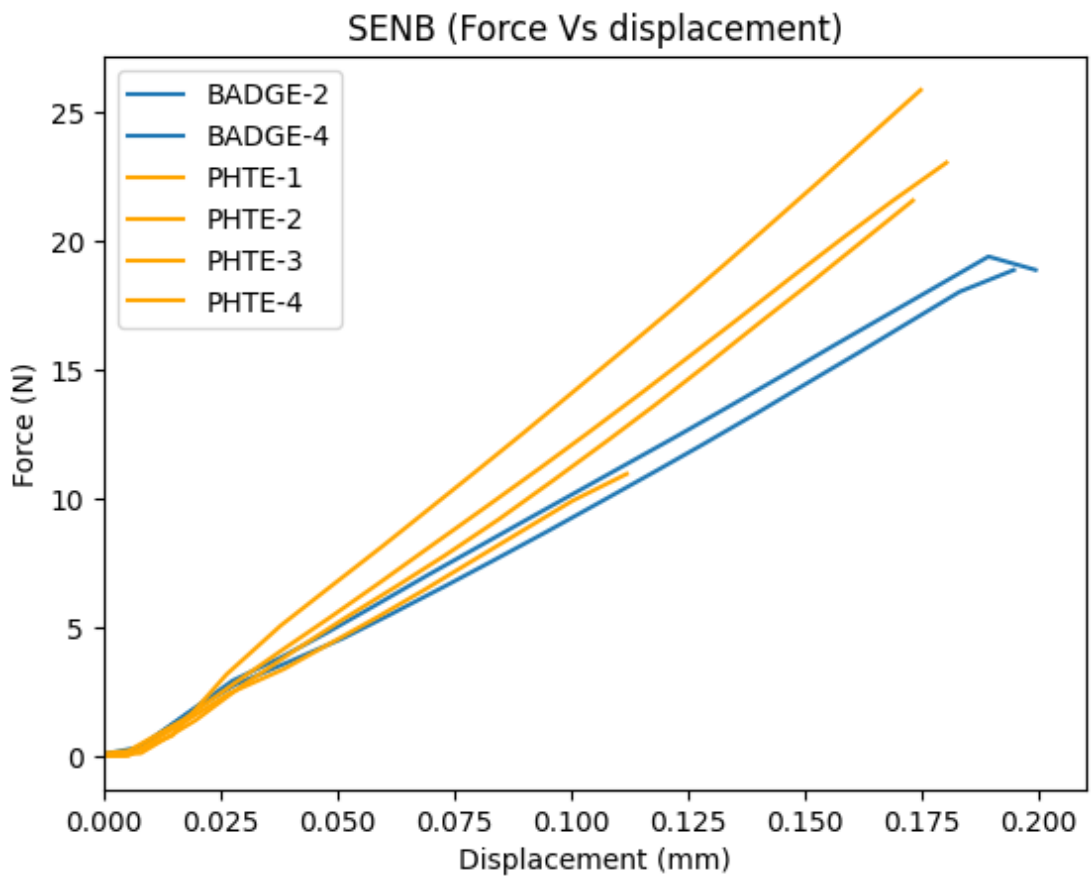


Figure 7.17: SENB Force Vs Displacement Plot

Testing was done and a Force vs. Displacement plot as shown in figure 7.17 was received. The following samples were deemed invalid:

- BADGE-1: The sample broke due to the fragile nature of the specimens.
- BADGE-2: The crack length was too long.
- BADGE-3: the data was lost and the machine gave noise as the output.
- PHTE-1: The crack length was too long, due to which a lower load was captured as in figure 7.17

The other samples give a consistent result to have validated results.

Test validation criteria

The testing standard mentions several parameter checks to be conducted for a test to be deemed valid. Thus, it is important to perform these checks before moving on to calculating the fracture toughness and comparing the resins.

To establish that a valid K_{IC} (Critical stress-intensity factor) has been determined, it is first necessary to calculate a conditional result, K_Q (the conditional or trial K_{IC} value). This involves checking if the results obtained are consistent with the size of the specimen. The standard mentions for a result to be considered valid, the following size criteria must be satisfied:

$$B, a, (W - a) > 2.5 \frac{K_Q}{\sigma_y^2}$$

where,

- K_Q = the conditional or trial K_{IC} value,
- σ_y = the yield stress of the material for the temperature and loading rate of the test.

According to the criteria, B must be adequate to provide plane strain, and $(W - a)$ must be adequate to prevent excessive plasticity. For SENB specimens, a maximum W/B ratio of 4 can be tried if $(W - a)$ is too small and non-linearity in loading happens.

K_Q value calculation

After getting the force vs. displacement plot, the standard mentions the determination of compliance (C) and determined load P_Q as in figure 7.18. The best-fit line was made and compliance was computed. Then a second line with a compliance 5% greater was plotted. Next, calculation of P_Q is required, if P_{max} lies between the two lines, $P_Q = P_{max}$.

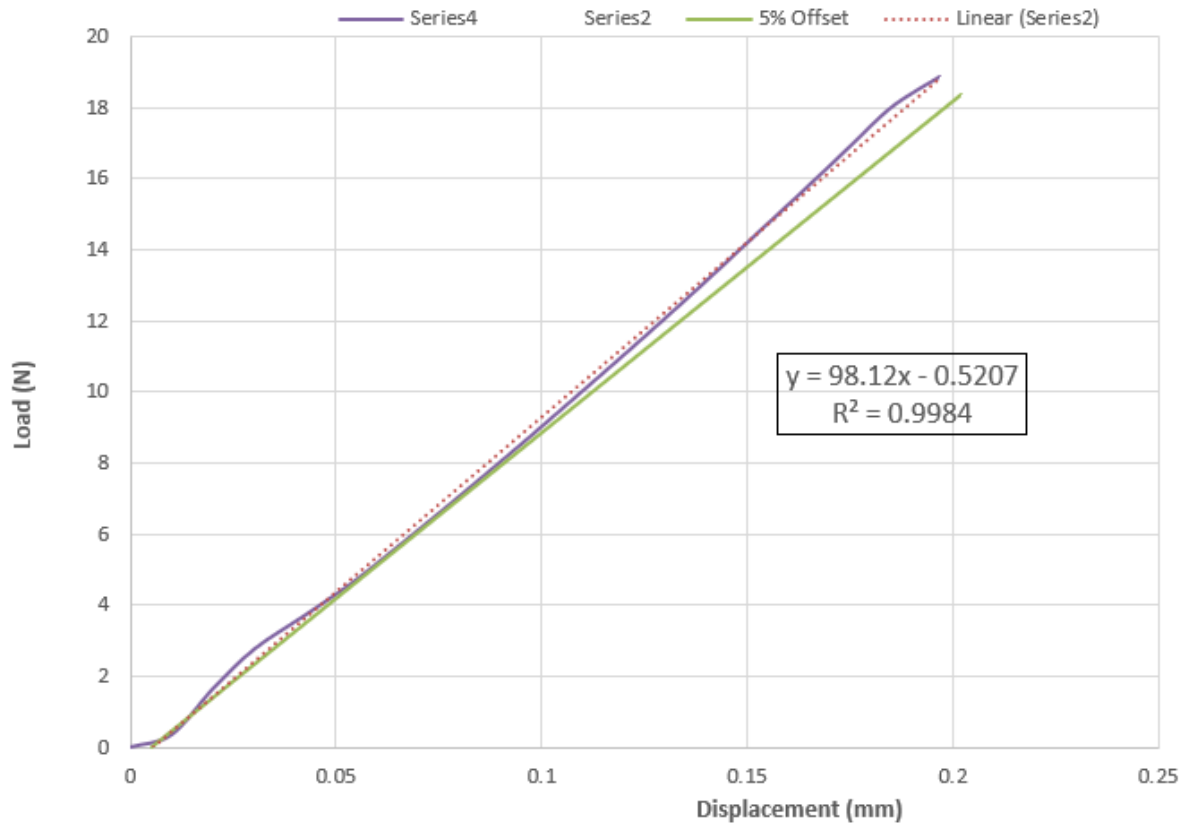


Figure 7.18: Determination of C and P_Q

After checking for P_Q , K_Q can be calculated, which is given as:

$$K_Q = \left(\frac{P_Q}{BW^{1/2}} \right) f(x)$$

where, ($0 < x < 1$):

$$f(x) = 6x^{1/2} \frac{[1.99 - x(1-x)(2.15 - 3.93x + 2.7^2)]}{(1+2x)(1-x)^{3/2}}$$

where,

- P_Q = determined load in kN
- B = specimen thickness in cm,
- W = specimen depth (width) in cm,
- a = crack length in, cm.

$$x = \frac{a}{W}$$

These steps were performed for all dimensionally valid samples and table 7.17 lists all the parameter calculations along with K_Q .

Sample	P_Q	x	f(x)	K_Q
	(N)			($MPa.m^{1/2}$)
BADGE-4	18.87	0.53	11.92	0.60
PHTE-2	21.56	0.51	11	0.67
PHTE-3	25.86	0.49	10.27	0.70
PHTE-4	23.03	0.53	11.62	0.70

Table 7.17: Calculation of K_Q , the conditional K_{IC} value

Fracture toughness calculation

As discussed before, for fracture toughness calculation, it is essential to first check for test validity. After calculating K_Q values, the following equation is checked in table 7.18 as discussed before:

$$B, a, (W - a) > 2.5 \frac{K_Q}{\sigma_y^2}$$

Sample	B	a	W-a	$2.5K_Q/\sigma_y^2$	Test Validity	K_{IC}
	(cm)	(cm)	(cm)			($MPa.m^{1/2}$)
BADGE-4	0.392	0.439	0.382	0.25	Valid	0.60
PHTE-2	0.392	0.417	0.401	0.31	Valid	0.67
PHTE-3	0.391	0.399	0.418	0.34	Valid	0.70
PHTE-4	0.393	0.433	0.388	0.34	Valid	0.70

Table 7.18: Check for validity of tests

It can be inferred that the tests mentioned were valid ones, and K_{IC} values in table 7.18 can be taken as K_Q from table 7.17. The fracture toughness can be taken as $0.69 MPa.m^{1/2}$ for PHTE which is 15 % higher as compared to $0.60 MPa.m^{1/2}$ for BADGE. However, more testing is essential to properly compare the resins.

8

Composite trials

After characterizing and comparing both the resins, it was decided to manufacture a composite as a proof-of-concept and assess the resins' workability.

8.1. Test selection

As the primary aim was to test and compare the resins, it was essential to prepare the composite by the kind of testing to be conducted. The initial kind of mechanical testing usually used is tensile testing or flexural testing, but they are mostly fiber-dominated as fibers are several times stronger than the matrix in tension. A technique suitable for testing resin is the Inter-Laminar shear strength. It gives the interaction of the resin with the fiber and its strength. Thus, it was decided to test composite samples for ILSS. The sample preparation and testing were done as per ASTM standard D2344 "Standard test method for short-beam strength of polymer matrix composite materials and their laminates". [54]

8.2. Reinforcement selection

After selecting the test, it was important to select the material, specifically the reinforcement properly as per the use case. As the study is concerned with high-strength and high-temperature resin systems, it was decided to prepare a composite with carbon fiber. To keep the influence of fibers to a minimum, uni-directional carbon fiber with 200 g/m^2 grammage was selected. A laminate thickness of 2 mm to 6 mm is specified in the standard. Considering a ply thickness of 0.2 mm, it was decided to manufacture 20-layer laminates.

8.3. Composite manufacturing

To prepare the composite, first, the resin mixes were prepared similar to the process of resin mixing defined in Chapter 7. Due to the nature of resins being viscous and the high-temperature requirements, it was decided to follow a similar process to thermoplastics for curing. A process of using metal molds and pressing in a hot press is used for thermoplastics, which was also used here.

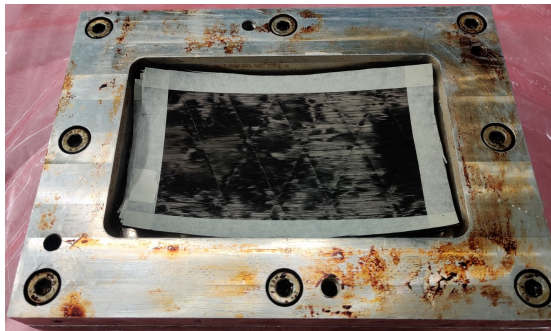
Due to a lack of time and to simplify the process, it was decided to use existing molds from other research works. Multiple trials were done to test the molds as well as finalize a laying process. The finalized composite manufacturing process consisted of the following steps:

1. Mold preparation

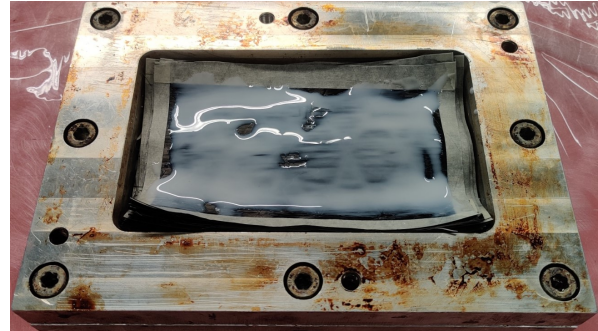
The mold was prepared by cleaning all the surfaces with acetone and isopropanol to get rid of dust and grease. Then, the mold release agent Marbokote 227 was applied 4 times with a time interval of 5 minutes on the contact surfaces. The bolts were also covered with beeswax to avoid getting the mold stuck in case of resin overflowing through the mold. The mold was assembled, and the bolts tightened, it was placed in an oven at $100 \text{ }^\circ\text{C}$ for heating.

2. Composite lay-up

It was decided to use a hand lay-up process, given the variation in parameters, the need to heat the resin for workability, and the expensive nature of the resin. Before starting the lay-up, the resin was maintained at 60 °C and the mold at 100 °C. It was essential to be swift in this process as the resin lowers in temperature raising its viscosity. The hand lay-up was done by alternating between fiber and resin layers as shown in figure 8.1.



(a) Fiber Layer



(b) Resin layer

Figure 8.1: Hand Lay-up process for Composite manufacturing

3. Curing of composite

After the hand lay-up is completed, the mold is closed as in figure 8.2 and wrapped with a high-temperature release film to avoid any excess resin damaging the heating plates on the hot press.



Figure 8.2: Closed with hand laid composite layers before curing

The same curing cycle developed previously of curing at 180 °C for 2 hours and post-curing at 220 °C for 1 hour was run for composite manufacturing as well. This was put into a program on the hot press.

The laminate manufactured from BADGE resin and 20 layers of Carbon fiber gave a thickness of around 6 mm. Thus, for the PHTe composite, the number of CF layers was reduced to 15, aiming for a thickness of around 4.5 mm. The manufactured laminates are as in figure 8.3.

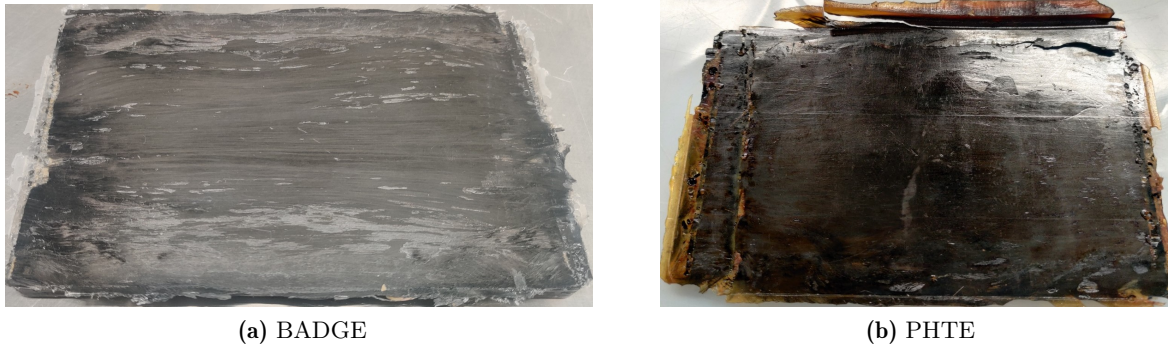


Figure 8.3: Composite laminate of both resins

8.3.1. Issues faced during composite manufacturing

A few challenges were faced during composite manufacturing, which are:

- High viscosity - Due to the high viscosity of the resin it is difficult to lay up at room temperature and heating is essential. While trying to spread the resin this also makes it easy to distort the fibers in the lay-up. As fibers are anisotropic and have significantly high strength in the longitudinal direction as compared to other directions, a slight change in the angle or distortion of fibers affects the strength of the composite heavily.
- High-temperature - As the viscosity of the resin reduces with temperature, the resin as well as the mold is heated. This makes it necessary to work swiftly with minimal handling.
- Safety issue - Due to the resin and the mold being heated, it poses a safety issue while laying up and proper care is essential to avoid mishaps.
- Type of fibers - It is also difficult to work with unidirectional fibers and a better composite can be prepared using a woven fabric as they have greater integrity and can be handled easily.

Due to these issues, the composite manufactured had a few voids present as well. The PHTE sample had a relatively low number of voids as compared to the BADGE composite, but this property is not due to the difference in the resin but rather the processing.

It was not possible to address these issues due to time limitations. More work can be put in the future to address a few of these issues, although the preferred method of composite would be heated Resin transfer moulding.

8.4. Inter-laminar shear strength testing (ILSS)

8.4.1. Sample preparation

After composite manufacturing, samples need to be prepared as per standard. The standard mentions a specimen length of 6 times the thickness and a width b twice the thickness. Due to the presence of voids and defects in the composite, only four proper samples of both resins could be prepared. A Secotom cutting machine equipped with a diamond-edge cutting blade was used to prepare the samples. The sample dimensions measured using a digital vernier caliper are as in the tables 8.1 and 8.2.

Sample	Length	Width	Thickness
1	37.15	12.87	5.85
2	36.94	11.80	5.81
3	37.05	12.62	5.86
4	36.97	12.18	5.82

Table 8.1: Sample Dimensions of Carbon composite with BADGE resin

Sample	Length	Width	Thickness
1	36.97	12.63	4.66
2	37.09	13.12	4.69
3	35	12.67	4.7
4	35.14	12.55	4.67

Table 8.2: Sample Dimensions of Carbon composite with PHTE resin

8.4.2. Testing

The standard mentions the loading nose diameter to be 6 mm and the support diameter to be 3mm. The standard mentions a loading span length-to-specimen thickness ratio of 4. The loading setup is shown in the figure 8.4. A span of 23.66 mm for BADGE and 18.7 mm for PHTE was taken for testing considering the thickness of the samples.

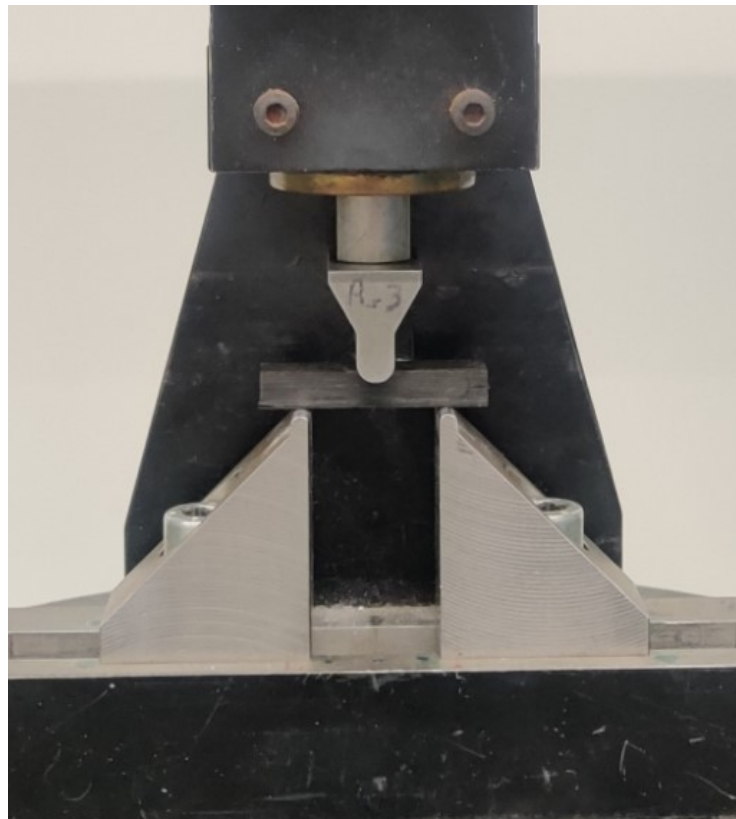


Figure 8.4: Short beam shear setup for ILSS (Inter-Laminar Shear Strength)

An initial test was done to understand the testing speed, and a crosshead rate of 0.5 mm/min was used for testing. All the samples were tested and force vs. displacement curve data was captured as in figure 8.5.

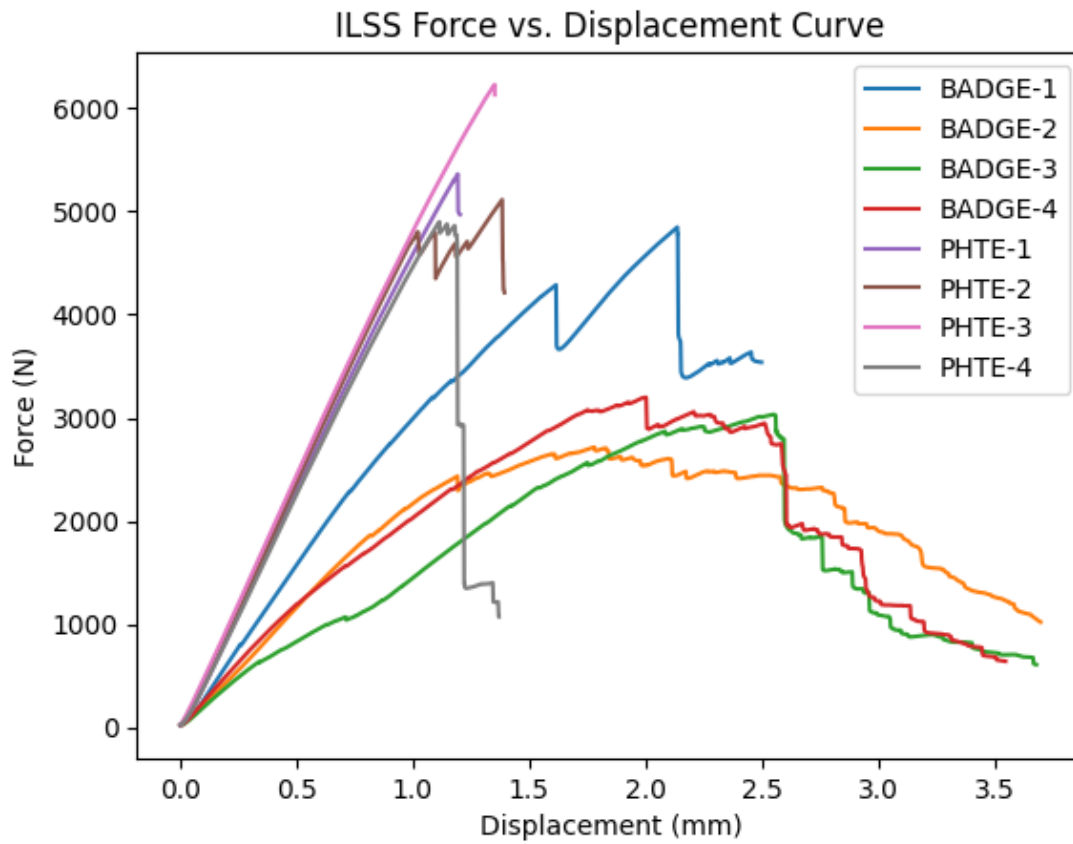


Figure 8.5: ILSS Force vs. Displacement testing data

8.4.3. Test Validity check

Before calculating shear stress and comparing the resins, it is essential to understand if the tests are valid or not. The expected results are sharp or clear laminar failures in shear as in figure 8.6.

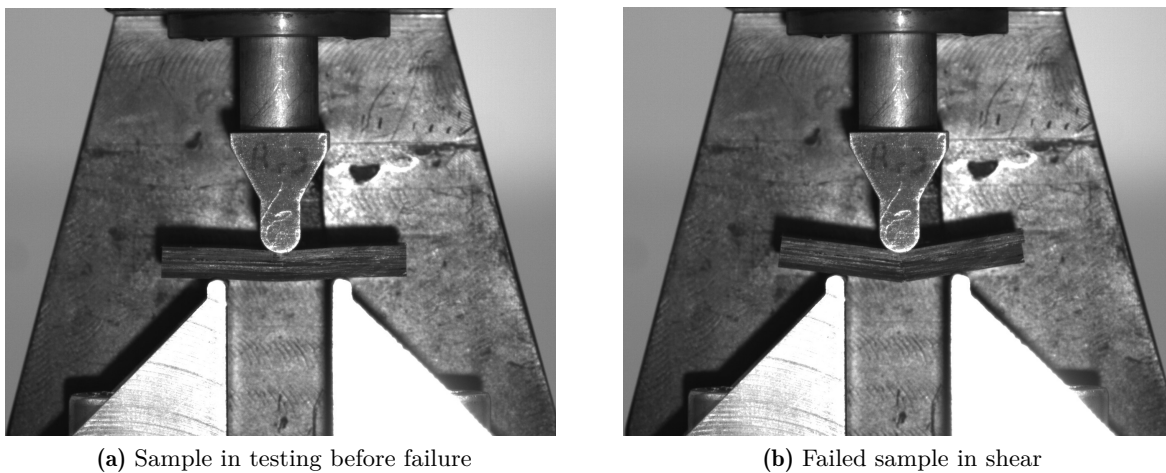


Figure 8.6: Successful ILSS test with failure through a lamina

From optical inspection of samples and the testing data, the BADGE sample does not give a valid test due to the presence of a lot of voids. Thus they cannot be used for shear strength estimation. PHTE samples had comparatively fewer voids and further discussion will be done on them.

8.4.4. Shear Strength Calculation

After checking for the validity of the test, we move on to shear strength calculation. ASTM D2344 recommends a closed-form approximation for the maximum shear stress,

$$\tau_{max} = \frac{3P}{4wt}$$

where,

- P = Applied load,
- w = Specimen Width,
- t = Specimen thickness.

BADGE Specimen	Maximum force P (N)	Maximum Shear Stress $\tau_{max}(MPa)$	Failure Mode
1	4847.61	48.26	Central cracking, no shear failure
2	2715.38	29.70	Multiple shears in layers with voids
3	3033.54	30.77	1 shear running along voids
4	3198.2	33.84	1 shear running along voids

Table 8.3: Inter-Laminar Shear strength calculation for Carbon composite with BADGE resin

Although table 8.3 mentions the maximum load and the maximum shear strength calculation for BADGE, the failure method of the samples was not inter-laminar shear. Thus, due to the invalidity of the tests, these values cannot be used for inter-laminar shear strength.

PHTE Specimen	Maximum force P (N)	Maximum Shear Stress $\tau_{max}(MPa)$	Failure Mode
1	5363.29	68.33	Proper laminar shear, negligible voids
2	5114.83	62.34	Proper laminar shear in the layer with a void
3	6230.09	78.47	Semi-laminar shear with the layer breaking in between
4	4900.31	62.72	Proper laminar shear in the layer with a void

Table 8.4: Inter-Laminar Shear Strength Calculation for Carbon Composite with PHTE resin

Table 8.4 consists of the maximum load and the maximum shear strength calculation for PHTE. The failure modes are also written for each sample. Apart from specimen 3, other specimens failed in inter-laminar shear. As can be inferred from table 8.4, samples 2 and 4 had a slight presence of voids at the failed interface which can be seen from a slightly less shear value as compared to sample 1.

Thus, the only sample that can be considered as true shear strength here is sample 1 for PHTE. Thus, for future testing reference, an ILSS value of 68.33 MPa can be considered. As no value of BADGE was obtained, an ILSS comparison value of 45.95 MPa was seen from a similar Carbon composite formed using a Bisphenol-A-based resin. [55] The inter-laminar shear strength of PHTE seems to be higher, however, extensive testing is essential to properly comment on and compare the inter-laminar shear strength of PHTE.

9

Conclusion

The primary aim of this thesis was to research a viable bio-based resin for high-performance applications. From the chemical structure and previous works, PHTE came up as a promising candidate. Thus, it was decided to move forward with PHTE as the epoxy of choice. There were a few existing studies with PHTE [22] [23] [33], but these studies were seen to have PHTE resin systems which performed lower than the BADGE resin systems. This was also attributed to the use of curing agents with low aromaticity in these studies or the use of reactive diluents for easier processing.

Thus, keeping in tandem with the aim of this thesis to prepare a resin system that holds the potential to compete with BADGE-based resin systems, it was decided to research PHTE with an aromatic curing agent. This aim was achieved by the following steps:

- Finalizing an appropriate curing agent.
- Stoichiometric ratio estimation
- Resin characterization
- Composite trials

To properly understand PHTE and for a fair comparison, BADGE was chosen as the comparison epoxy. It is a resin system widely used in aerospace and other high-performance applications. To keep the comparison fair, BADGE monomer was used rather than a commercial product to avoid disparity in data due to additives and inhibitors which are often used in commercial products to alter their properties. As that is dependent on the application and required properties, it varies and widens the scope a lot.

The existing studies were seen to be comparing the resin systems with only a handful of parameters. Thus, it was decided to compare the resin systems with a wide variety of parameters useful for real-life composite applications. To create an extensive database and easily repeatable and comparable results, ASTM standards were followed for all testing.

9.1. Curing agent selection

Through the literature review, four curing agents were found to be of interest:

- DDS,
- DDM,
- DDE, and
- DICY.

Out of these DDM and DDE were eliminated due to their toxic properties and large particle

size. For further selection, a qualitative analysis using the kofler bench was used to finalize the curing agent. DDS was selected as the curing agent of interest, as it has aromatic structures and gives a good processing window and workability as opposed to DICY which had a really short processing window. DDS being a commercial product is also available in a micronized powder form, which makes the process of creating homogeneously dispersing the curing agent in the resin system fairly easy. The curing agent was also kept common for both systems to avoid further variations.

From the kofler bench, a reduction in viscosity was also observed with slight heating. This gave a direction for easier working of the resin during the whole study.

9.2. Stoichiometric ratio estimation

After the selection of the materials, it was important to calculate the mixing ratio. Each epoxy reacts with one hydrogen at the ends of a curing agent. Thus, the functionality of:

- DDS is 4 (4 hydrogens at the ends),
- PHTE is 3 (3 epoxy groups), and
- BADGE is 2 (2 epoxy groups).

Thus, the theoretical molar ratios were calculated to be 1.33:1 (4:3) for PHTE:DDS and 2:1 (4:2) for BADGE:DDS as per the monomer structures.

However, during the synthesis of epoxy monomers, the reaction or the product is not purely monomeric and some internal oligomericity is present. This drives the overall functionality of the monomer down and thus it is important to determine the mixing ratio for proper cross-linking, also known as stoichiometric ratio. This was done by maximizing the glass transition temperature (T_g), as it depends on the cross-linking in the material which promises the best possible properties.

This process was done in two phases:

- Phase 1 consisted of estimating the first decimal place of the ratio. five different mixes with the first decimal place varying were prepared and tested i.e. 1.4, 1.5 to 1.8 for PHTE:DDS and 1.9, 2 to 2.3 for BADGE:DDS.
- Then the second phase was run with the finalized ratio from the first phase for the second decimal estimation. Again, five resin mixes were prepared and tested i.e. 1.46, 1.48 to 1.54 for PHTE:DDS and 2.06, 2.08 to 2.12 for BADGE:DDS.

The final stoichiometric ratios estimated were:

- 1.52:1 for PHTE:DDS, and
- 2.06:1 for BADGE:DDS.

To determine the ratios, especially for PHTE, DMA had to be used as opposed to the common practice of using DSC for T_g estimation. This was essential due to the lack of a clear glass transition drop in DSC curves, which was attributed to the bulky structure of all the components.

9.3. Resin characterization

Once, the mixing ratios were finalized, the resins were characterized and compared. The study encompassed a thorough material analysis and testing phase, which involved examining chemical properties and mechanical performance through various material characterization techniques which are summarized in table 9.1.

We can infer that PHTE can compete with BADGE and even surpasses a few properties. The onset temperature is higher for BADGE, but the T_g and ash content are higher for PHTE, which

is beneficial. Also, the mass or property loss in BADGE upon surpassing onset temperature is considerably high in BADGE, which is not preferable as it imposes a hard limit on temperature.

Parameter	Technique used	PHTE:DDS (1.52:1)	BADGE:DDS (2.06:1)	Difference
Onset of weight loss	Thermo-gravimetry analysis	310 °C	360 °C	50 °C lower
Char yield (at 850 °C)	Thermo-gravimetry analysis	26.22 %	1.3 %	
Activation energy	Differential scanning calorimetry	59.974 kJ/mol	63.417 kJ/mol	5.4 % lower
Coefficient of thermal expansion (CTE)	Thermo-mechanical analysis	$97.75 \times 10^{-6}/K$	$84.45 \times 10^{-6}/K$	
Glass transition temperature (T _g)	Dynamic mechanical analysis	260 °C	226 °C	34 °C higher
Viscosity (at 25 °C)	Dynamic rheometry	12300 Pa-s	19.3 Pa-s	
Viscosity (at 60 °C)	Dynamic rheometry	101 Pa-s	0.5 Pa-s	
Water contact angle	Optical tensiometer	69.2°	79.72°	
Water absorption % - 14 Days	Submersion in de-ionized water	1.3 %	0.96 %	
Gel content	Submersion in toluene for 72 hours	99.95 %	100 %	
Bio-based content	Bio-based carbon/fossil carbon	64.31 %	0 %	
Density	Weight measurement	1217 kg/m ³	1333 kg/m ³	10.1 % higher
Tensile strength	Mechanical tensile testing	67 MPa	83 MPa	23.8 % lower
Young's modulus	Mechanical tensile testing	1.794 GPa	1.296 GPa	33.6 % higher
Flexural strength	3-point bend testing	122 MPa	124 MPa	≈
Flexural modulus	3-point bend testing	3.77 GPa	2.6 GPa	39.6 % higher
Fracture toughness (K _{IC})	Single edge notched bend - 3-point bend test	0.69 MPa.m ^{1/2}	0.60 MPa.m ^{1/2}	15 % higher

Table 9.1: Comparison table - PHTE and BADGE resin systems with DDS

The viscosity is higher for PHTE which will require slightly more intensive processing as compared to BADGE but it drops suddenly with some heating. This can also be controlled by additives and depends on the application. The water affinity of PHTE is also higher as compared to BADGE, which is to be expected from bio-based materials.

The PHTE:DDS resin system also has a good bio-based content of 64.31 %. In terms of mechanical properties, the density is slightly higher for PHTE but the stiffness or modulus is higher for PHTE which is beneficial for a matrix material and might counter the higher density as per application. A beneficial property is the fracture toughness which is higher for PHTE. This helps to stop crack propagation in the material, as it is impossible to avoid defects in a structure.

9.4. Composite trials

To assess the resins in an actual use case, a composite preparation was attempted. Hand lay-up of carbon fiber uni-directional fibers and heated resins was done in a heated mold and cured as per the defined curing cycle. The viscous nature of the resins also makes hand lay-up difficult and results in a composite with lots of voids. A comparative comment cannot be made on the manufacturing as not a lot of composite manufacturing was done, but the composite prepared with PHTE was good with a few voids. This promises the workability of PHTE resin system for composite and a high-temperature RTM system is advised as the method of manufacturing.

For a quantitative analysis, tensile and flexural tests were not performed as they are highly dependent on the fiber as compared to the matrix. Thus it was decided to test for inter-laminar shear strength (ILSS), which is dependent on the matrix. A few good samples were cut from the prepared laminates and tested in a short beam shear setup. The BADGE samples did not fail in shear and thus invalid test results were obtained. PHTE samples broke in shear and an average ILSS value of 68.33 MPa was received. PHTE was seen to have a higher inter-laminar shear strength as compared to 45.95 MPa for a similar carbon fiber composite made with a Bisphenol-A-based resin. [55]

9.5. Conclusion and cost considerations

In conclusion, PHTE promises good properties and emerges as a potential epoxy for high-performance applications. This is a promising result as the majority of the current work on bio-based composites gives low thermal and mechanical properties, making it unsuitable for structural applications. The high thermal and mechanical properties with a high bio-based content of 64.31 % place PHTE as a contender for future sustainable matrix material for high-performance composite applications and further work can be done on it to tailor the properties as per application. This environmentally friendly feature is a big step in the right direction toward satisfying the growing need in a variety of industrial sectors for more ecologically friendly materials.

The current issues are its high viscosity and high temperature requirements which need further work. Along with these, a major challenge is the current market price of Phloroglucinol and PHTE. This is because Phloroglucinol is majorly used in pharmaceutical applications. Although competition with pharmaceuticals is not preferable it does not seem to be an issue of concern as phloroglucinol has various sources of origin and can even be obtained from the bark of fruit trees. The phloroglucinol is already an 11 million dollar market and is expected to grow year on year. Also, with further industrialization, brown algae can be grown on farms and a lower purity product as compared to pharmaceuticals can be used, which will significantly drive the price down.

Resolving these issues is essential to realizing the full promise of PHTE in a range of industrial applications, particularly in fields where material resilience and environmental sustainability are critical.

10

Recommendations and Future Work

As concluded, PHTE gives promising results and holds potential as a bio-based alternative to toxic fossil-fuel-based resins. Due to its amazing thermal and mechanical properties, it deserves a place in the development of next-generation sustainable composite materials. However, further research and investigation are required for it to replace a matrix material as commercial and well-researched as BADGE. Future endeavors, derived and based on this study, could encompass several areas of research and development regarding PHTE formulation and its use in composite systems. These may include:

- **Purity of PHTE monomer:** As we can understand from the stoichiometric ratios, PHTE has quite a lot of deviation from the monomer as compared to BADGE. Thus further work can be done for better synthesis techniques to achieve better products.
- **Exploration of other curing agents:** PHTE can be investigated with other curing agents to cater to different requirements. Liquid low-viscosity curing agents for lowering viscosity with good mechanical properties or curing agents with higher aromatic ratios or smaller structures to increase thermal properties for applicability in space applications.
- **Further development of the resin system:** Investigating and developing the resin system with additives for influencing properties as per requirement. Toughening agents can be used to reduce the brittle nature of the resin system and accelerators would be useful to reduce the energy requirements for curing. Investigating the use of high-quality, functional reactive diluents to mimic industrial resin recipes for high-performance applications, and ensuring consistent and reliable results would also be beneficial.
- **Exploration of bio-based curing agents:** To further increase the bio-based content of the resin system, a bio-based curing agent can be investigated. This might also generate a need for research on an aromatic bio-based curing agent.
- **Recyclability:** A curing agent selection can be done to achieve a recyclable or partially recyclable resin system. A curing agent that is capable of forming vitrimeric systems would be of interest, although extensive testing on creep behavior would be essential.
- **Curing cycle development:** The curing cycle can be further investigated to optimize and reduce the temperature and times to reduce energy utilization and overall environmental impact. The dispersion and dissolution of solid curing agents can be studied using hot-stage microscopy.
- **Expanding the resin characterization:** The resin system can be further characterized so that the system can potentially be utilized commercially. More SENB testing can be done to properly characterize fracture toughness.
- **Exploration of composite manufacturing techniques:** As mentioned hand lay-up is not the best method for composite manufacturing utilizing the PHTE:DDS resin system. Thus it

is essential to explore other manufacturing techniques especially high-temperature Resin Transfer Moulding.

- **Bio-based fibers:** Although it is not possible to use natural fibers with PHTE:DDS resin system due to the high-temperature curing, it can be explored with a different curing agent with lower curing temperatures for secondary structural applications to create more environmentally friendly fiber-reinforced composites with high bio-content.
- **Comparison with other high-performance resin systems:** As PHTE is one of the contenders in the search for a sustainable bio-based resin, it will be beneficial to compare PHTE with Tactix and other bio-based resin systems with the possibility of high thermal and mechanical properties such as resveratrol and vanillin.
- **Exploration for prepreg system:** As the PHTE:DDS resin system is a slow cure system requiring post-cure, semi-curing can be studied for prepreg production to facilitate faster and better composite production.
- **Life cycle assessment (LCA) Studies:** Although a lot of analysis on mechanical and thermal properties has been done while being stated that PHTE is bio-based, it is essential to properly assess the change brought about by green materials and to proceed with caution. LCA studies are a good measure to properly assess the overall change or impact brought about by a process/material and avoid green-washing from the virtue of the material being bio-based. Sometimes bio-based materials might require greater processing leading to overall negative effects.

References

- [1] Victor Giurgiutiu. "Introduction". In: *Stress, Vibration, and Wave Analysis in Aerospace Composites*. Elsevier, 2022, pp. 1–27. DOI: [10.1016/b978-0-12-813308-8.00006-5](https://doi.org/10.1016/b978-0-12-813308-8.00006-5).
- [2] Shivi Kesarwani. *Polymer Composites in Aviation Sector A Brief Review Article*. URL: www.ijert.org.
- [3] William E. Dyer and Baris Kumru. "Polymers as Aerospace Structural Components: How to Reach Sustainability?" In: *Macromolecular Chemistry and Physics* 224.24 (2023), p. 2300186. DOI: <https://doi.org/10.1002/macp.202300186>. eprint: <https://onlinelibrary.wiley.com/doi/pdf/10.1002/macp.202300186>. URL: <https://onlinelibrary.wiley.com/doi/abs/10.1002/macp.202300186>.
- [4] E. Frank, D. Ingildeev, and M.R. Buchmeiser. "2 - High-performance PAN-based carbon fibers and their performance requirements". In: *Structure and Properties of High-Performance Fibers*. Ed. by Gajanan Bhat. Woodhead Publishing Series in Textiles. Oxford: Woodhead Publishing, 2017, pp. 7–30. ISBN: 978-0-08-100550-7. DOI: <https://doi.org/10.1016/B978-0-08-100550-7.00002-4>. URL: <https://www.sciencedirect.com/science/article/pii/B9780081005507000024>.
- [5] Pranshul Gupta et al. "Enhancing the mechanical properties of jute fiber reinforced green composites varying cashew nut shell liquid composition and using mercerizing process". In: *Materials Today: Proceedings* 19 (2019), pp. 434–439. ISSN: 2214-7853. DOI: <https://doi.org/10.1016/j.matpr.2019.07.631>.
- [6] Fu Gu et al. "Can bamboo fibres be an alternative to flax fibres as materials for plastic reinforcement? A comparative life cycle study on polypropylene/flax/bamboo laminates". In: *Industrial Crops and Products* 121 (2018), pp. 372–387. ISSN: 0926-6690. DOI: <https://doi.org/10.1016/j.indcrop.2018.05.025>. URL: <https://www.sciencedirect.com/science/article/pii/S0926669018304369>.
- [7] K. Subrahmanya Bhat Deepa G. Devadiga and GT Mahesha. "Sugarcane bagasse fiber reinforced composites: Recent advances and applications". In: *Cogent Engineering* 7.1 (2020). Ed. by Julio Sánchez, p. 1823159. DOI: [10.1080/23311916.2020.1823159](https://doi.org/10.1080/23311916.2020.1823159). eprint: <https://doi.org/10.1080/23311916.2020.1823159>. URL: <https://doi.org/10.1080/23311916.2020.1823159>.
- [8] Anshuman Shrivastava. "1 - Introduction to Plastics Engineering". In: *Introduction to Plastics Engineering*. Ed. by Anshuman Shrivastava. Plastics Design Library. William Andrew Publishing, 2018, pp. 1–16. ISBN: 978-0-323-39500-7. DOI: <https://doi.org/10.1016/B978-0-323-39500-7.00001-0>. URL: <https://www.sciencedirect.com/science/article/pii/B9780323395007000010>.
- [9] J.S. Bergstrom. *Mechanics of Solid Polymers: Theory and Computational Modeling*. Plastics Design Library. Elsevier Science, 2015. ISBN: 9780323322966. URL: <https://books.google.nl/books?id=DfucBAAAQBAJ>.

- [10] Nathan J. Van Zee and Renaud Nicolay. “Vitrimers: Permanently crosslinked polymers with dynamic network topology”. In: *Progress in Polymer Science* 104 (2020). ISSN: 00796700. DOI: [10.1016/j.progpolymsci.2020.101233](https://doi.org/10.1016/j.progpolymsci.2020.101233).
- [11] Mitsuhiro Okayasu, Yuki Tsuchiya, and Hiroaki Arai. “Experimentally and analyzed property of carbon fiber reinforced thermoplastic and thermoset plates”. In: *Journal of Materials Science Research* 7.3 (2018), p. 12. ISSN: 1927-0585. DOI: [10.5539/jmsr.v7n3p12](https://doi.org/10.5539/jmsr.v7n3p12).
- [12] Maxime Roux et al. “Processing and recycling of thermoplastic composite fibre/PEEK aerospace part”. In: Jan. 2014.
- [13] Vahid Yaghoubi and Baris Kumru. “Retrosynthetic Life Cycle Assessment: A Short Perspective on the Sustainability of Integrating Thermoplastics and Artificial Intelligence Into Composite Systems”. In: *Advanced Sustainable Systems* n/a.n/a (), p. 2300543. DOI: <https://doi.org/10.1002/adsu.202300543>. eprint: <https://onlinelibrary.wiley.com/doi/pdf/10.1002/adsu.202300543>. URL: <https://onlinelibrary.wiley.com/doi/abs/10.1002/adsu.202300543>.
- [14] Cristina Cantarutti, Roxana Dinu, and Alice Mija. “Biorefinery Byproducts and Epoxy Biorenewable Monomers: A Structural Elucidation of Humins and Triglycidyl Ether of Phloroglucinol Cross-Linking”. In: 21 (Feb. 2020), pp. 517–533. ISSN: 15264602. DOI: [10.1021/acs.biomac.9b01248](https://doi.org/10.1021/acs.biomac.9b01248).
- [15] Fan Long Jin, Xiang Li, and Soo Jin Park. “Synthesis and application of epoxy resins: A review”. In: *Journal of Industrial and Engineering Chemistry* 29 (2015), pp. 1–11. ISSN: 22345957. DOI: [10.1016/j.jiec.2015.03.026](https://doi.org/10.1016/j.jiec.2015.03.026).
- [16] Roxana Dinu et al. “High Glass Transition Materials from Sustainable Epoxy Resins with Potential Applications in the Aerospace and Space Sectors”. In: *ACS Applied Polymer Materials* (2022). ISSN: 26376105. DOI: [10.1021/acsapm.2c00183](https://doi.org/10.1021/acsapm.2c00183).
- [17] David Santiago et al. “Bio-based epoxy shape-memory thermosets from triglycidyl phloroglucinol”. In: *Polymers* 12.3 (Mar. 2020). ISSN: 20734360. DOI: [10.3390/polym12030542](https://doi.org/10.3390/polym12030542).
- [18] Roxana Dinu et al. “Development of Sustainable High Performance Epoxy Thermosets for Aerospace and Space Applications”. In: *Polymers* 14.24 (Dec. 2022). ISSN: 20734360. DOI: [10.3390/polym14245473](https://doi.org/10.3390/polym14245473).
- [19] Aratz Genua et al. “Build-to-specification vanillin and phloroglucinol derived biobased epoxy-amine vitrimers”. In: *Polymers* 12.11 (Nov. 2020), pp. 1–14. ISSN: 20734360. DOI: [10.3390/polym12112645](https://doi.org/10.3390/polym12112645).
- [20] Samira El Gazzani et al. “High-temperature epoxy foam: Optimization of process parameters”. In: *Polymers* 8.6 (June 2016). ISSN: 20734360. DOI: [10.3390/polym8060215](https://doi.org/10.3390/polym8060215).
- [21] Yongxiang Yang et al. “Recycling of composite materials”. In: *Chemical Engineering and Processing: Process Intensification* 51 (Jan. 2012), pp. 53–68. ISSN: 02552701. DOI: [10.1016/j.cep.2011.09.007](https://doi.org/10.1016/j.cep.2011.09.007).
- [22] Roxana Dinu et al. “Sustainable and recyclable thermosets with performances for high technology sectors. An environmental friendly alternative to toxic derivatives”. In: *Frontiers in Materials* 10 (2023). ISSN: 22968016. DOI: [10.3389/fmats.2023.1242507](https://doi.org/10.3389/fmats.2023.1242507).
- [23] Roxana Dinu et al. “Recyclable, Repairable, and Fire-Resistant High-Performance Carbon Fiber Biobased Epoxy”. In: *ACS Applied Polymer Materials* 5.4 (Apr. 2023), pp. 2542–2552. ISSN: 26376105. DOI: [10.1021/acsapm.2c02184](https://doi.org/10.1021/acsapm.2c02184).

- [24] Songqi Ma et al. “Bio-based epoxy resin from itaconic acid and its thermosets cured with anhydride and comonomers”. In: *Green Chemistry* 15.1 (2013), pp. 245–254. ISSN: 14639270. DOI: [10.1039/c2gc36715g](https://doi.org/10.1039/c2gc36715g).
- [25] Emilie Darroman et al. “Improved cardanol derived epoxy coatings”. In: *Progress in Organic Coatings* 91 (2016), pp. 9–16. ISSN: 03009440. DOI: [10.1016/j.porgcoat.2015.11.012](https://doi.org/10.1016/j.porgcoat.2015.11.012).
- [26] Fengshuo Hu et al. “Synthesis and characterization of thermosetting furan-based epoxy systems”. In: *Macromolecules* 47.10 (2014), pp. 3332–3342. ISSN: 15205835. DOI: [10.1021/ma500687t](https://doi.org/10.1021/ma500687t).
- [27] P. Niedermann, G. Szebényi, and A. Toldy. “Novel high glass temperature sugar-based epoxy resins: Characterization and comparison to mineral oil-based aliphatic and aromatic resins”. In: *Express Polymer Letters* 9.2 (2015), pp. 85–94. ISSN: 1788618X. DOI: [10.3144/expresspolymlett.2015.10](https://doi.org/10.3144/expresspolymlett.2015.10).
- [28] Lise Maisonneuve et al. “Structure-properties relationship of fatty acid-based thermoplastics as synthetic polymer mimics”. In: *Polymer Chemistry* 4.22 (2013), pp. 5472–5517. ISSN: 17599962. DOI: [10.1039/c3py00791j](https://doi.org/10.1039/c3py00791j).
- [29] Carla Vilela et al. “Polymers and copolymers from fatty acid-based monomers”. In: *Industrial Crops and Products* 32.2 (2010), pp. 97–104. ISSN: 09266690. DOI: [10.1016/j.indcrop.2010.03.008](https://doi.org/10.1016/j.indcrop.2010.03.008).
- [30] Jean Mathieu Pin, Nicolas Sbirrazzuoli, and Alice Mija. “From epoxidized linseed oil to bioresin: An overall approach of epoxy/anhydride cross-linking”. In: *ChemSusChem* 8.7 (Apr. 2015), pp. 1232–1243. ISSN: 1864564X. DOI: [10.1002/cssc.201403262](https://doi.org/10.1002/cssc.201403262).
- [31] Qiuyu Tang et al. “Bio-Based Epoxy Resin from Epoxidized Soybean Oil”. In: *Soybean*. Ed. by Minobu Kasai. Rijeka: IntechOpen, 2018. Chap. 8. DOI: [10.5772/intechopen.81544](https://doi.org/10.5772/intechopen.81544). URL: <https://doi.org/10.5772/intechopen.81544>.
- [32] Eric Ramon, Carmen Sguazzo, and Pedro M.G.P. Moreira. “A review of recent research on bio-based epoxy systems for engineering applications and potentialities in the aviation sector”. In: *Aerospace* 5.4 (2018). ISSN: 22264310. DOI: [10.3390/aerospace5040110](https://doi.org/10.3390/aerospace5040110).
- [33] Dimitrios Apostolidis et al. “Algae-derived partially renewable epoxy resin formulation for glass fibre reinforced sustainable polymer composites”. In: *RSC Applied Polymers* 2 (Jan. 2024). DOI: [10.1039/D3LP00174A](https://doi.org/10.1039/D3LP00174A).
- [34] Xin Song et al. “High-performance and fire-resistant epoxy thermosets derived from plant-derived ferulic acid”. In: *Industrial Crops and Products* 187 (Nov. 2022). ISSN: 09266690. DOI: [10.1016/j.indcrop.2022.115445](https://doi.org/10.1016/j.indcrop.2022.115445).
- [35] A.C. Grillet et al. “Effects of the structure of the aromatic curing agent on the cure kinetics of epoxy networks”. In: *Polymer* 30.11 (1989), pp. 2094–2103. ISSN: 0032-3861. DOI: [https://doi.org/10.1016/0032-3861\(89\)90300-5](https://doi.org/10.1016/0032-3861(89)90300-5). URL: <https://www.sciencedirect.com/science/article/pii/0032386189903005>.
- [36] Sizhu Yu et al. “Effect of the aromatic amine curing agent structure on properties of epoxy resin-based syntactic foams”. In: *ACS Omega* 5.36 (Sept. 2020), pp. 23268–23275. ISSN: 24701343. DOI: [10.1021/acsomega.0c03085](https://doi.org/10.1021/acsomega.0c03085).
- [37] Heru Sukanto et al. “Epoxy resins thermosetting for mechanical engineering”. In: *Open Engineering* 11 (Jan. 2021), pp. 797–814. ISSN: 23915439. DOI: [10.1515/eng-2021-0078](https://doi.org/10.1515/eng-2021-0078).

- [38] Emmanouil D. Tsochatzis, Georgios Theodoridis, and Milena Corredig. “Analysis of oligomers to assess exposure to microplastics from foods. A perspective”. In: *Frontiers in Nutrition* 10 (2023). ISSN: 2296861X. DOI: [10.3389/fnut.2023.1186951](https://doi.org/10.3389/fnut.2023.1186951).
- [39] “Thermal Analysis and Thermal Properties[1]”. In: *Characterization and Failure Analysis of Plastics*. ASM International, Dec. 2003. ISBN: 978-1-62708-281-5. DOI: [10.31399/asm.tb.cfap.t69780115](https://doi.org/10.31399/asm.tb.cfap.t69780115). eprint: <https://dl.asminternational.org/book/chapter-pdf/598550/t69780115.pdf>. URL: <https://doi.org/10.31399/asm.tb.cfap.t69780115>.
- [40] A. W. Coats and J. P. Redfern. “Thermogravimetric analysis. A review”. In: *Analyst* 88 (1053 1963), pp. 906–924. DOI: [10.1039/AN9638800906](https://doi.org/10.1039/AN9638800906). URL: <http://dx.doi.org/10.1039/AN9638800906>.
- [41] Xiaoyan Liu and Weidong Yu. “Evaluating the thermal stability of high performance fibers by TGA”. In: *Journal of Applied Polymer Science* 99.3 (2006), pp. 937–944. DOI: <https://doi.org/10.1002/app.22305>. eprint: <https://onlinelibrary.wiley.com/doi/pdf/10.1002/app.22305>. URL: <https://onlinelibrary.wiley.com/doi/abs/10.1002/app.22305>.
- [42] Dailyn Guzmán et al. “Novel bio-based epoxy thermosets based on triglycidyl phloroglucinol prepared by thiol-epoxy reaction”. In: *Polymers* 12.2 (Feb. 2020). ISSN: 20734360. DOI: [10.3390/polym12020337](https://doi.org/10.3390/polym12020337).
- [43] T. Hatakeyama and F. X. Quinn. *Thermal analysis: fundamentals and applications to polymer science*. Wiley, 1999. ISBN: 0471983624. DOI: [10.1002/9780470423837](https://doi.org/10.1002/9780470423837).
- [44] Pooria Gill, Tahereh Tohidi Moghadam, and Bijan Ranjbar. *Differential Scanning Calorimetry Techniques: Applications in Biology and Nanoscience*. 2010.
- [45] Kodre Kv et al. *Research and Reviews: Journal of Pharmaceutical Analysis Differential Scanning Calorimetry: A Review*. Vol. 3.
- [46] “Standard Test Method for Transition Temperatures and Enthalpies of Fusion and Crystallization of Polymers by Differential Scanning Calorimetry”. In: (). DOI: [10.1520/D3418](https://doi.org/10.1520/D3418). URL: <https://standards.iteh.ai/catalog/standards/sist/3f54b9ed-4d1b-4b3c-8607-187d614af4ac/astm-d3418-21>.
- [47] W.M. GROENEWOUD. “CHAPTER 4 - DYNAMIC MECHANICAL ANALYSIS”. In: *Characterisation of Polymers by Thermal Analysis*. Ed. by W.M. GROENEWOUD. Amsterdam: Elsevier Science B.V., 2001, pp. 94–122. ISBN: 978-0-444-50604-7. DOI: <https://doi.org/10.1016/B978-044450604-7/50005-4>. URL: <https://www.sciencedirect.com/science/article/pii/B9780444506047500054>.
- [48] Mukesh Kumar Singh and Annika Singh. “Chapter 11 - Dynamic mechanical analysis”. In: *Characterization of Polymers and Fibres*. Ed. by Mukesh Kumar Singh and Annika Singh. The Textile Institute Book Series. Woodhead Publishing, 2022, pp. 241–271. ISBN: 978-0-12-823986-5. DOI: <https://doi.org/10.1016/B978-0-12-823986-5.00005-1>. URL: <https://www.sciencedirect.com/science/article/pii/B9780128239865000051>.
- [49] *Test Method for Plastics: Dynamic Mechanical Properties: In Flexure (Three-Point Bending) 1*. DOI: [10.1520/D5023-15](https://doi.org/10.1520/D5023-15). URL: www.astm.org.

-
- [50] “Standard Test Method for Water Absorption of Plastics”. In: (). DOI: [10.1520/D0570](https://doi.org/10.1520/D0570). URL: <https://standards.iteh.ai/catalog/standards/sist/96e87ef8-a79c-4880-a714-dbd20160c276/astm-d570-22>.
- [51] “Standard Test Methods for Determination of Gel Content and Swell Ratio of Crosslinked Ethylene Plastics”. In: (). DOI: [10.1520/D2765-16](https://doi.org/10.1520/D2765-16). URL: www.astm.org.
- [52] “Standard Test Methods for Flexural Properties of Unreinforced and Reinforced Plastics and Electrical Insulating Materials”. In: (). DOI: [10.1520/D0790-10](https://doi.org/10.1520/D0790-10). URL: <http://www.ansi.org>.
- [53] *Standard Test Methods for Plane-Strain Fracture Toughness and Strain Energy Release Rate of Plastic Materials*. URL: www.astm.org.
- [54] “Standard Test Method for Short-Beam Strength of Polymer Matrix Composite Materials and Their Laminates”. In: (). DOI: [10.1520/D2344_D2344M](https://doi.org/10.1520/D2344_D2344M). URL: www.astm.org.
- [55] Junsen Ma et al. “Study on the inter-laminar shear properties of carbon fiber reinforced epoxy composite materials with different interface structures”. In: *Materials and Design* 214 (2022). ISSN: 18734197. DOI: [10.1016/j.matdes.2022.110417](https://doi.org/10.1016/j.matdes.2022.110417).

Woven fabric composite trials

Multiple trials for composite manufacturing with the resin systems included preparing a composite with woven carbon fabric as well. These trials included multiple mold trials as well to finalize a processing method. A readily available woven carbon fabric of 200 g/m^2 was used to conduct these trials.



(a) Woven carbon composite with PHTE



(b) Woven carbon composite with BADGE

Figure 11.1: Composite laminate manufacturing trials with the resin systems

Figure 11.1 shows the laminate prepared with both the resin systems and woven carbon fiber. These laminates were prepared from 4 layers. The laminates received were good in quality with a few surface issues. As discussed in chapter 8 for composites, several issues were faced here as well, and resin transfer molding utilizing a heated mold would be a better manufacturing procedure as compared to hand lay-up.